DUDLEY KNOX LIBRARY
NAVAL POSTGRADUATE SCHOOL
MONTEREY, CALIFORNIA 93943

DEPARTMENT OF OCEAN ENGINEERING

MASSACHUSETTS INSTITUTE OF TECHNOLOGY

CAMBRIDGE, MASSACHUSETTS 02139

MULTIVARIABLE CONTROL SYSTEM DESIGN FOR A SUBMARINE USING ACTIVE ROLL CONTROL

by

Richard James Martin

COURSE XIII-A

© JUNE 1985

MULTIVARIABLE CONTROL SYSTEM DESIGN FOR A SUBMARINE USING ACTIVE ROLL CONTROL

by

Richard James Martin

B.S., Purdue University
(1978)

SUBMITTED TO THE DEPARTMENTS OF OCEAN ENGINEERING AND MECHANICAL ENGINEERING IN PARTIAL FULFILLMENT OF THE REQUIREMENTS FOR THE DEGREE OF OCEAN ENGINEER AND MASTER OF SCIENCE IN MECHANICAL ENGINEERING

at the

MASSACHUSETTS INSTITUTE OF TECHNOLOGY

May 1985

© Richard James Martin, 1985

Thesis
M3585
C.1

Permission is hereby granted to the Charles Stark Draper Laboratory, Inc., to the Massachusetts Institute of Technology, and to the United States Government and its agencies to reproduce and to distribute copies of this thesis document in whole or in part.

MULTIVARIABLE CONTROL SYSTEM DESIGN FOR A SUBMARINE USING ACTIVE ROLL CONTROL

by

Richard James Martin

Submitted to the Departments of Ocean Engineering and Mechanical Engineering in Partial Fulfillment of the Requirements for the Degrees of Ocean Engineer and Master of Science in Mechanical Engineering.

ABSTRACT

A Multivariable Control System is designed for a deeply submerged submarine using the Linear Quadratic Gaussian (LQG) with Loop Transfer Recovery (LTR) methodology. The differential stern, bow, and rudder control surfaces are dynamically coordinated to cause the submarine to follow independent and simultaneous commanded changes in roll, yaw rate, depth rate and pitch attitude. Linear models of the submarine are developed at a ship speed of 30 knots with various rudder angles and then analyzed using the method of modal analysis. The linear models are then augmented with integral control, loop shaping techniques are applied to design a Kalman Filter transfer function, and the LTR technique is applied to recover the Kalman Filter loop shapes. The resulting model-based compensator and plant is tested using a non-linear mathematical model of the submarine, and comparisons are made with an equivalent compensator design that lacks active roll control capability. The performance characteristics of the closed loop design with roll control capability was significantly better than the characteristics of the design without roll control.

THESIS SUPERVISORS: Dr. Michael Athans, Professor of Systems Science and Engineering
Dr. Lena Valavani, Assistant Professor of Aeronautics and Astronautics

ACKNOWLEDGEMENTS

I would like to thank my thesis supervisors, Professors Michael Athans and Lena Valavani, for their support in shaping the ideas of this thesis and for their never-ending patience in its completeness.

I would also like to thank the Charles Stark Draper Laboratory for the use of their facilities over the last three years, including the computer resources and use of modem upon which this thesis strongly depended.

Additionally, I sincerely thank Mr. William Bonnice of Draper, for his technical and programming support for the submarine model.

This research was conducted at the MIT Laboratory for Information and Decision Systems with partial support provided by the Office of Naval Research under contract ONR/N00014-82-K-0582(NR606-003).

TABLE OF CONTENTS

LIST OF FIGURES 7

LIST OF TABLES 8

Chapter 1 INTRODUCTION AND SUMMARY 9

1.1 Background 9
1.2 Prior Work 10
1.3 Contributions of the Thesis 11
1.4 Outline of the Thesis 11

Chapter 2 THE SUBMARINE MODEL 13

2.1 Introduction 13
2.2 Model Development 14
2.2.1 Ship Coordinates 15
2.2.2 Fixed Coordinates 15
2.2.3 Definitions of Submarine States and Control Variables 16
2.3 Model Implementation 19
2.4 Model Linearization 20
2.5 Output and Control Variable Selections 23
2.5.1 Constraints of the Methodology 23
2.5.2 Output Variable Selection 30
2.5.3 Control Variable Selection 31
2.6 Summary 32

Chapter 3 ANALYSIS OF THE LINEAR MODEL 33

3.1 Introduction 33
3.2 Reduction of the model 34
3.3 Scaling 35
3.4 Modal Analysis of the System 38
3.5 Controllability and Observability 43
3.6 Structure of the Poles, Zeroes, and Singular Values 46
3.7 Summary 49

Chapter 4 MULTIVARIABLE CONTROL SYSTEM DESIGN 52

4.1 Introduction 52
4.2 The LQG/LTR Design Methodology 52
4.3 Controller Specifications 60
4.4 Controller Design 62
4.4.1 Augmentation of the Model Dynamics 62
4.4.2 Kalman Filter Design 65
4.4.3 Application of LQG/LTR 68
4.5 The Closed Loop System 70
4.6 Summary of LQG/LTR Design Sequence for Model without Roll Control 73
4.7 Summary 76

Chapter 5 EVALUATION OF THE MODEL BASED COMPENSATOR....77

5.1 Introduction 77
5.2 Implementation of the Compensator 77
5.3 Testing of the Compensator Design 78
5.4 Comparison of the Linear and Nonlinear Simulations 79
5.5 Roll versus Non-roll Control Model 86
5.5.1 Mild Turning Maneuver 87
5.5.2 Moderate Turning Maneuver 93
5.5.3 Combined Maneuver 99
5.5.4 Hard Turning Maneuver 105
5.6 Summary 111

Chapter 6 SUMMARY, CONCLUSIONS, AND DIRECTIONS FOR FUTURE RESEARCH 112

6.1 Summary 112
6.2 Conclusions 113
6.3 Directions for Future Research 115

References 116

Appendix A DETAILED DEFINITION OF THE SUBMARINE PROBLEM 118

Appendix B SUMMARY OF THE SUBMODEL PROGRAM 122

Appendix C STATE SPACE MATRICES FOR THE LINEARIZED MODELS 127

Appendix D MODAL ANALYSIS RESULTS 136

Appendix E GAIN MATRICES AND PROPERTIES OF THE CLOSED LOOP SYSTEM 141

LIST OF FIGURES

Figure 2.1 Sketch showing positive directions of axes, angles, velocities, forces, and moments 16

Figure 2.2 Comparison of Linear and Non-linear dynamics for Model S30R0 24

Figure 2.3 Comparison of Linear and Non-linear dynamics for Model S30R15 27

Figure 2.4 Submarine Control Surface Configurations 32

Figure 3.1 Block Diagram of Plant Transformed for Units, and Weightings of Inputs and Outputs 37

Figure 3.2 Modal Analysis for the Linearized Roll Control Model 41

Figure 3.3 Controllability Analysis for the Linearized Roll Control Model 45

Figure 3.4 Singular Value Plot of the Scaled Linear Model 47

Figure 3.5 Singular Value Decomposition for the Scaled Linear Model at DC 50

Figure 4.1 Block Diagram of a MIMO Compensated Plant 53

Figure 4.2 Plot of Desired Singular Value Shapes 55

Figure 4.3 Model Based Compensator in a feedback configuration 59

Figure 4.4 Integrators placed in the control channel of plant 63

Figure 4.5 Comparison of Open Loop Singular Values with and without augmenting dynamics 64

Figure 4.6 Singular Values of G_{FOL} 67

Figure 4.7 Summary of LQG/LTR Design Sequence 69

Figure 4.8 Singular Values of the Closed Loop 71

LIST OF FIGURES (continued)

Figure 4.9 Compensator Singular Values 72

Figure 4.10 Singular Values for the Transfer Function broken at the Plant Input 73

Figure 4.11 Summary of LQG/LTR Design Sequence for Model without Roll Control 74

Figure 4.12 Block Diagram of the Closed Loop System 76

Figure 5.1 Modifications of the MBC Feedback Design for Weightings on Inputs and Outputs 78

Figure 5.2 Comparison of the Linear and Non-linear Response of the Roll Control Model for a commanded 1.5° pitch angle 81

Figure 5.3 Comparison of the Non-linear Response of Models with and without Roll Control for a Mild Turn 89

Figure 5.4 Comparison of the Non-linear Response of Models with and without Roll Control for a Moderate Turn 95

Figure 5.5 Comparison of the Non-linear Response of Models with and without Roll Control for a Combined Maneuver ..101

Figure 5.6 Comparison of the Non-linear Response of Models with and without Roll Control for a Hard Turn 107

LIST OF TABLES

Table 2.1 Definition of Submarine States and Control Variables 18

Table 3.1 Input to Ouptut Coupling 48

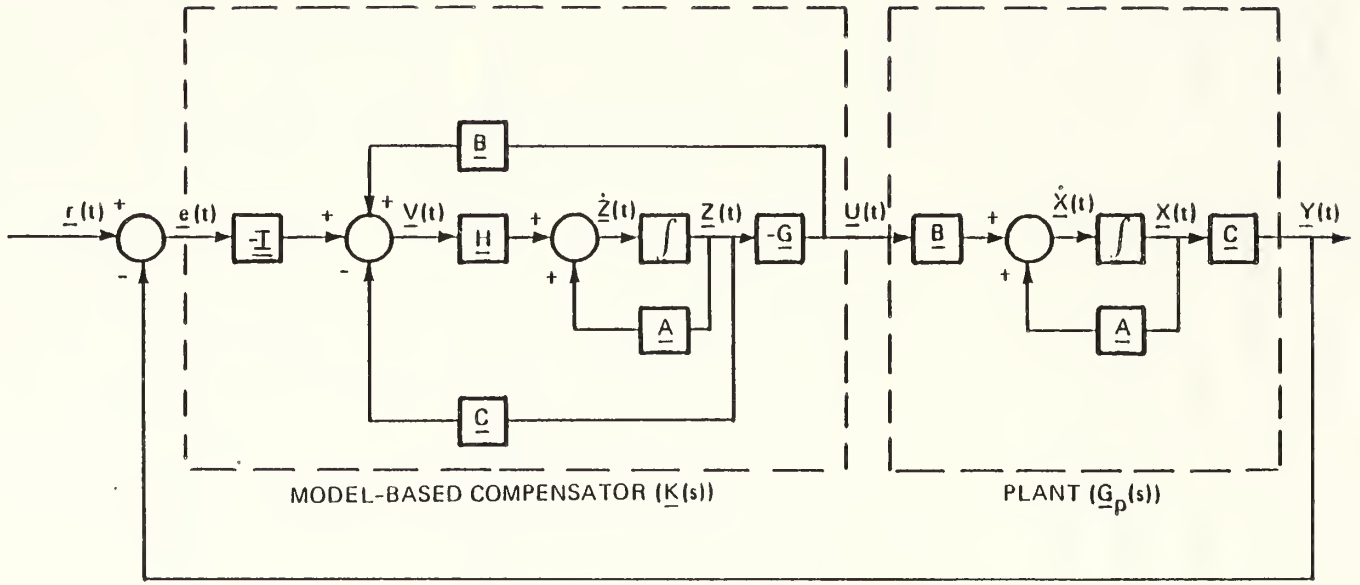


Figure 4.3 Model-Based Compensator in a feedback configuration.

Providing the plant is minimum phase [2], the singular values of $\underline{G}(s)\underline{K}_{MBC}(s)$ converge to the singular values of $\underline{G}_{KF}(s)$ as the design parameter $q \rightarrow \infty$. Above crossover frequencies, additional rolloff is produced by the recovery phase, which further enhances the high frequency robustness characteristics. As a result, the loop shape of $\underline{G}_{KF}(s)$ is recovered, and the resulting controller will have the desired performance characteristics.

4.3 Controller Specifications

Performance specifications outlined in this thesis are not all encompassing and do not necessarily reflect established Navy specifications for submarine control systems. The performance requirements are mainly driven by the intuitive engineering approach to obtain good command following, good system response, robustness, and disturbance rejection. These performance requirements will be met through loop shaping techniques.

Two performance requirements are imposed on the controller design. First, the steady state error to step commands and step disturbances is to be zero. Second, the maximum crossover frequency is limited by the ability of the submarine to respond and by the rate at which the compensator deflects the control surfaces.

The zero steady state requirement is met by placing integrators in each of the four input channels. Since the error signal appears at the input to the plant, this is

where the integrators will be placed. In this manner, the integrators will then become part of the compensator which is before the plant in the feedback loop. Note that the use of integral control in the input channels will not prevent the specification for maximum crossover frequency from being met.

The maximum crossover frequency of the compensator determines the rapidity of the control surface deflections based on the error signals which are generated by the difference between the reference commands and the measured outputs. Various models were analyzed during this research to determine the effects of the maximum crossover frequency. As the maximum crossover frequency was varied from 0.1 rad/sec to 1.0 rad/sec, two major observations were made. The first observation was that for high crossover frequencies the dynamic response of the submarine reacted more quickly and improved. The second observation was that the control surface deflections occurred more rapidly, which contributed to the improved dynamic response of the submarine. Since actuator dynamics are not directly modelled in this thesis, the maximum crossover frequency was selected based on control surface deflections which approximate actuator dynamics as listed in section 3.3.

Although not explicitly stated as a performance specification, from the performance aspect, it is desirable to have all singular values cross over at about the same frequency. Also, on the high frequency side, the controller

must be capable of rejecting noise and be robust to high frequency modelling errors. Noise sources generally originate from the environment, or from the sensor itself. Sensor noise typically occurs at a higher frequency than the system bandwidth and should not affect the dynamics of the ship since ship eigenvalues will typically lie in the lower frequency band.

4.4 Controller Design

4.4.1 Augmentation of the Model Dynamics

Augmenting the dynamics of the submarine control system normally serves a dual purpose. One is to model the actuator dynamics to make the model as accurate as possible and to achieve desirable rolloff at crossover for robustness. The other is to include integrators to cause the compensator to permit the submarine to achieve zero steady state error to step inputs and disturbances (i.e., good command following). The actuator dynamics are above the maximum expected crossover frequency, and thus are neglected [11,12,13]. This is perfectly valid as long as the rolloff above crossover is fast enough and satisfies the robustness criteria.

A block diagram of the augmented model appears in Figure 4.4. It is seen that the integrators are placed in the control channels. The mathematics of the augmented states will be manipulated in such a way as to provide a means to achieve the desired loop shapes of $\underline{G}_{FOL}(s)$.

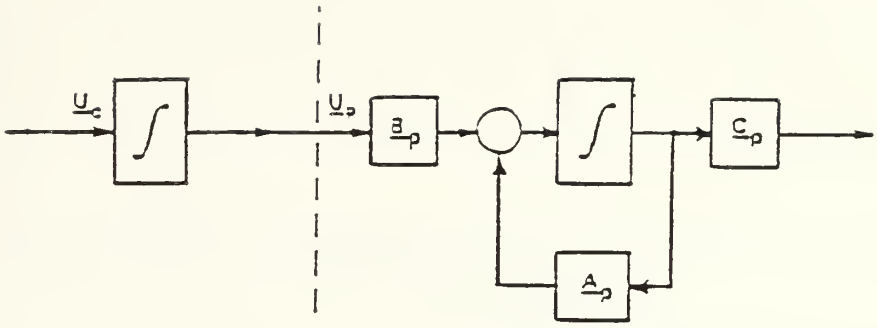
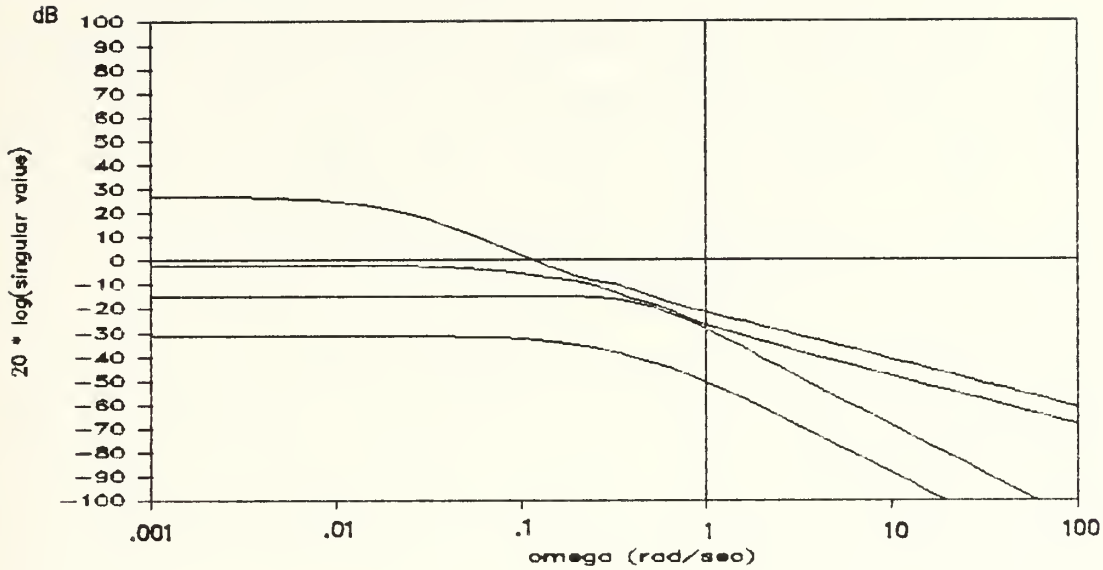


Figure 4.4 Integrators placed in the control channel of plant.

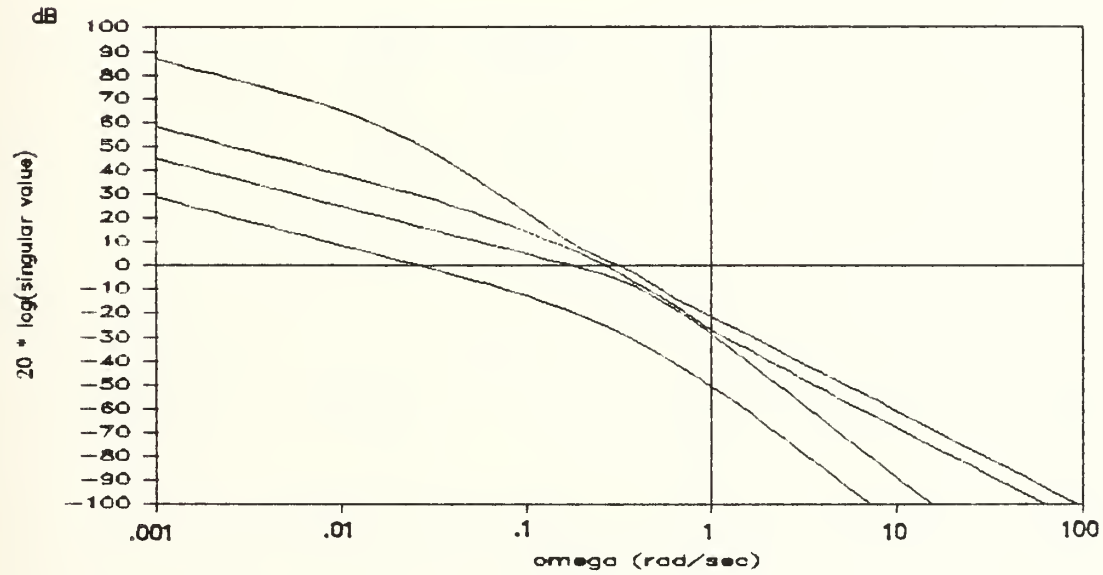
We define the augmentation dynamics by $\underline{G}_a(s)$, whose state space description is

$$\dot{\underline{u}}_p(t) = \underline{u}_c(t) \quad ; \quad \underline{G}_a(s) = \underline{I}/s$$

where each matrix is [4 x 4]. The augmenting dynamics are introduced to the 8th order system using state space multiplication, producing a 12th order system. Note that the physical input to the plant is labelled $\underline{u}_p(s)$ to distinguish it from the output of the compensator $\underline{u}_c(s)$. Although the augmentation dynamics $\underline{G}_a(s)$ will eventually be lumped with the compensator, they are kept separate until the LQG/LTR procedure is complete. Figure 4.5 shows a comparison of the unaugmented and augmented model. As shown, the integrators at the input produce a high dc gain increase at 0.001 rad/sec.



(a) Unaugmented Plant



(b) Plant augmented with integral control

Figure 4.5 Comparison of Open Loop Singular Values with and without augmenting dynamics

4.4.2 Kalman Filter Loop Design

In section 4.2, it was stated that at high and low frequencies the singular values of the Kalman filter transfer function matrix are approximated by the singular values of $(1/\sqrt{\mu})\underline{G}_{FOL}(s)$. For each choice of $\underline{L}$, $\underline{G}_{FOL}(s)$ is easily calculated using available software.

To meet the loop shaping requirements displayed in Figure 4.2, the maximum and minimum singular values of $\underline{G}_{KF}(s)$ should be identical at high and low frequencies, and as close as possible at crossover. The choice of the design parameter $\underline{L}$ will thus be based on this philosophy.

Recall from section 4.2 that $\underline{G}(s) = \underline{G}_p(s)\underline{G}_a(s)$, and define $\underline{G}(s) = \underline{C}[s\underline{I} - \underline{A}]^{-1}\underline{B}$, where

$$\underline{A} = \begin{bmatrix} \underline{0} & \underline{0} \\ \underline{B}_p & \underline{A}_p \end{bmatrix} \qquad \underline{C} = [\underline{0} \quad \underline{C}_p],$$

and

$$s\underline{I}-\underline{A} = \begin{bmatrix} s\underline{I} & \underline{0} \\ -\underline{B}_p & s\underline{I}-\underline{A}_p \end{bmatrix}, \quad [s\underline{I}-\underline{A}]^{-1} = \begin{bmatrix} \underline{I}/s & \underline{0} \\ [s\underline{I}-\underline{A}_p]^{-1}\underline{B}_p/s & [s\underline{I}-\underline{A}_p]^{-1} \end{bmatrix}.$$

At low frequencies, $s\underline{I}-\underline{A}_p \approx -\underline{A}_p$ and $[s\underline{I}-\underline{A}_p]^{-1} \approx -\underline{A}_p^{-1}$. Since $\underline{A}_p$ has distinct and non-zero eigenvalues, $\underline{A}_p^{-1}$ exists. We now partition the $\underline{L}$ matrix into $\underline{L}_1$ and $\underline{L}_2$, where $\underline{L}_1$ will be selected for low frequency matching, and $\underline{L}_2$ will be selected for high frequency matching.

Forming $\underline{G}_{FOL}(s)$ for low frequencies,

$$\underline{G}_{FOL}(s) = \underline{C}[s\underline{I}-\underline{A}]^{-1}\underline{L}$$

$$\underline{G}_{FOL}(s) \approx [\underline{0} \quad \underline{C}_p] \begin{bmatrix} \underline{I}/s & \underline{0} \\ -\underline{A}_p^{-1}\underline{B}_p/s & -\underline{A}_p^{-1} \end{bmatrix} \begin{bmatrix} \underline{L}_1 \\ \underline{L}_2 \end{bmatrix}$$

$$\approx - \underline{C}_p\underline{A}_p^{-1}\underline{B}_p\underline{L}_1/s - \underline{C}_p\underline{A}_p^{-1}\underline{L}_2. \qquad (4.14)$$

It is now seen that the singular values can be matched at low frequencies if we select the matrix $\underline{L}_1$ as follows:

$$\underline{L}_1 = -[\underline{C}_p\underline{A}_p^{-1}\underline{B}_p]^{-1}. \qquad (4.15)$$

At high frequencies, $s\underline{I}-\underline{A}_p \approx s\underline{I}$, and $[s\underline{I}-\underline{A}_p]^{-1} \approx \underline{I}/s$. Forming $\underline{G}_{FOL}(s)$ for high frequencies,

$$\underline{G}_{FOL}(s) = [\underline{0} \quad \underline{C}_p] \begin{bmatrix} \underline{I}/s & \underline{0} \\ \underline{B}_p/s^2 & \underline{I}/s \end{bmatrix} \begin{bmatrix} \underline{L}_1 \\ \underline{L}_2 \end{bmatrix}$$

$$\approx \underline{C}_p\underline{B}_p\underline{L}_1/s^2 + \underline{C}_p\underline{L}_2/s.$$

The singular values can now be matched at high frequencies if we select $\underline{L}_2$ as follows:

$$\underline{L}_2 = \underline{C}_p'(\underline{C}_p\underline{C}_p')^{-1}, \qquad (4.16)$$

since as $s \to \infty$, $1/s > 1/s^2$, and the second term dominates the maximum singular values.

The above method for constructing the $\underline{L}$ matrix provides the designer with a guarantee of identical behavior of the Kalman filter loop singular values at both high and low

frequencies. However, this method does not provide an opportunity to directly control the shape of the singular values at crossover.

Once the $\underline{L}$ matrix is determined, the parameter μ is used to move the singular value plots up or down to obtain the desired crossover frequency. Then we can solve the FARE and calculate $\underline{G}_{KF}(s)$. The final value of μ used for the model during the Kalman filter design process is 4. The Kalman filter gain matrices are included in Appendix E.

Figure 4.6 is a plot of the singular values of the Kalman filter transfer matrix $\underline{G}_{FOL}(s)$ for the $\underline{L}$ matrix as defined in equations 4.15 and 4.16, and for $\mu = 4.0$. Although the singular values match at high and low frequencies, some differences exist at crossover.

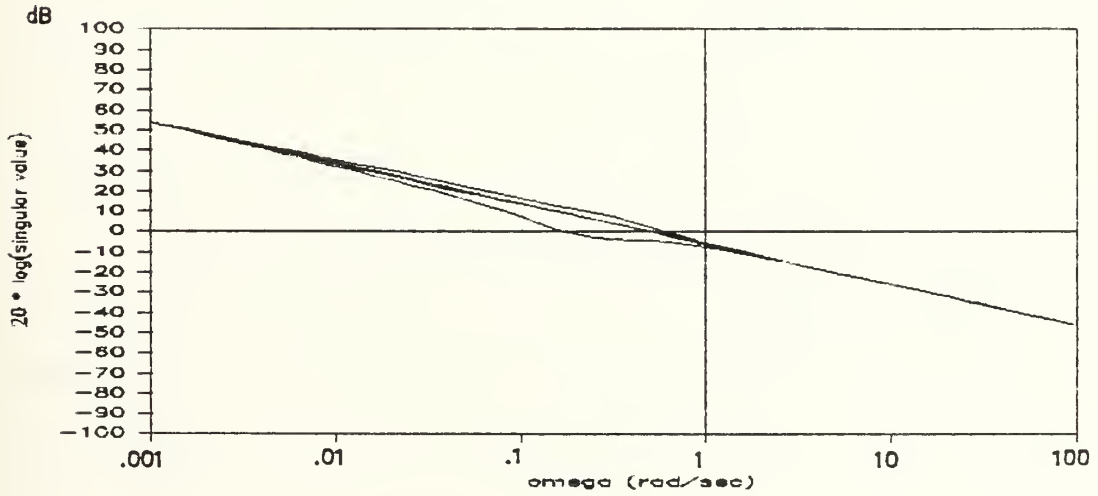


Figure 4.6 Singular Values of $\underline{G}_{FOL}(s)$

If the dynamic response of the model is not satisfactory, it is necessary to investigate the elements of the transfer function matrix $\underline{G}_{FOL}(s)$ in an attempt to control the separation of the singular values at crossover. The purpose is to achieve a scaling matrix for $\underline{C}_p$ which will result in a tight crossover pattern of the singular values.

4.4.3 Application of LQG/LTR

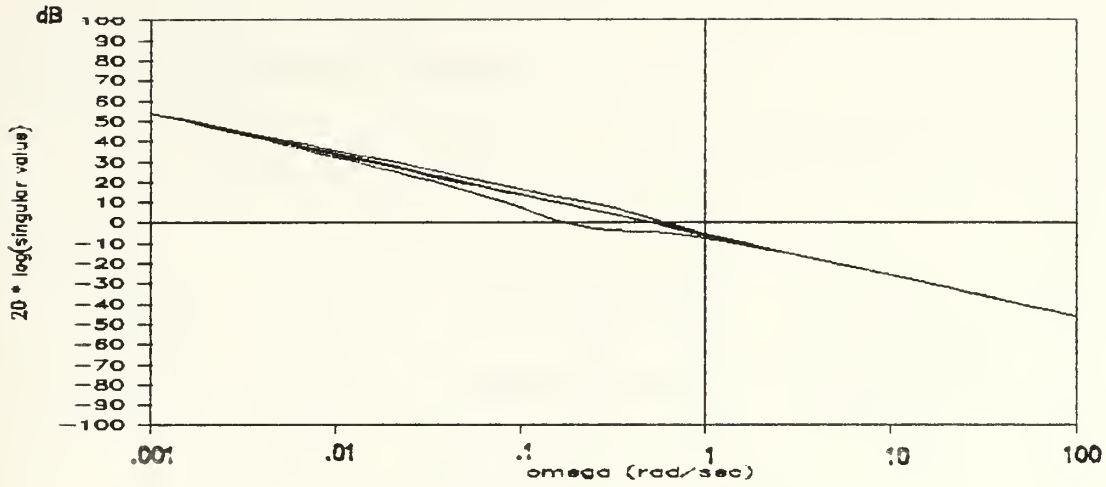
As stated in the overview of the LQG/LTR design procedure, once the Kalman filter design is complete, the remainder of the design process is quite straightforward.

It is now necessary to choose the design parameter q, and solve the CARE to obtain the $\underline{K}$ matrix. Then, we determine the Control gain matrix

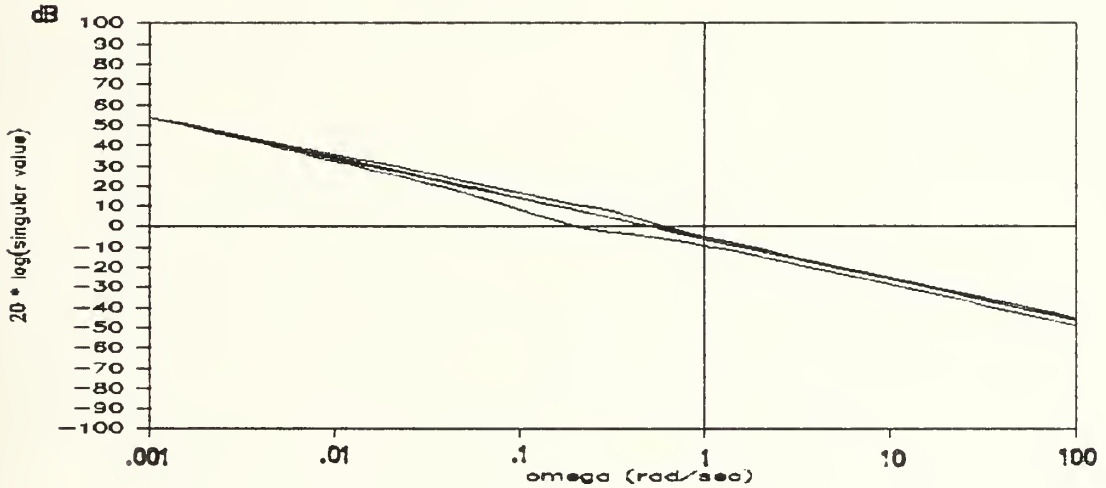
$$\underline{G} = \underline{B}'\underline{K}.$$

Recall that for this recovery method to work well, the submarine model must not have low frequency transmission zeros. A value of $q = 1000$ was used for the model, producing the Control gain matrices in Appendix E1.

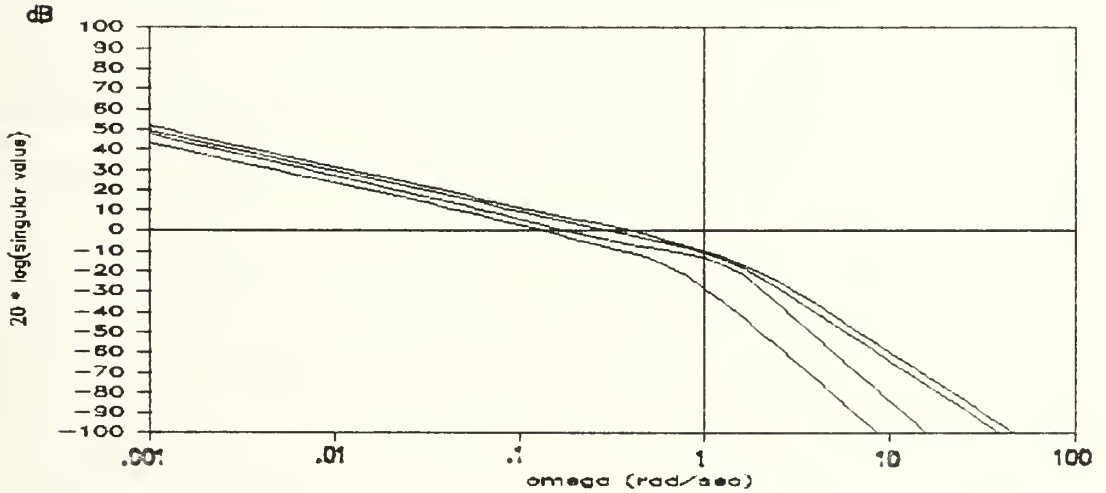
The entire design sequence is summarized in Figure 4.7, which are the singular value plots of $\underline{G}_{FOL}(s)$, $\underline{G}_{KF}(s)$, and $\underline{G}(s)\underline{K}(s)$. The minimum and maximum crossover frequencies are 0.2 rad/sec and 0.5 rad/sec, respectively.



(a) Kalman Filter Open Loop, $\underline{G}_{FOL}$



(b) Kalman Filter Loop, $\underline{G}_{KF}$



(c) Recovered Open Loop Transfer Function, $\underline{G}(s)\underline{K}(s)$ with q = 1000

Figure 4.7 Summary of the LQG/LTR Design Sequence

4.5 The Closed Loop System

The closed loop system can be written in state space form as

$$\begin{bmatrix} \dot{\underline{x}}(t) \\ \dot{\underline{z}}(t) \end{bmatrix} = \begin{bmatrix} \underline{A} & -\underline{B}\underline{G} \\ \underline{H}\underline{C} & \underline{A}-\underline{B}\underline{G}-\underline{H}\underline{C} \end{bmatrix} \begin{bmatrix} \underline{x}(t) \\ \underline{z}(t) \end{bmatrix} + \begin{bmatrix} \underline{0} \\ -\underline{H}\underline{C} \end{bmatrix} \underline{r}(t)$$

$$\underline{y}(t) = \begin{bmatrix} \underline{C} & \underline{0} \end{bmatrix} \begin{bmatrix} \underline{x}(t) \\ \underline{z}(t) \end{bmatrix} ,$$

where:

$\underline{x}(t)$ = the state of the nominal design model, and

$\underline{z}(t)$ = the state of the compensator.

The poles and zeros for the closed loop system are contained in Appendix E1. Since all the poles are in the left half plane, the system is in fact stable.

Referring to the overall loop transfer function of the closed loop system (section 4.2), from command input to output, then the singular values of the closed loop plant should be approximately 0 dB from dc up to the crossover frequency, and then rolloff at frequencies above crossover. This is shown in Figure 4.8, which is a singular value plot of the closed loop system.

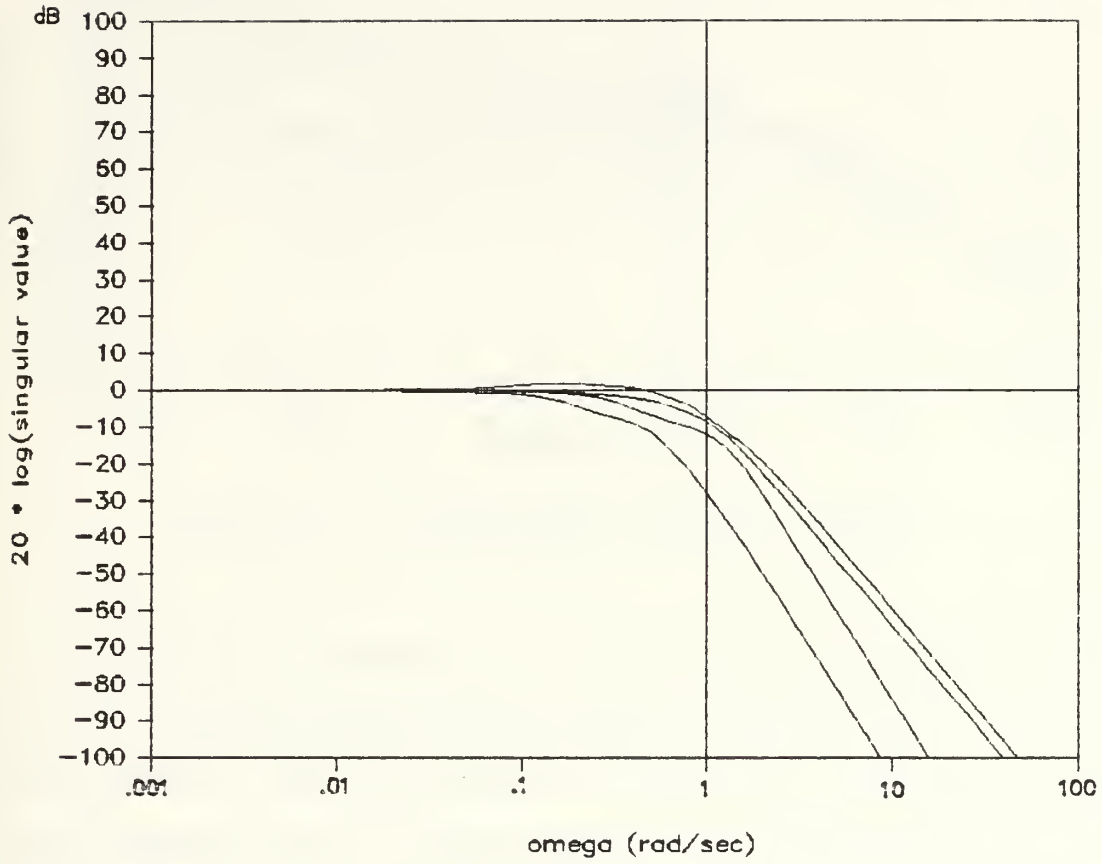


Figure 4.8 Singular Values of the Closed Loop

The singular values of the compensator are shown in Figure 4.9. Here we observe the lead-lag characteristics of the compensator over the frequency range of interest. Note the large amplifications at frequencies below crossover. The large spread in the singular values indicates certain directions are being amplified more than others.

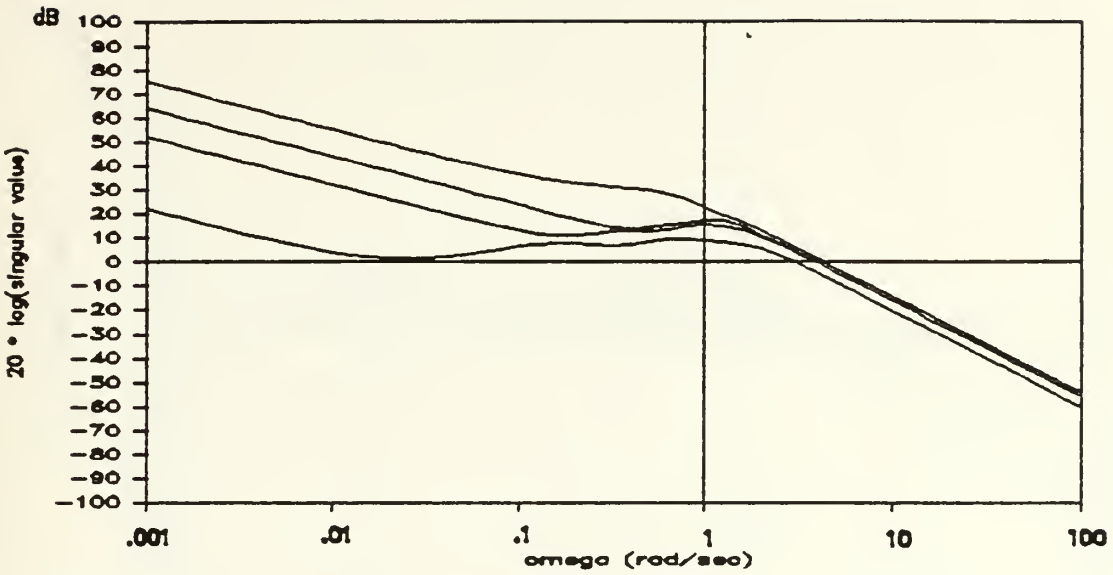


Figure 4.9 Compensator Singular Values

Figure 4.10 represents the singular values for the loop transfer function broken at the plant input instead of the plant output. Referring back to Figure 4.1, we see that the plots represent the net amplification from reference commands $\underline{r}(s)$ to the controls $\underline{u}_p(s)$, where

$$\underline{u}_p(s) = [\underline{I} + \underline{K}(s)\underline{G}(s)]^{-1}\underline{K}(s)\ \underline{r}(s) \ .$$

The figure shows that there are certain directions where amplification is required more than in others.

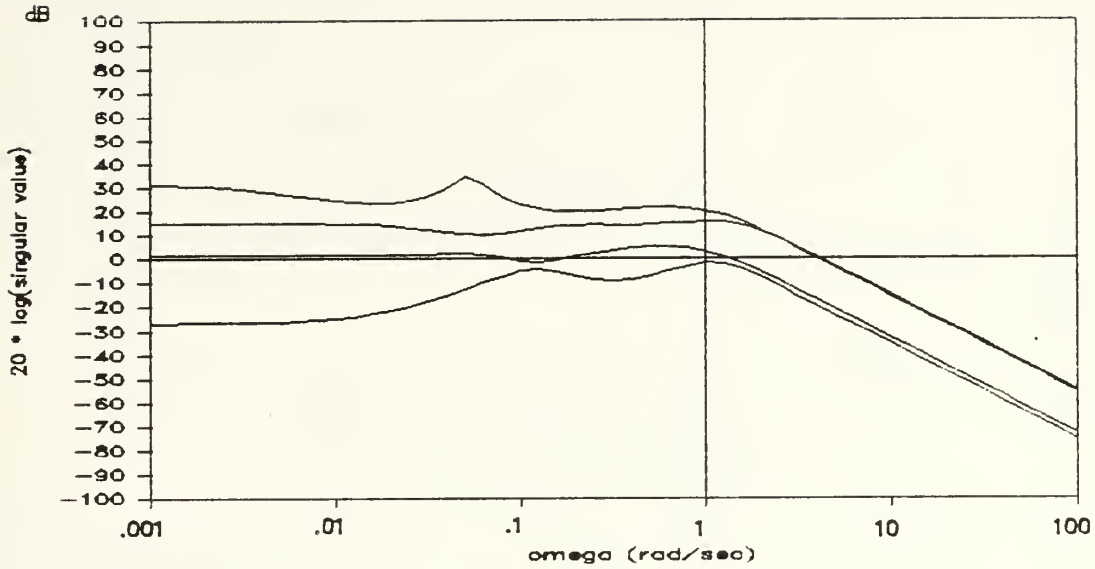
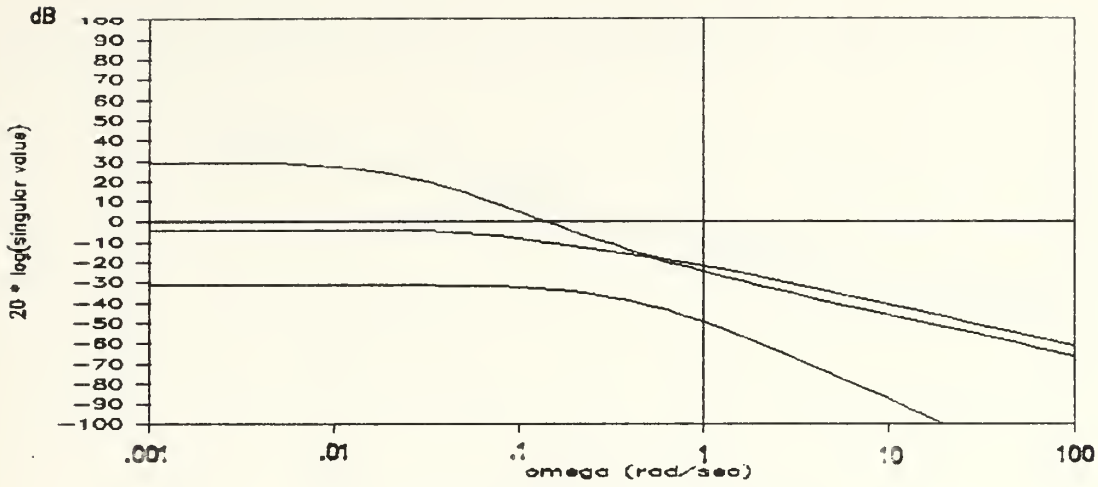


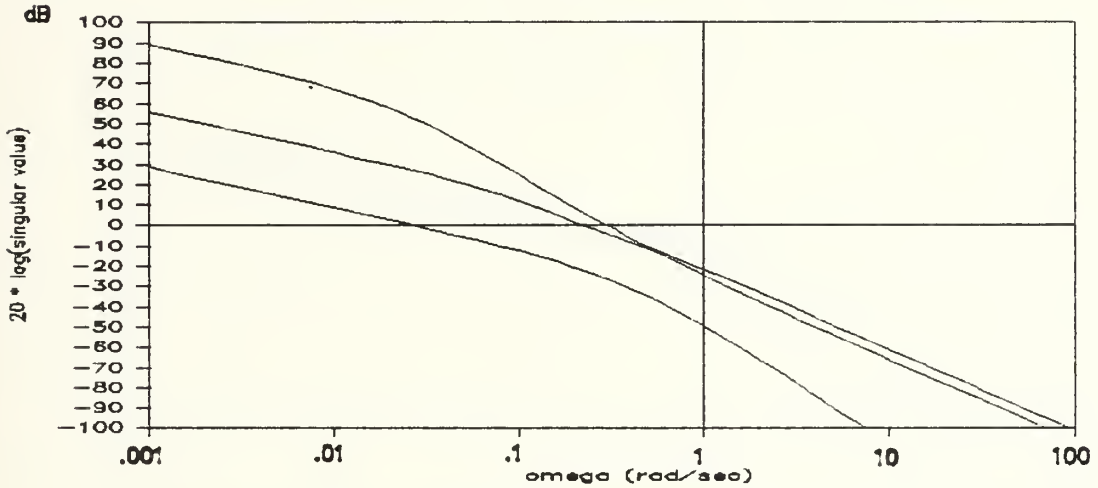
Figure 4.10 Singular Values for the Transfer Function broken at the Plant Input

4.6 Summary of LQG/LTR Design Sequence for Model without Roll Control

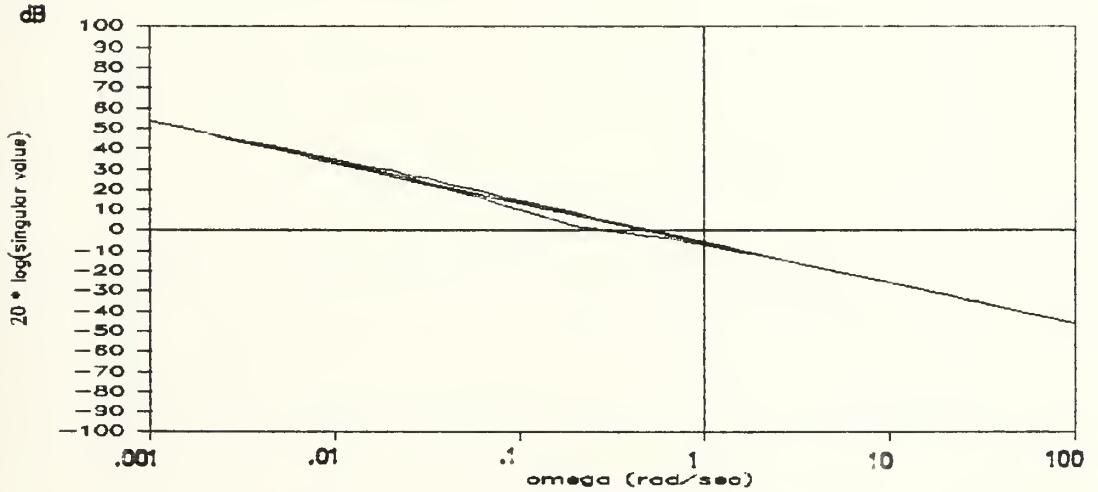
Figure 4.11 displays a summary of the LQG/LTR design sequence for a model which does not have active roll control. The entire design sequence is illustrated from the singular values of the original 3-input 3-output plant, through the loop transfer recovery process. For completeness, the singular value plot of the closed loop is also presented.



(a) Open Loop Plant

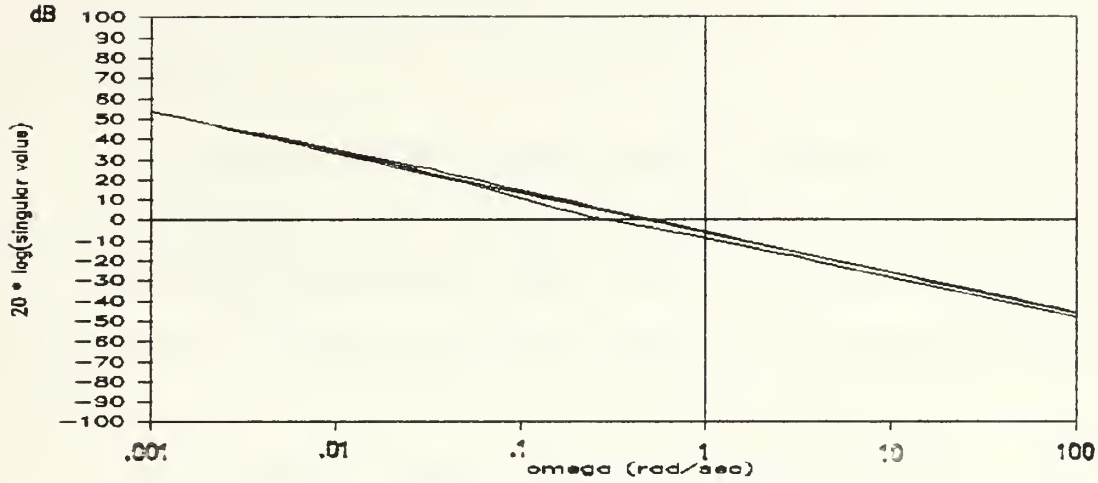


(b) Augmented Open Loop Plant

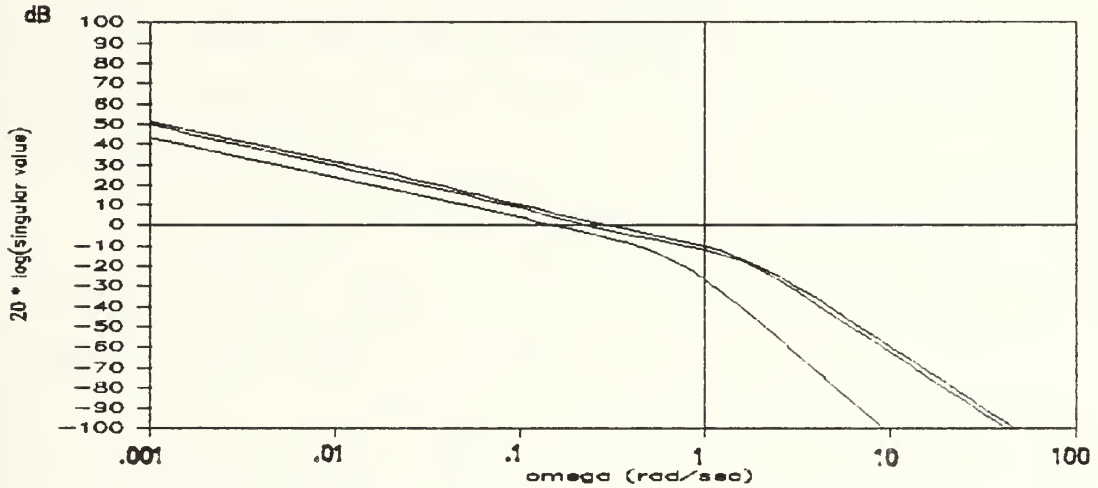


(c) Kalman Filter Open Loop, $\underline{G}_{FOL}$

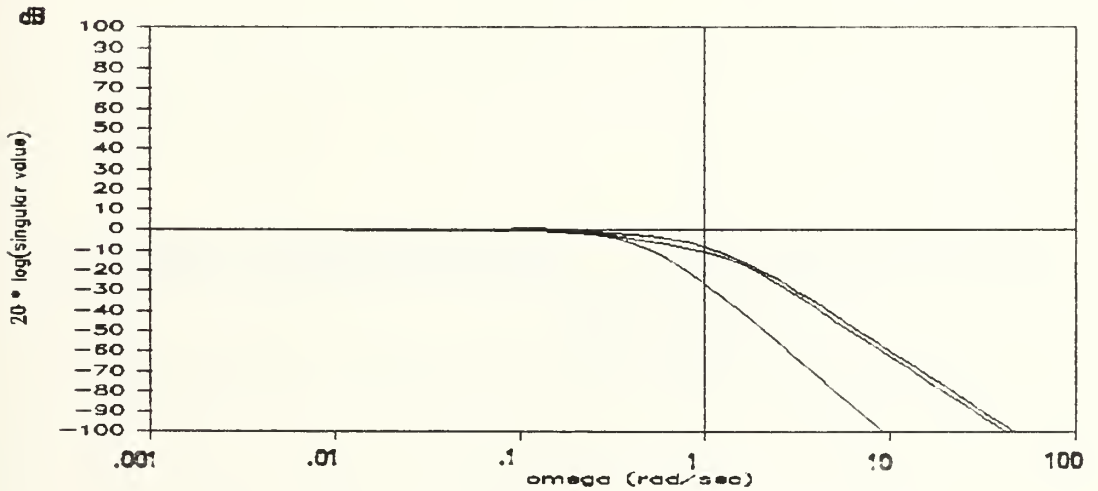
Figure 4.11 Summary of the LQG/LTR Design Sequence for Model without Roll Control



(d) Kalman Filter Loop, $\underline{G}_{KF}$



(e) Recovered Open Loop Transfer Function, $\underline{G}(s)\underline{K}(s)$



(f) Singular Values of the Closed Loop

Figure 4.11 Summary of the LQG/LTR Design Sequence for Model without Roll Control

4.7 Summary

This chapter demonstrated the application of the LQG/LTR control system design methodology. Specifications for the controller design were also presented, and then the methodology was applied to the design of a submarine control system.

Compensator designs were studied for various crossover frequencies, and then a compensator was selected which provided system response characteristics which were desirable, and which deflected the control surfaces in a reasonable manner.

Additionally, summary plots of the design sequence for a control system design without active roll control capability was also provided.

Figure 4.12 represents the final closed loop design on which Chapter Five is based.

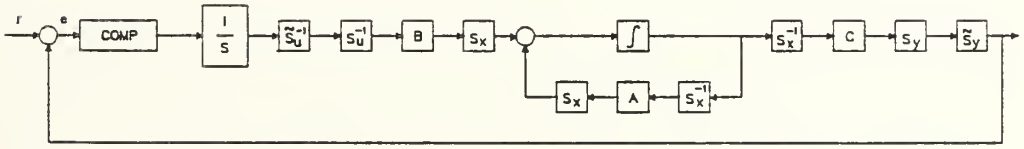


Figure 4.12 Block Diagram of the Closed Loop System

CHAPTER FIVE

EVALUATION OF THE MODEL BASED COMPENSATOR

5.1 Introduction

In this chapter, the performance of the controller design is evaluated. The controller is tested using both the linear and non-linear submarine simulations to determine how closely the performance specifications are met, and to test for instabilities in the design.

The 4-input, 4-output design is also compared to a 3-input, 3-output design that does not have the capability of active roll control. The comparisons provide a measure of performance improvements for the submarine when active roll control using the differential stern planes are employed.

5.2 Implementation of the Compensator

To implement the compensator on the computer facility at Draper, programming changes were necessary in two subroutines which are needed by the submarine simulation program. Subroutines OUTPTS and MBDCMP were modified to reflect scaling for consistent units from radians to degrees. Additionally, to maintain a properly scaled error vector to the compensator, it was necessary to apply appropriate scaling matrices to the $\underline{B}$ and $\underline{C}$ matrices of the MBC. These matrices reflect the weightings which were applied to the input and output vectors of the open loop model during the compensator designs of Chapter Four.

Once complete, the linear plant dynamics, upon which the compensator was designed, were replaced with the submarine simulation program to evaluate the performance of the compensator. This implies then, that the error vector, $\underline{e}(t)$, at the input to the Model Based Compensator is always the true difference between the commanded input and the output variables.

Figure 5.1 displays how the MBC feedback configuration for this design is modified by scaling. The block identified as COMP is now the MBC with the augmenting dynamics as discussed in the previous chapter. Describing the MBC with $\underline{A}$, $\underline{B}$, and $\underline{C}$ matrices (as shown in section 4.5) we now include the scaling matrices $\tilde{\underline{S}}_u^{-1}$ and $\tilde{\underline{S}}_y$ into the compensator, and define the resulting compensator as the compensator provided to the computer simulation at Draper.

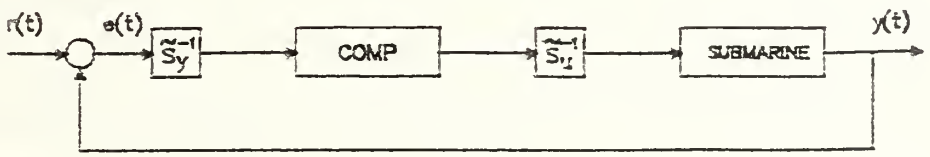


Figure 5.1 Modifications of the MBC Feedback Design for Weightings on Inputs and Outputs

5.3 Testing of the Compensator Design

The LQG/LTR compensator design was tested by providing the computer simulation at Draper with a data file

the computer simulation at Draper with a data file containing time sequenced command inputs and then integrating either the linear or non-linear equations of motion. Transient and steady state maneuvers were performed to validate the resulting designs. To provide comparisons for the various models, however, only the steady state maneuvers will be displayed in this thesis.

The evaluations of the Model Based Compensators are performed by first comparing the linear and non-linear simulations of the roll control model. The evaluations are completed by comparing a second MBC, designed without roll control capability, to the MBC designed with roll control capability.

5.4 Comparison of the Linear and Non-linear Simulations

Use of the LQG/LTR design methodology allows us to analyze the linear and non-linear applications of the design to ascertain whether the design is valid. Discounting effects due to non-linearities, the resulting linear simulation provides a prediction of initial derivatives, natural frequencies, and damping effects which can be expected in the non-linear simulation.

Figure 5.2 represents a comparison of the linear (LQG/LTR) and non-linear responses of the submarine simulation for a commanded 1.5° pitch angle. In the linear model, we observe that the forward velocity is essentially constant, while in the non-linear model we observe a

decrease of approximately 0.5 knots in the ship's forward velocity. Because the linear model neglects the non-linear dynamics of the submarine, we see a roll angle develop for the linear model which causes a heading change and depth excursion which is much more significant than in the non-linear response.

Comparing the control surface deflections, we see that the linear model requires slightly more deflection to obtain the desired response, which indicates that, in the linear case, the control surfaces are less effective. The fact that the linear model indicates less control surface authority explains the fact that the controller error signal does not disappear until much later than in the non-linear simulation.

For completeness, the outputs are also provided. Note that the outputs essentially exhibit the mirror image of the controller error, but additionally provide indication of the true output in the variable commanded for the maneuver, in this case, pitch angle θ.

The purpose of this comparison was to establish the validity of both the compensator design, and the computer software used for the simulations. This was particularly important because of the modifications made to the computer subroutines for scaling and selection of output variables. The simulations performed in the next section use only the non-linear computer models.

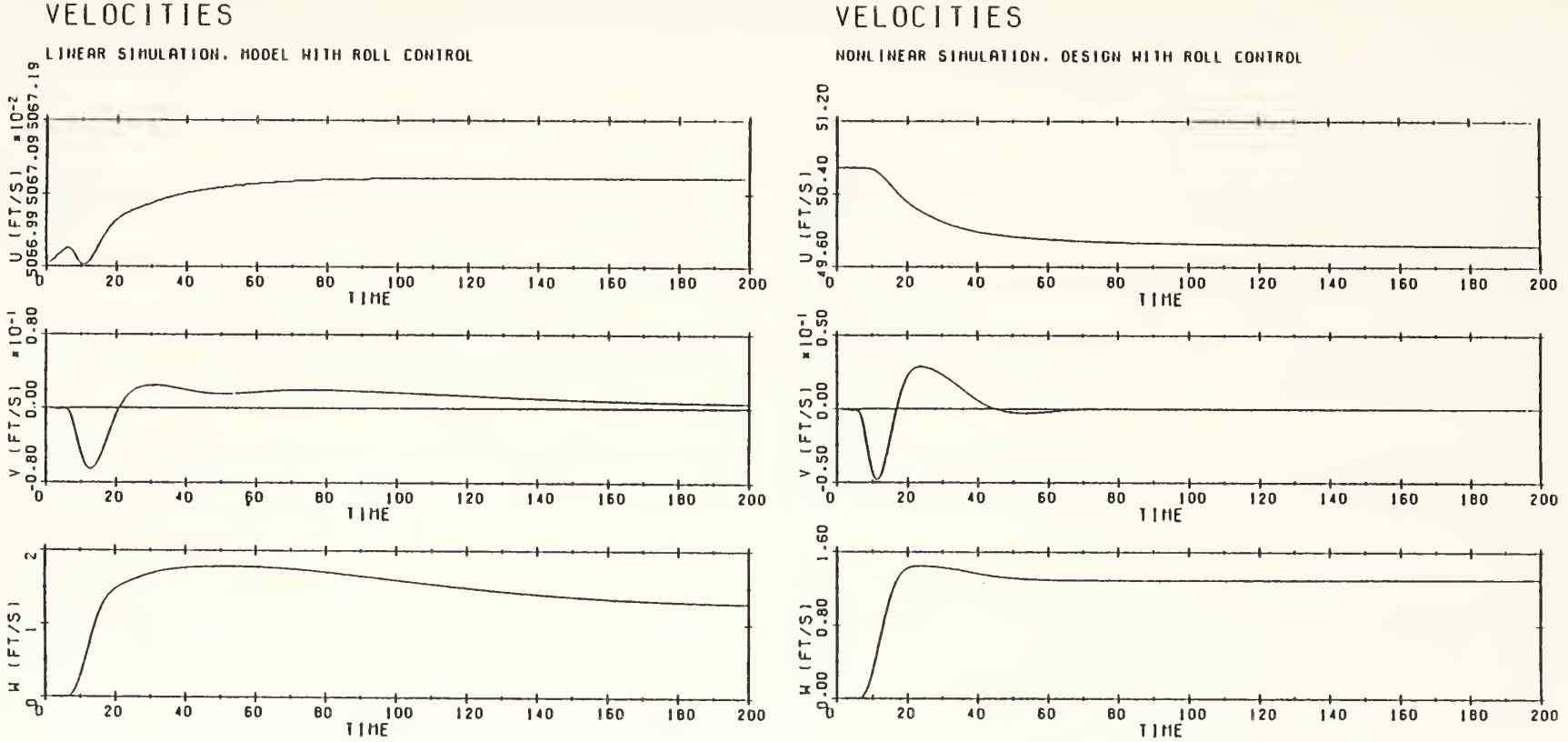


Figure 5.2(a) Comparison of the Linear and Non–linear Response of the Roll Control Model for a 1.5 degree pitch angle

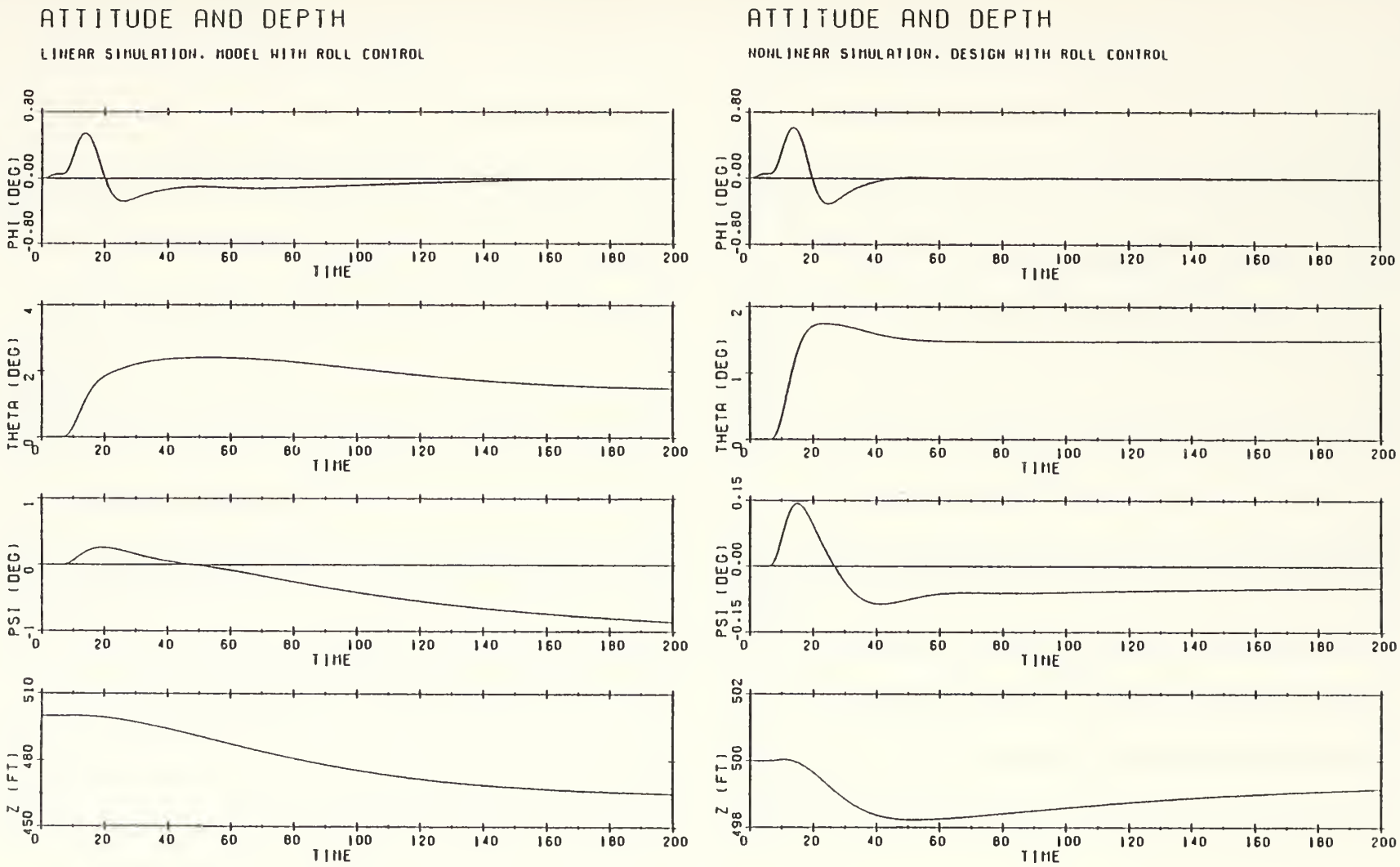


Figure 5.2(b) Comparison of the Linear and Non-linear Response of the Roll Control Model for a 1.5 degree pitch angle

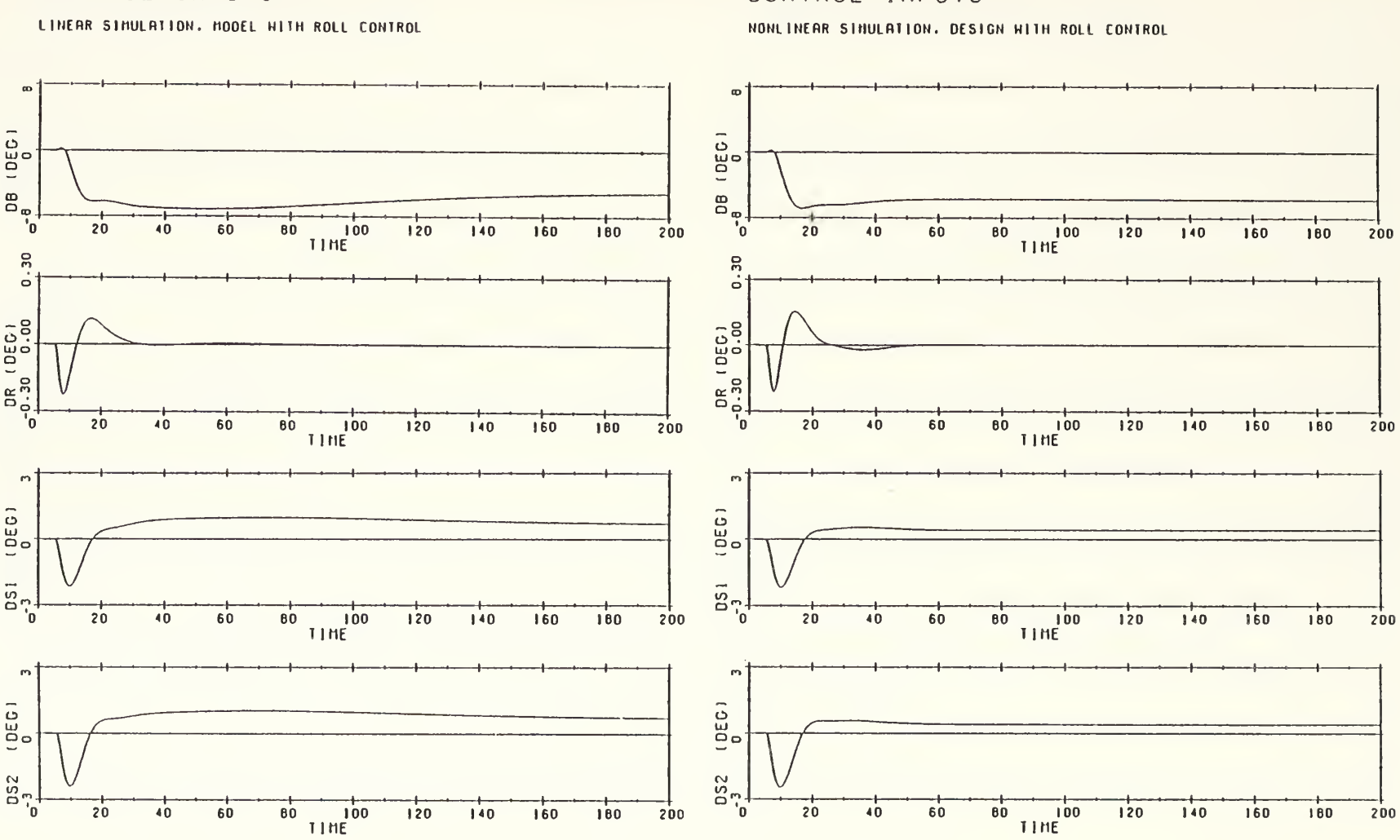


Figure 5.2(c) Comparison of the Linear and Non-linear Response of the Roll Control Model for a 1.5 degree pitch angle

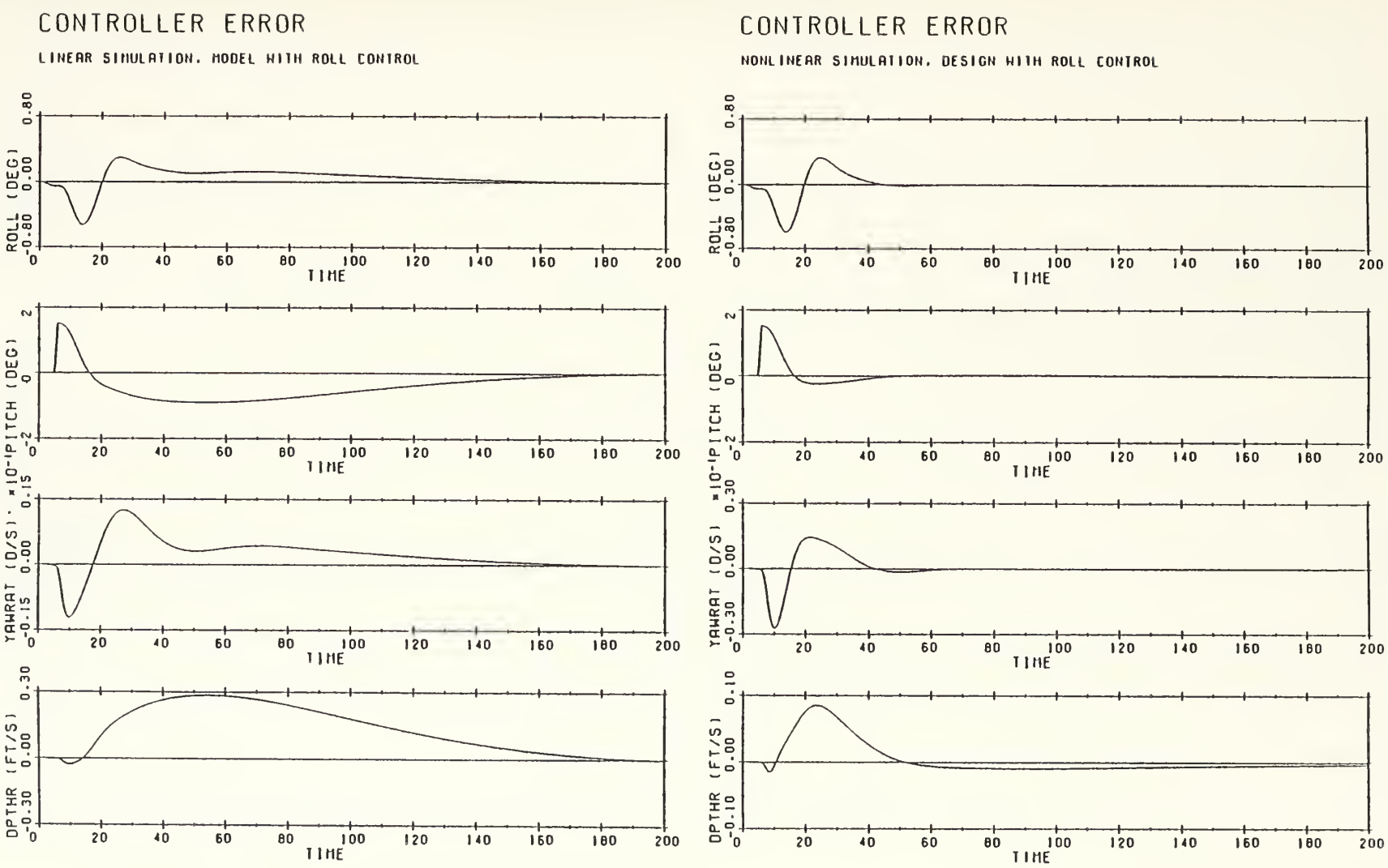


Figure 5.2(d) Comparison of the Linear and Non-linear Response of the Roll Control Model for a 1.5 degree pitch angle

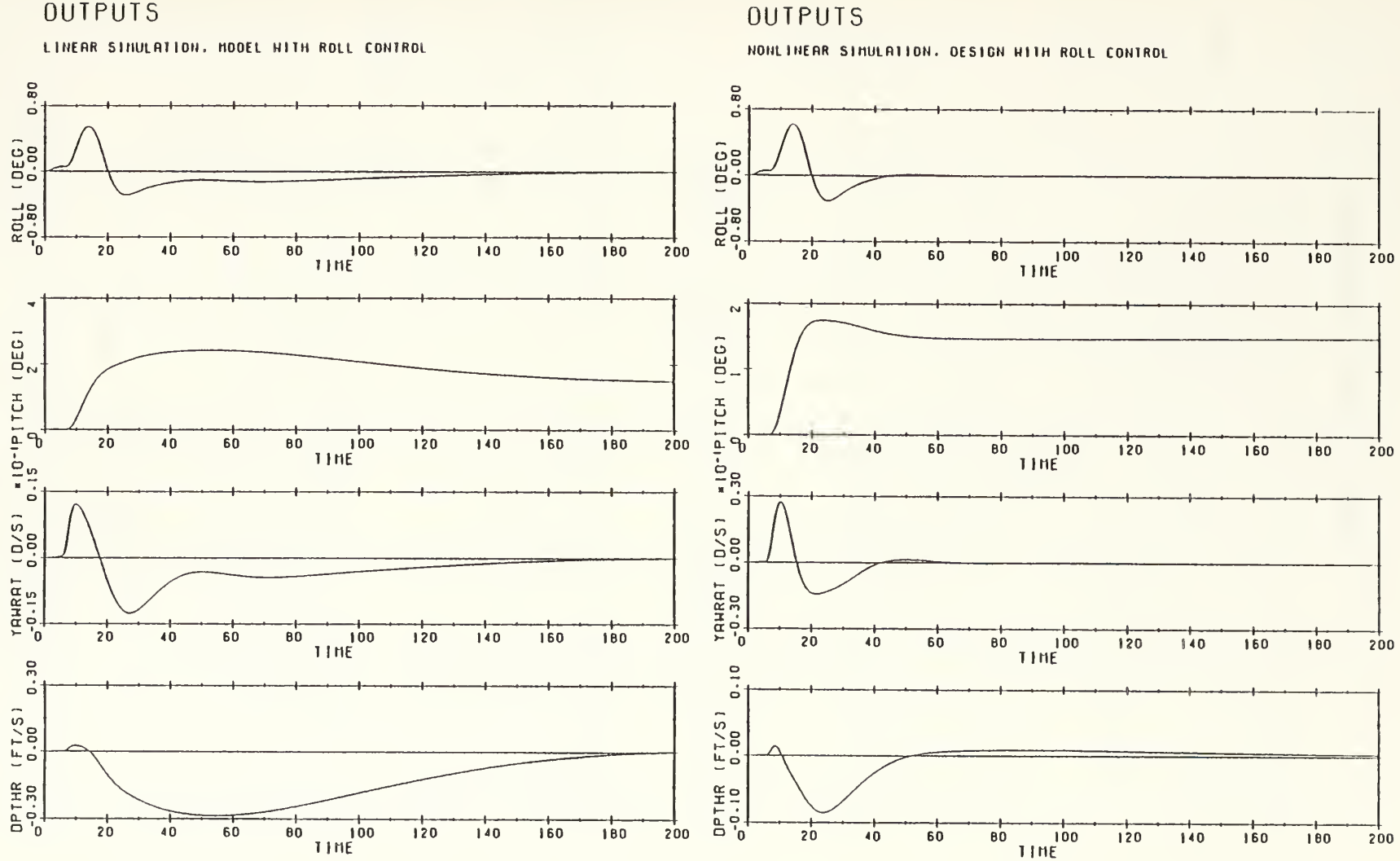


Figure 5.2(e) Comparison of the Linear and Non-linear Response of the Roll Control Model for a 1.5 degree pitch angle

5.5 Roll vs Non-roll Control Model

Having established the validity of the compensator design and the compensator software, it is now necessary to demonstrate the performance characteristics of the roll control model as compared to a comparably designed compensator without roll control capability.

Using the criteria presented in Chapter Four, a Model Based Compensator was designed which does not have roll control capability. The elimination of roll angle, Φ, as a state of the output vector resulted in an input vector $\underline{u}(t)$, where

$$\underline{u}(t) = \begin{bmatrix} \delta b \\ \delta r \\ \delta s \end{bmatrix} \quad \text{and} \quad \delta s = \delta s_1 + \delta s_2 \ .$$

Information regarding the state space descriptions of the model without roll control capability is provided in Appendix C4. Modal analysis results are provided in Appendix D2, and properties of the closed loop system are provided in Appendix E2.

To allow comparisons between the two models that provide useful information, the same design parameters were used for both models. The output vector for this model is $\underline{y}(t)$, where

$$\underline{y}(t) = [\ \underline{\theta}(t) \quad \dot{\underline{\psi}}(t) \quad \dot{\underline{z}}(t)\ ]^T \ .$$

Comparisons are made for four simulations. The first two simulations are for heading changes by commanding a step

input of 1 deg/second, and 2 deg/second, respectively. The intent of these two simulations is to display the submarine trajectory when a steady turning rate is commanded. A larger commanded heading rate should accelerate the nonlinear characteristics of the system. The third comparison is for a combined maneuver in which step commands of 1 degree of pitch, 0.5 feet/second of depth rate, and 1 degree/second of heading change are provided to the compensators. The fourth simulation is less detailed than the three preceding ones, however, the commanded turning rate is 3 degrees/second, and provides additional insight into the differences in the two compensators.

In all four simulations the commands are applied as step inputs at t = 5 seconds. Additionally, in the simulations for the design without roll control, the stern plane deflections δs_1 and δs_2 are shown separately to further illustrate the stern plane deflections in the design with roll control.

5.5.1 Mild Turning Maneuver

Figure 5.3 displays the results of commanding a mild turning maneuver of 1 deg/sec. For this turning rate, the ship experiences a decrease in forward velocity of 6%.

Looking first at the design with roll control, we observe that the submarine initially rolls outward, then snap rolls into the turn at t = 12 seconds. The maximum inward roll angle is 2° at t = 22 seconds. The ship has a

maximum downward pitch angle of -1°. The ship loses 8 feet in depth during the entire maneuver. It is observed the stern planes deflect differentially to compensate for the roll moment, with a steady state difference of 6°. Note the use of bow planes to minimize the depth rate. Once depth rate error has been eliminated, the bow planes return to their neutral position.

To obtain the commanded turning rate, the rudder initially deflects 5°. As the error in yaw rate decreases, the rudder steadies at slightly less than 2° deflection.

Looking now at the model without roll control, it is immediately observed that the ship experiences a snap roll of 10°, with roll angle steadying out at 8°. Due to the roll angle, and the effect of the rudder, the ship experiences a downward pitch angle of approximately 2°, which causes the ship to experience a depth loss of almost 65 feet. Because the roll angle is contributing to the depth rate, the bow planes are deflected 7°, with stern plane deflections of -1°. The combination of stern planes and bow planes are minimizing the depth excursion. Note, however, that since roll angle strongly influences pitch and depth rate, that these two terms are not being damped as readily as they were in the roll control model.

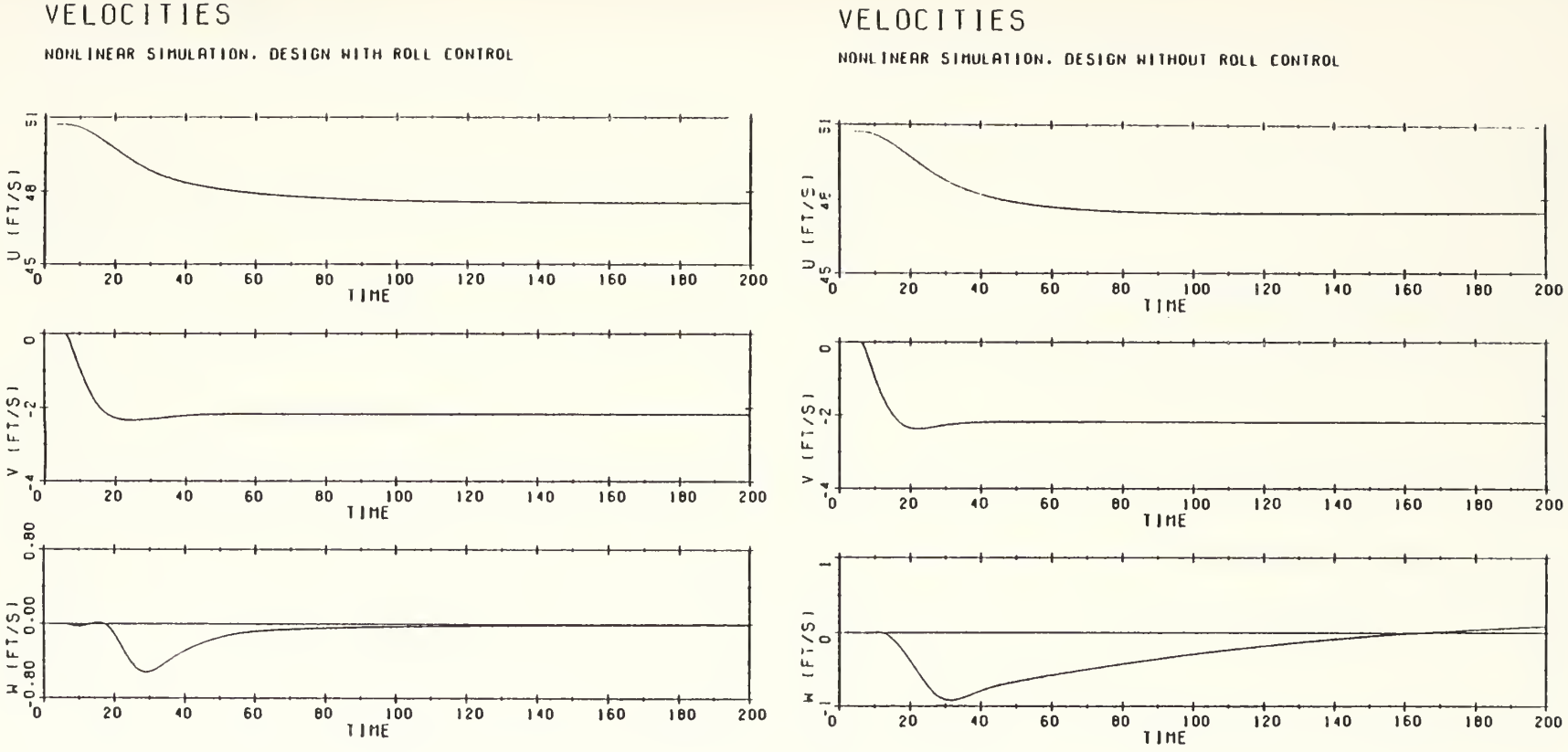


Figure 5.3(a) Comparison of the Non-linear Response of Models with and without Roll Control for a Mild Turn

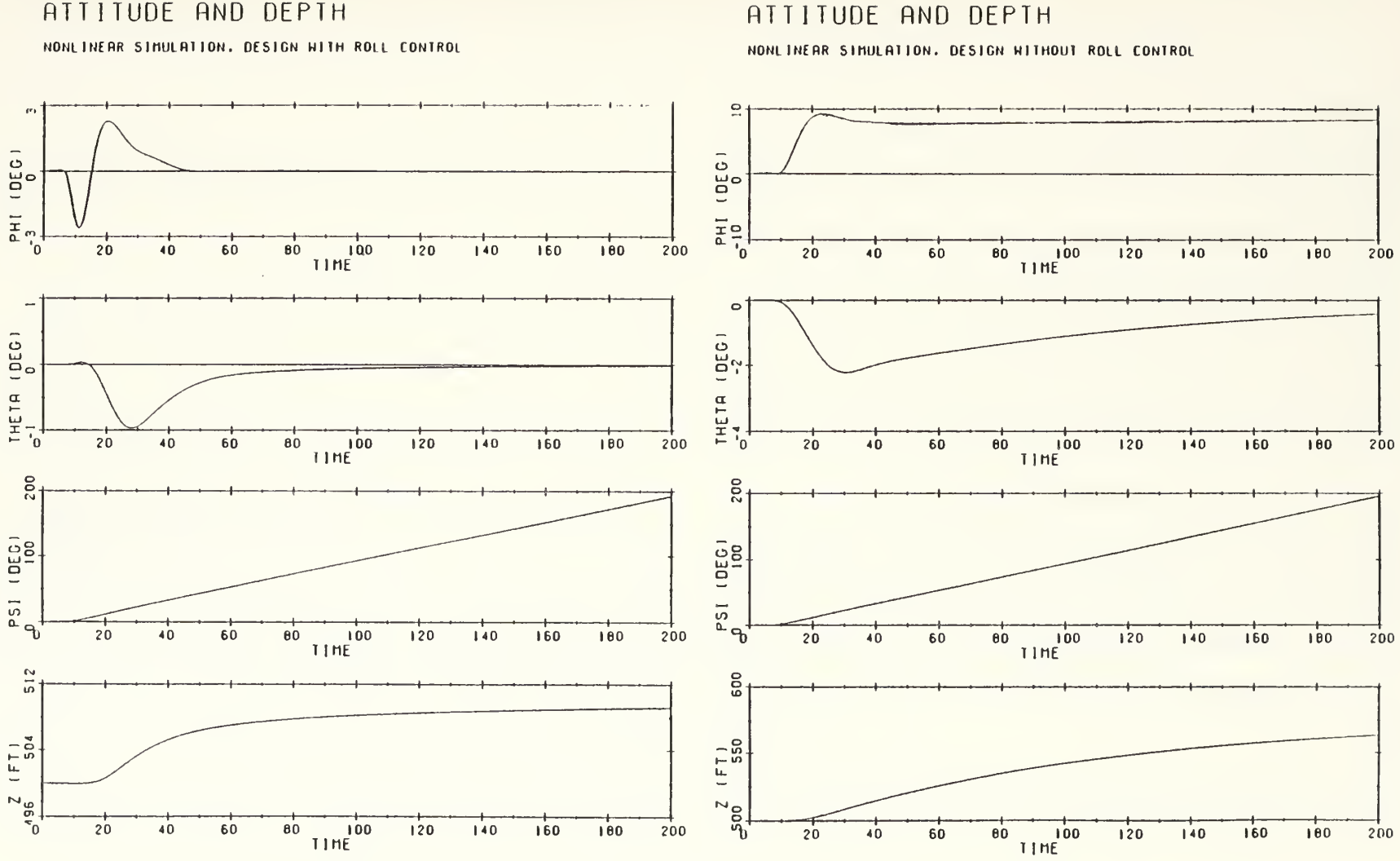


Figure 5.3(b) Comparison of the Non-linear Response of Models with and without Roll Control for a Mild Turn

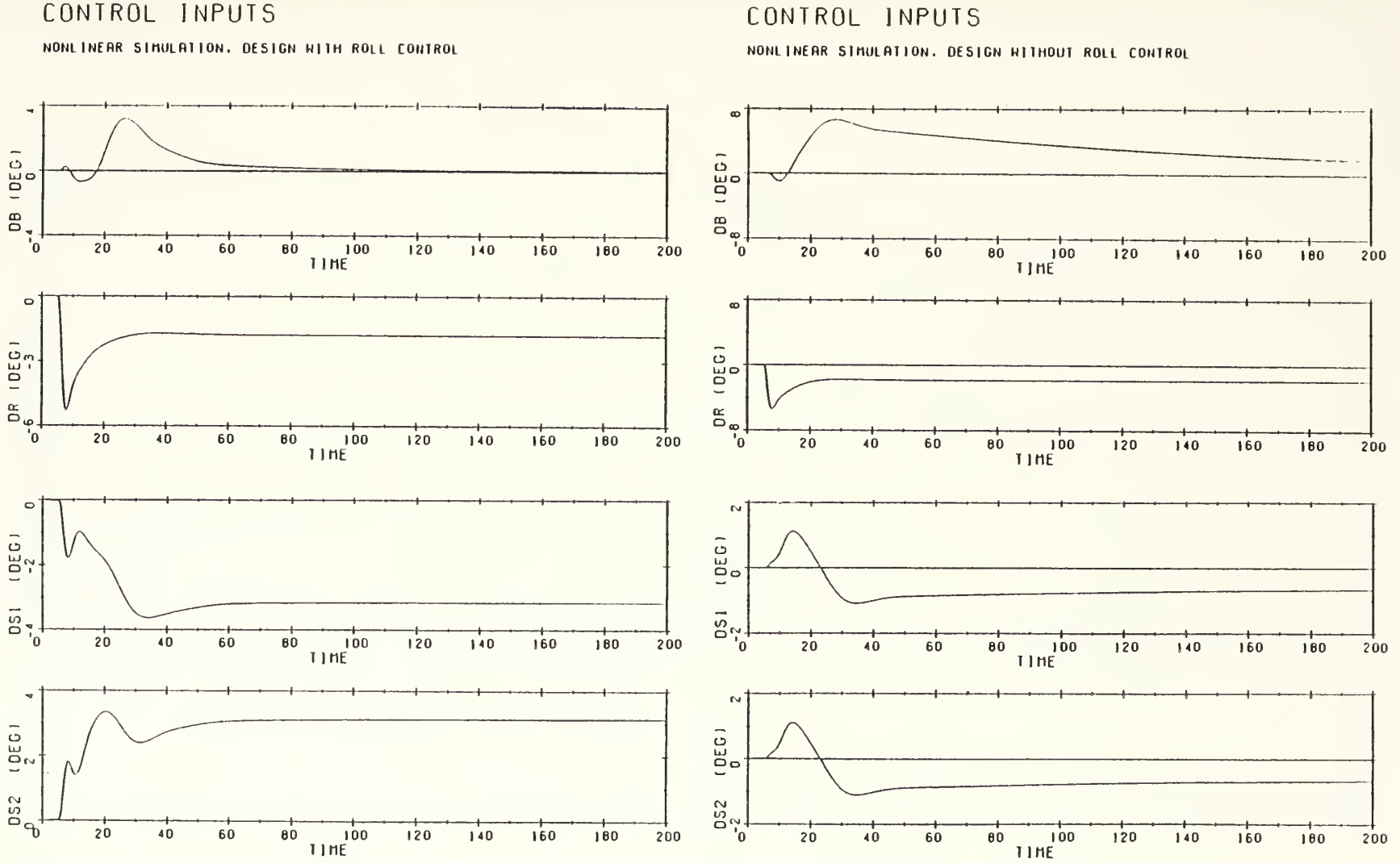


Figure 5.3(c) Comparison of the Non-linear Response of Models with and without Roll Control for a Mild Turn

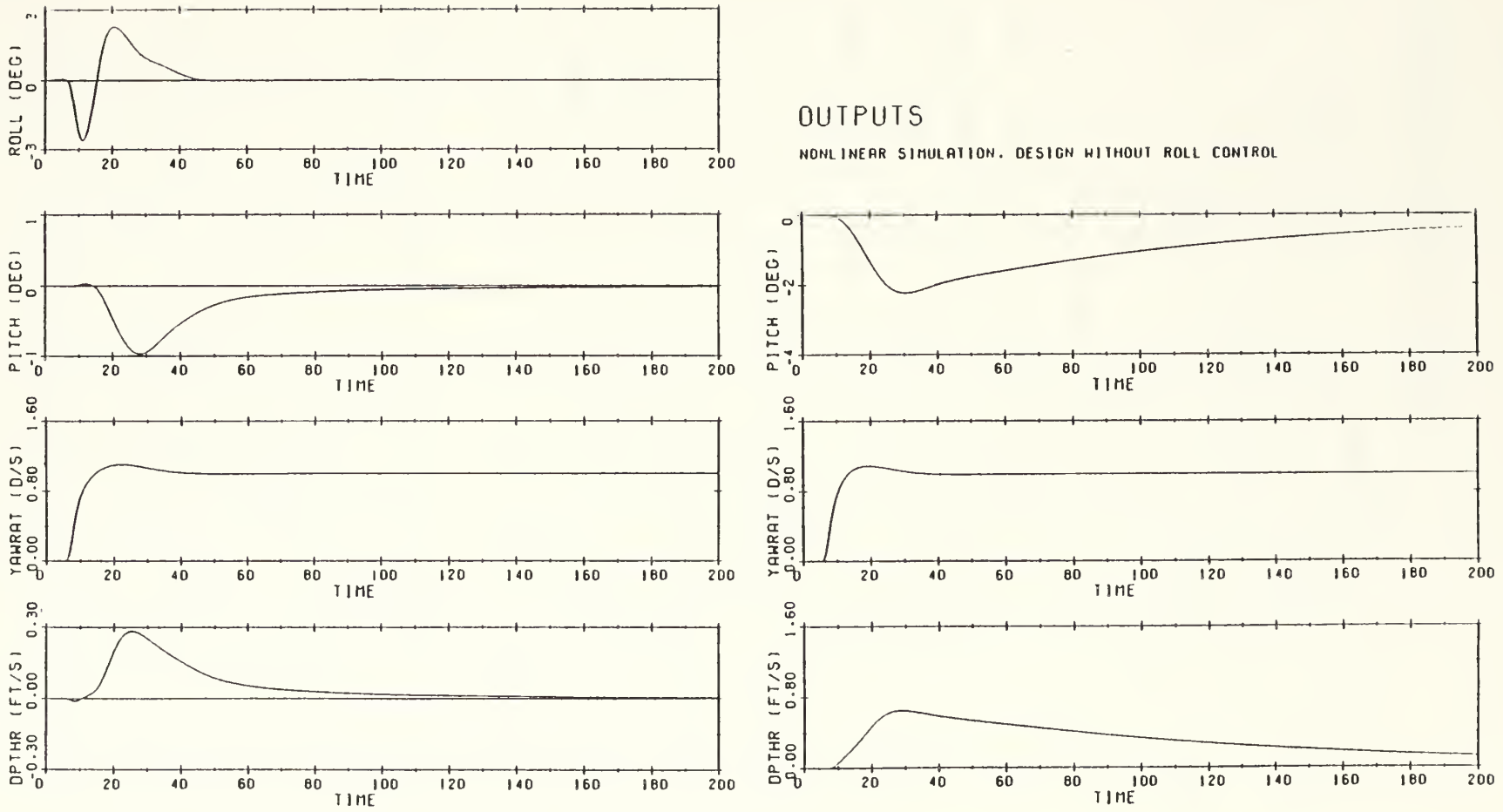


Figure 5.3(d) Comparison of the Non-linear Response of Models with and without Roll Control for a Mild Turn

5.5.2 Moderate Turning Maneuver

This simulation is for a commanded yaw rate of 2 deg/sec. Referring to Figure 5.4, we observe a 25% decrease in forward velocity. The model with roll control experiences an outward roll of 6°, then snap rolls inward to 3°. By t = 30 seconds, the roll angle is essentially zero. The ship initially pitches upward due to the outward roll and rudder deflection. When the snap roll occurs, the pitch angle achieves an angle of -2°, but steadies out at -1.3° at t = 55 seconds. This negative pitch angle contributes to the constant depth rate of 0.4 ft/sec. The significant loss of speed contributes to the lack of ability of the control surfaces to minimize vertical plane errors. For this simulation, the stern planes a deflecting a difference of 12° to compensate for the roll moment in the turn. To minimize depth rate, we see the bow planes are deflecting 3°, and to maintain the turn, the rudder is deflecting almost 8°.

Comparing the model without roll control, we observe the ship snap rolls inward 15°, then comes to a steady roll angle of 12°. Because of the large roll angle, the ship pitches down 6° initially, with pitch angle coming to -2.5° at t= 200 seconds. The depth loss in the turn is 225 feet. The bow planes almost saturate initially, deflecting to 18° to counteract the depth rate. At t = 200 seconds, the bow planes are deflected 9° (or three times the deflection in the roll control model). The rudder is deflected

approximately 8°, which is similar in the roll control model. Additionally, the stern planes are deflected to minimize the depth rate, whereas, in the roll control model, they were deflected only to minimize roll angle because the bow planes were better able to minimize depth rate.

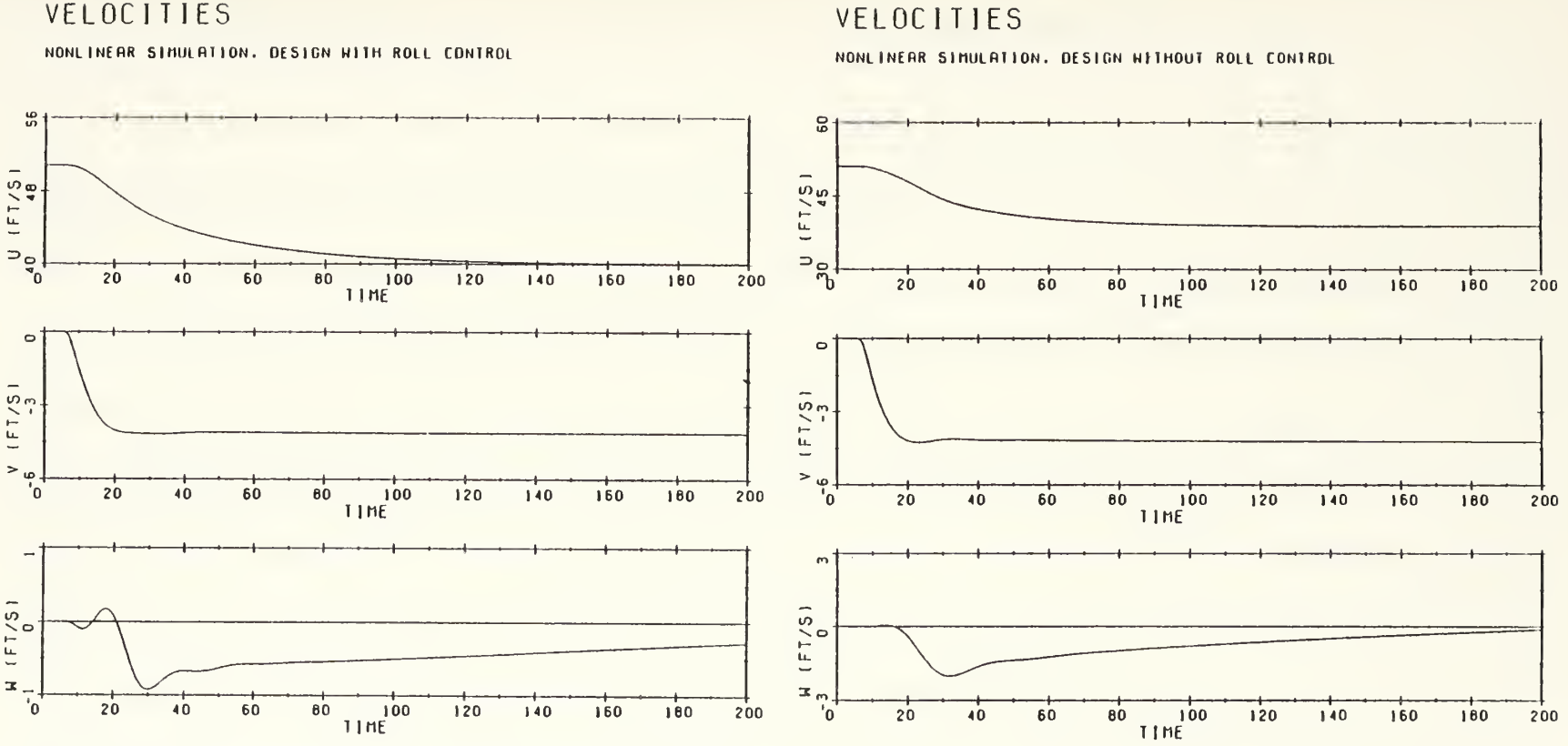
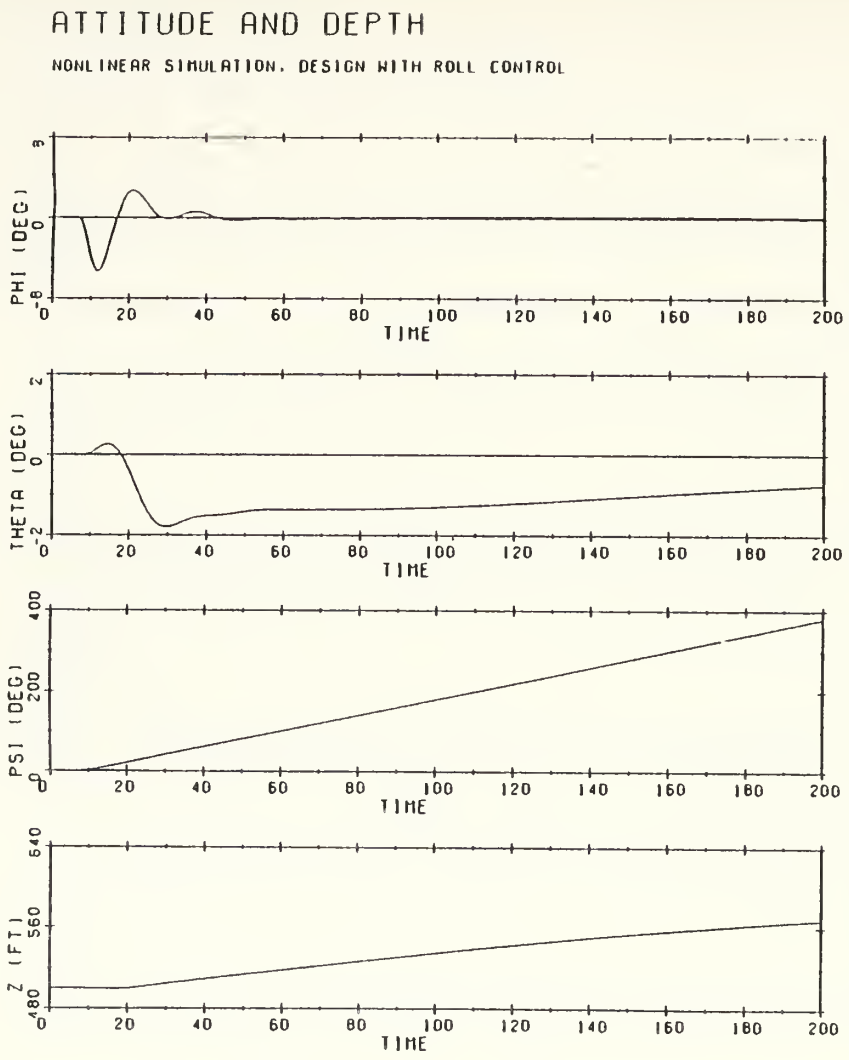


Figure 5.4(a) Comparison of the Non-linear Response of Models with and without Roll Control for a Moderate Turn



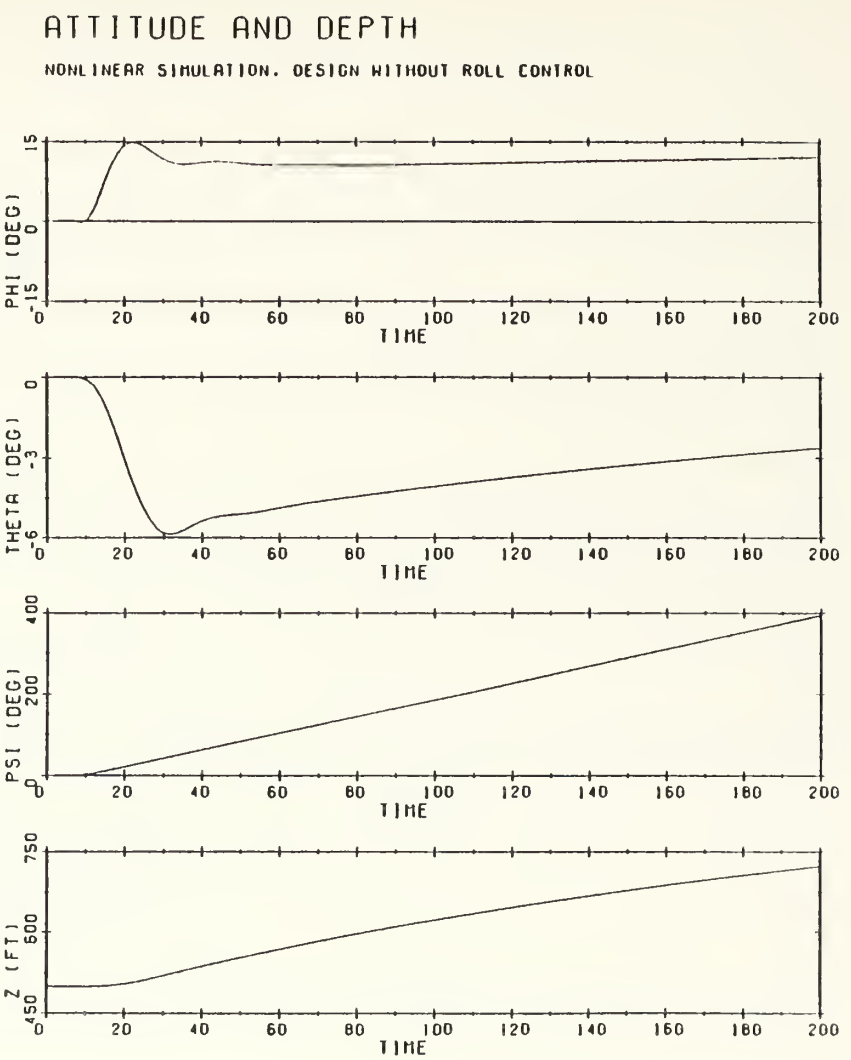


Figure 5.4(b) Comparison of the Non-linear Response of Models with and without Roll Control for a Moderate Turn

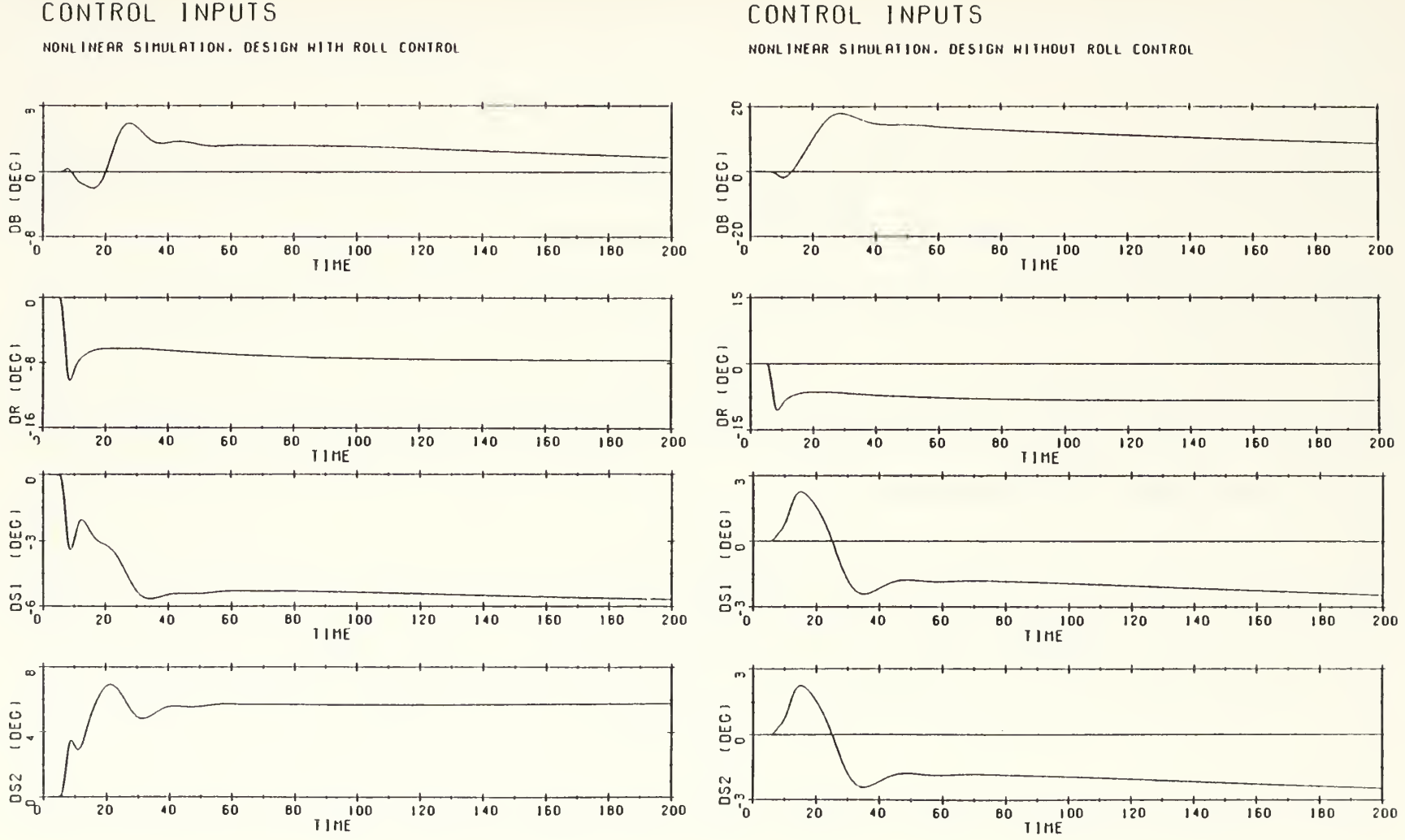


Figure 5.4(c) Comparison of the Non-linear Response of Models with and without Roll Control for a Moderate Turn

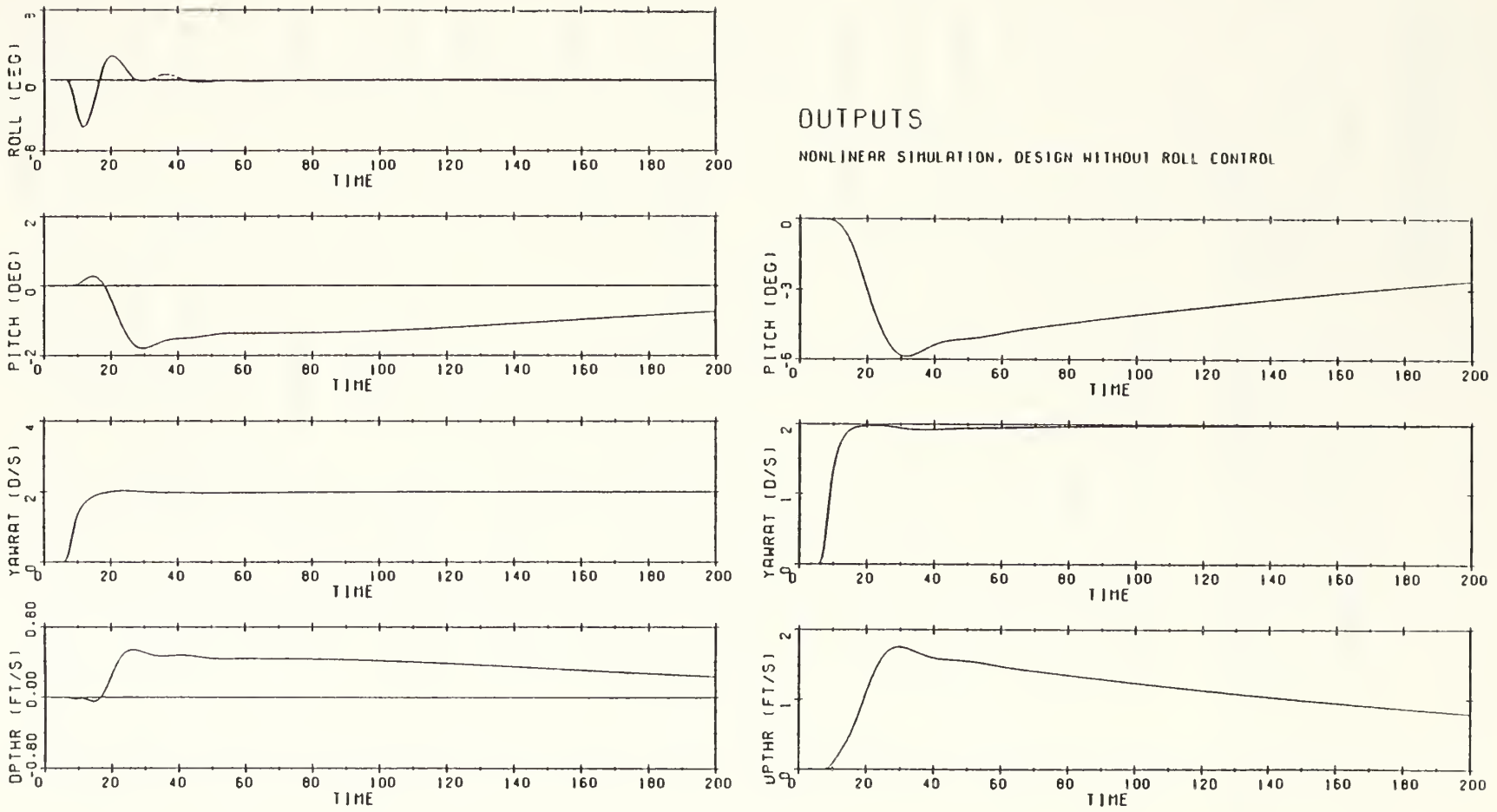


Figure 5.4(d) Comparison of the Non-linear Response of Models with and without Roll Control for a Moderate Turn

5.5.3 Combined Maneuver

This maneuver is for step input commands of -0.5 ft/sec in depth rate, 1 deg/sec in yaw rate, and 1 degree in pitch. Referring to Figure 5.5, we observe a 6% decrease in the forward velocity.

Looking first at the model with roll control, it is observed that the errors in roll angle and yaw rate are damped by t = 40 seconds. The errors in pitch and depth rate, however, are not damped until t = 140 seconds. By t = 200 seconds, the ship has experienced a depth rise of 80 feet. Again, the stern planes are deflected differentially to counteract the roll moment, with a steady differential deflection of 6°. The bow planes are deflected at -1.5° to maintain the commanded depth rate, and the rudder is deflected -2° to maintain the commanded yaw rate.

Comparing the design without roll control, it is observed that the ship experiences a snap roll of 10°. This roll angle causes a pitch angle of -2° which results in a large pitch error. In fact, at t = 200 seconds, there is still an error in pitch of 0.5°, or 50% of the commanded pitch angle. This also causes a -0.35 ft/sec depth rate instead of the commanded -.5 ft/sec. The net result of these errors is displayed in the depth of the ship. The depth rise in this design is 25 feet, instead of 80 feet, as in the model with roll control. Note here, that a depth rise is commanded.

The steady state stern planes angle is -0.75°, which indicates the stern planes are being used to obtain the ordered pitch angle. Because the depth rate is a result of the combination of pitch angle and ship's speed, we observe the bow planes are being used to obtain the ordered depth rate. In the roll control model, the ship obtained the ordered pitch angle rather quickly, thus, the bow planes are deflected in the opposite direction to limit the depth rate to -0.5 ft/sec.

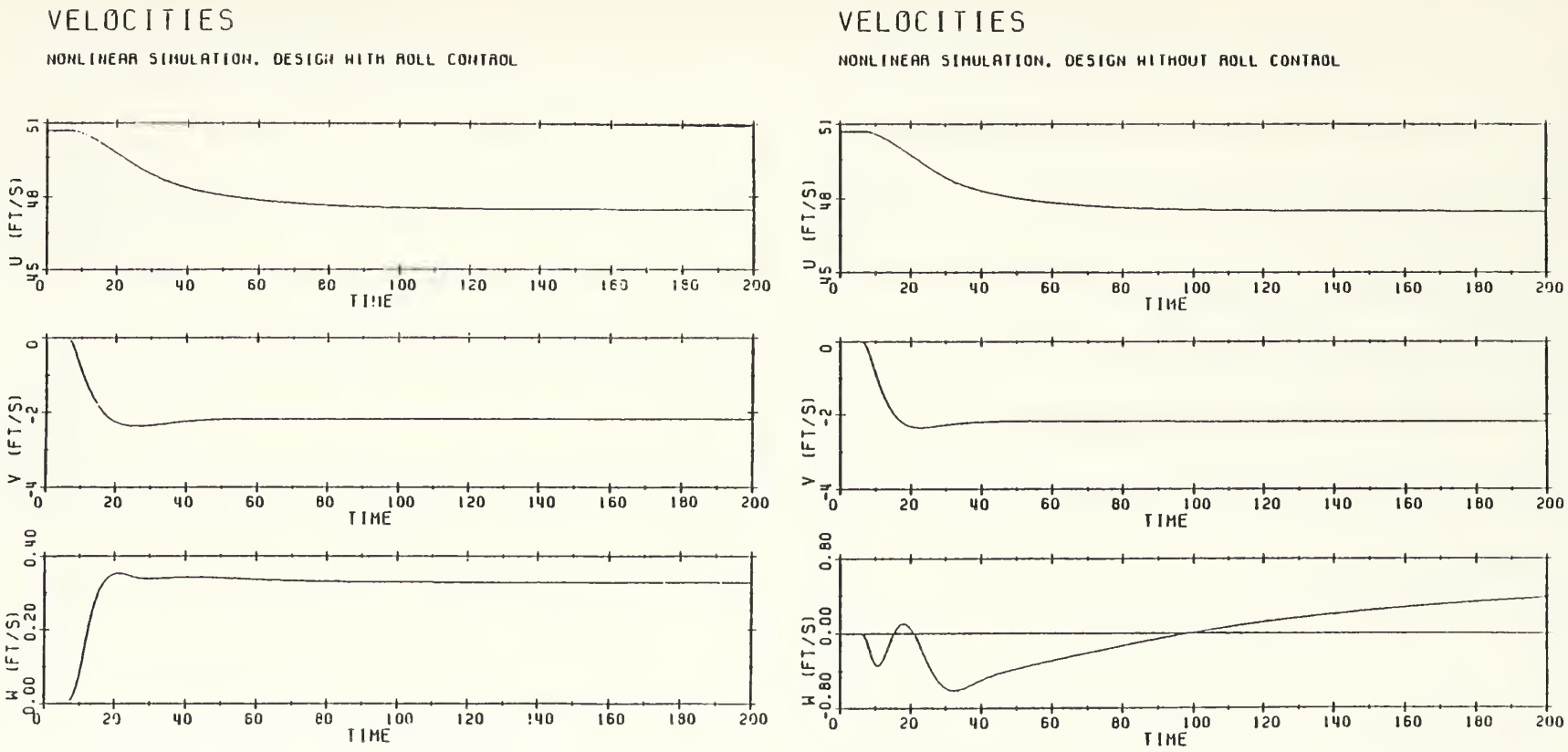


Figure 5.5(a) Comparison of the Non-linear Response of Models with and without Roll Control for a Combined Maneuver

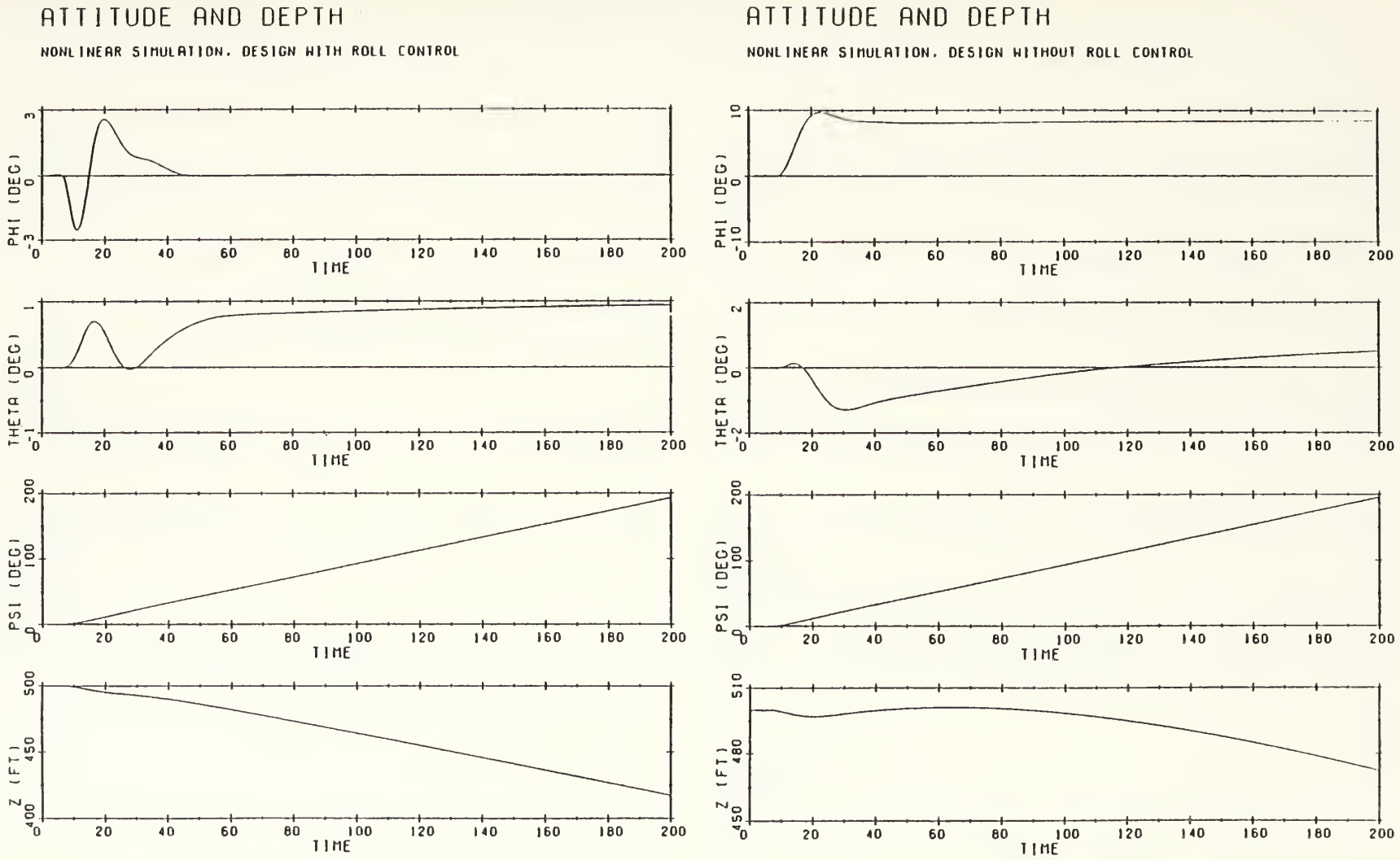


Figure 5.5(b) Comparison of the Non-linear Response of Models with and without Roll Control for a Combined Maneuver

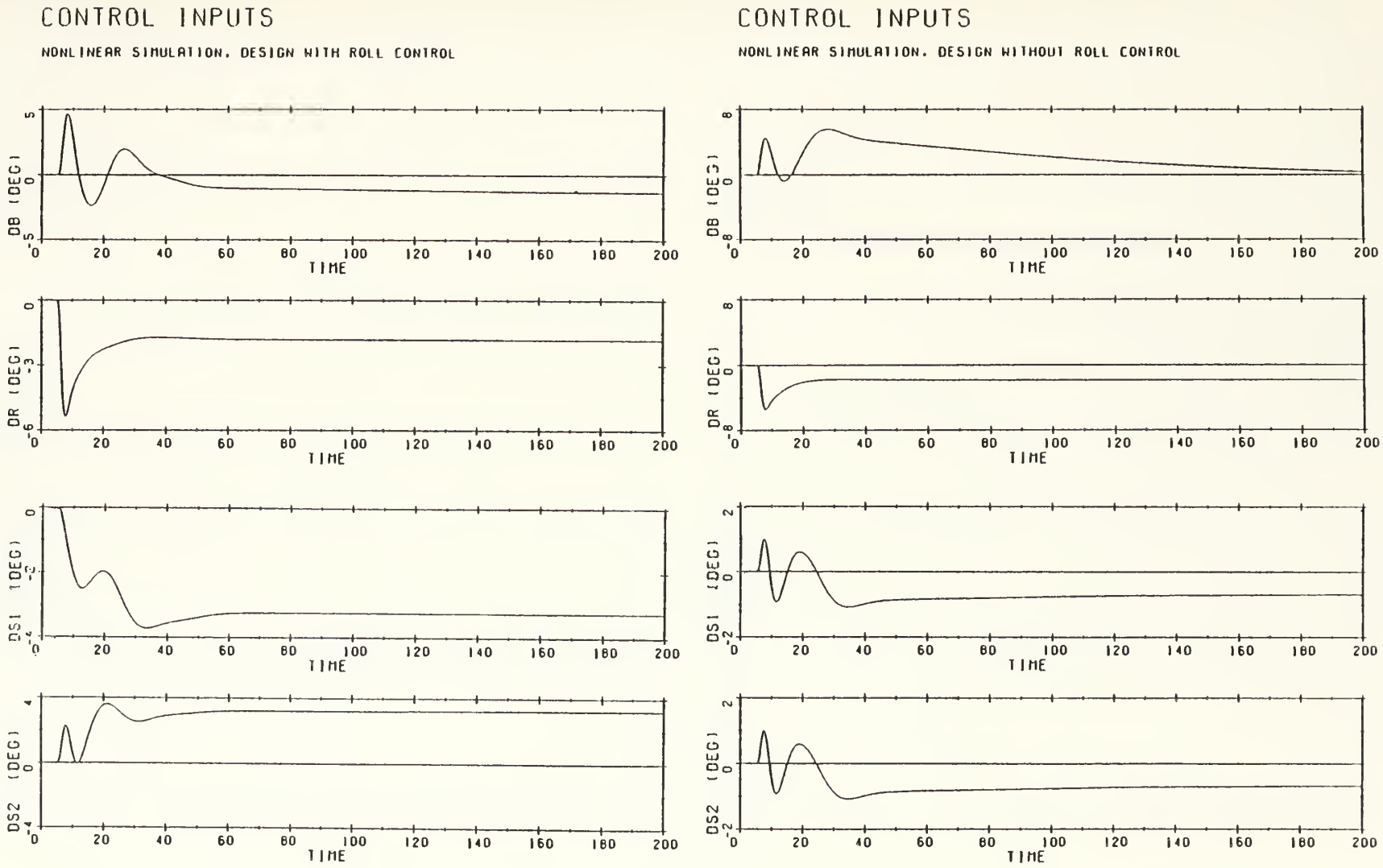
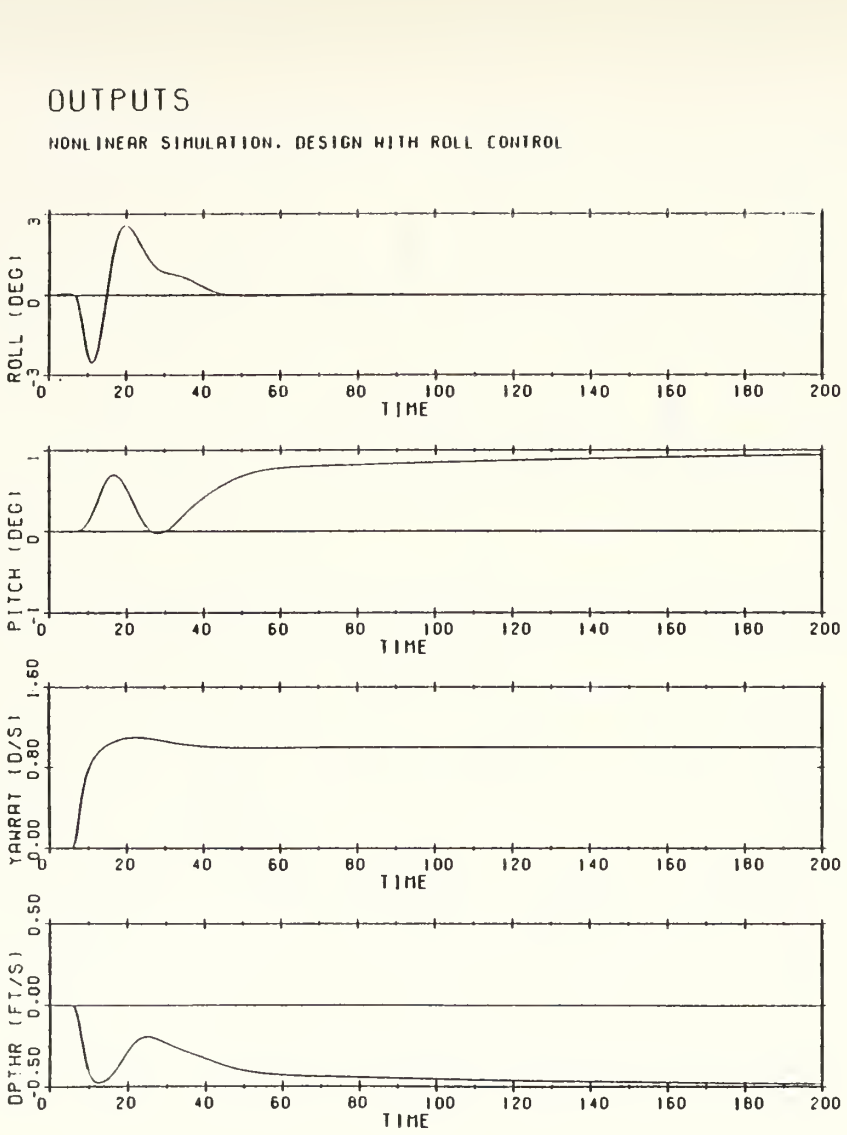


Figure 5.5(c) Comparison of the Non-linear Response of Models with and without Roll Control for a Combined Maneuver



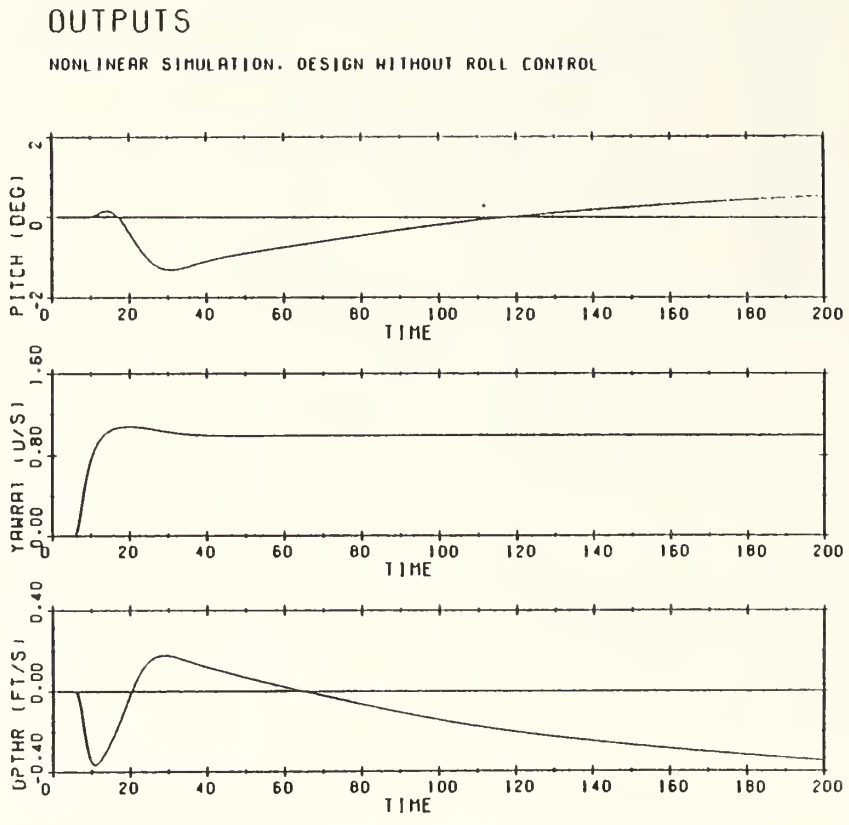


Figure 5.5(d) Comparison of the Non-linear Response of Models with and without Roll Control for a Combined Maneuver

5.5.4 Hard Turning Maneuver

This maneuver is for a commanded yaw rate of 3 deg/sec, and is provided to display the effects of control surface saturation. Referring to Figure 5.6, we observe a drop in ship's speed of almost 45%. Looking at the model with roll control, it is observed that the ship initially rolls outward approximately 8°, then snaps inward at t = 14 seconds. The maximum downward pitch angle reaches 4° at t = 160 seconds, and starts to reduce by the end of the run. The depth loss in this case is 184 ft. The stern planes again deflect differentially to counteract the roll moment, but now, we observe the port stern planes are deflected at -3.9° at t =200 seconds whereas the starboard stern planes are deflected at 7.8°. This indicates that the stern planes, although deflecting differentially for roll control, are also being deflected for control of pitch angle. The bow planes are deflected at 6.25° in an attempt to minimize depth rate. To maintain the ordered yaw rate, the rudder is deflected -27° at the end of the run.

Comparing the model without roll control, we observe that the ship snap rolls inboard 19°, and pitch angle approaches -12°. The stern planes deflect to limit the pitch angle, and the bow planes deflect to limit depth rate. The bow planes, however, saturate in this run at t = 22 seconds. Up to this point, the ship's depth was maintained fairly well. As soon as the bow planes saturate, the depth rate increases, causing the ship to lose depth. This causes

the stern planes to deflect in the opposite direction in an attempt to minimize pitch angle and depth rate. At t = 25 seconds, the pitch angle steadies, and starts to come off. At t = 108 seconds, the depth rate goes negative, and it is observed the bow planes come out of saturation. By t = 200 seconds, we observe that the roll angle has been reduced to 8°, maximum negative pitch angle is 7°, depth rate is significantly reduced, and none of the control surfaces are saturated. Depth at the end of the run is 820 feet, which equates to a depth loss of 320 feet, as compared to the roll control model's depth loss of 184 feet.

The purpose of this run was to demonstrate how different the submarine's trajectory is when the control surfaces saturate.

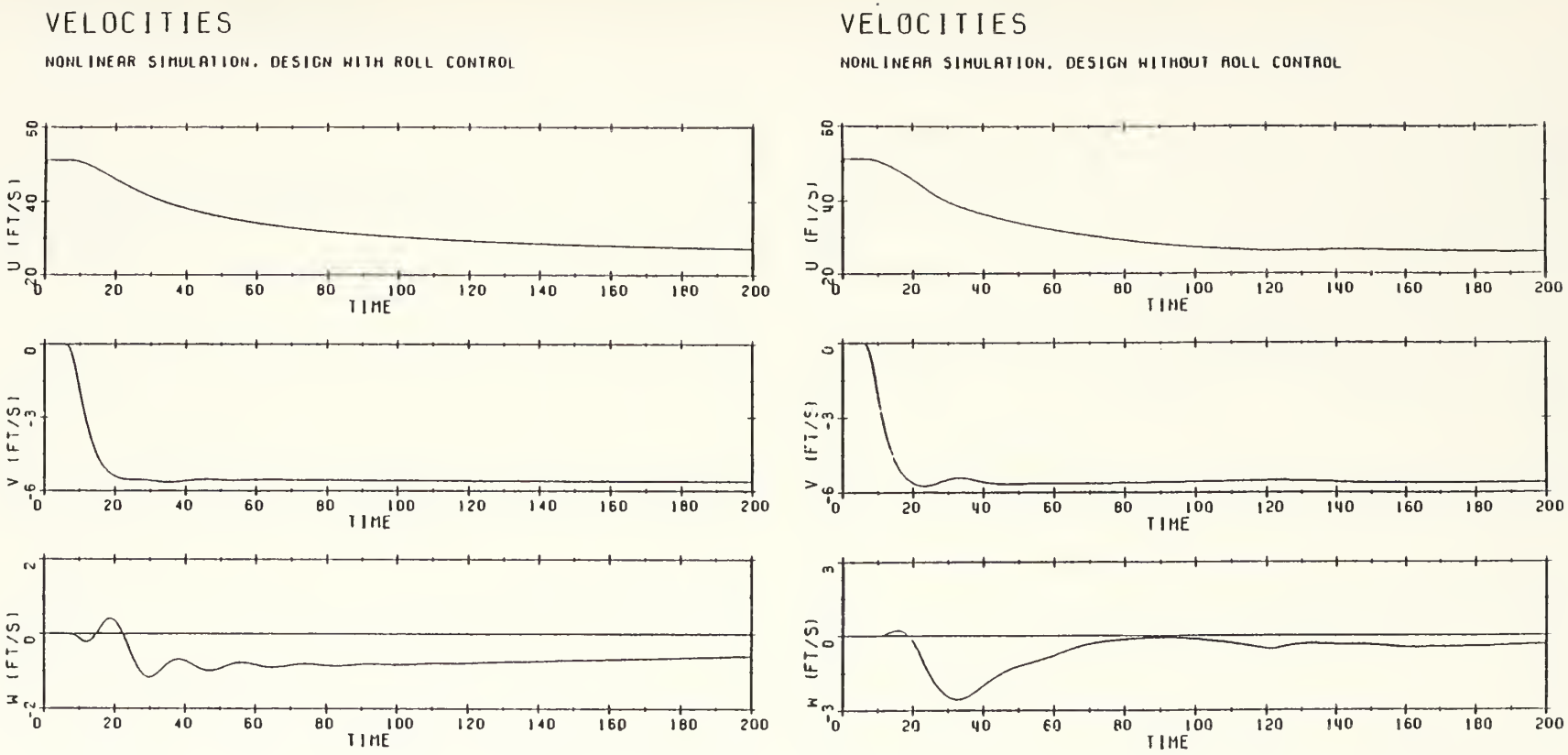


Figure 5.6(a) Comparison of the Non-linear Response of Models with and without Roll Control for a Hard Turn

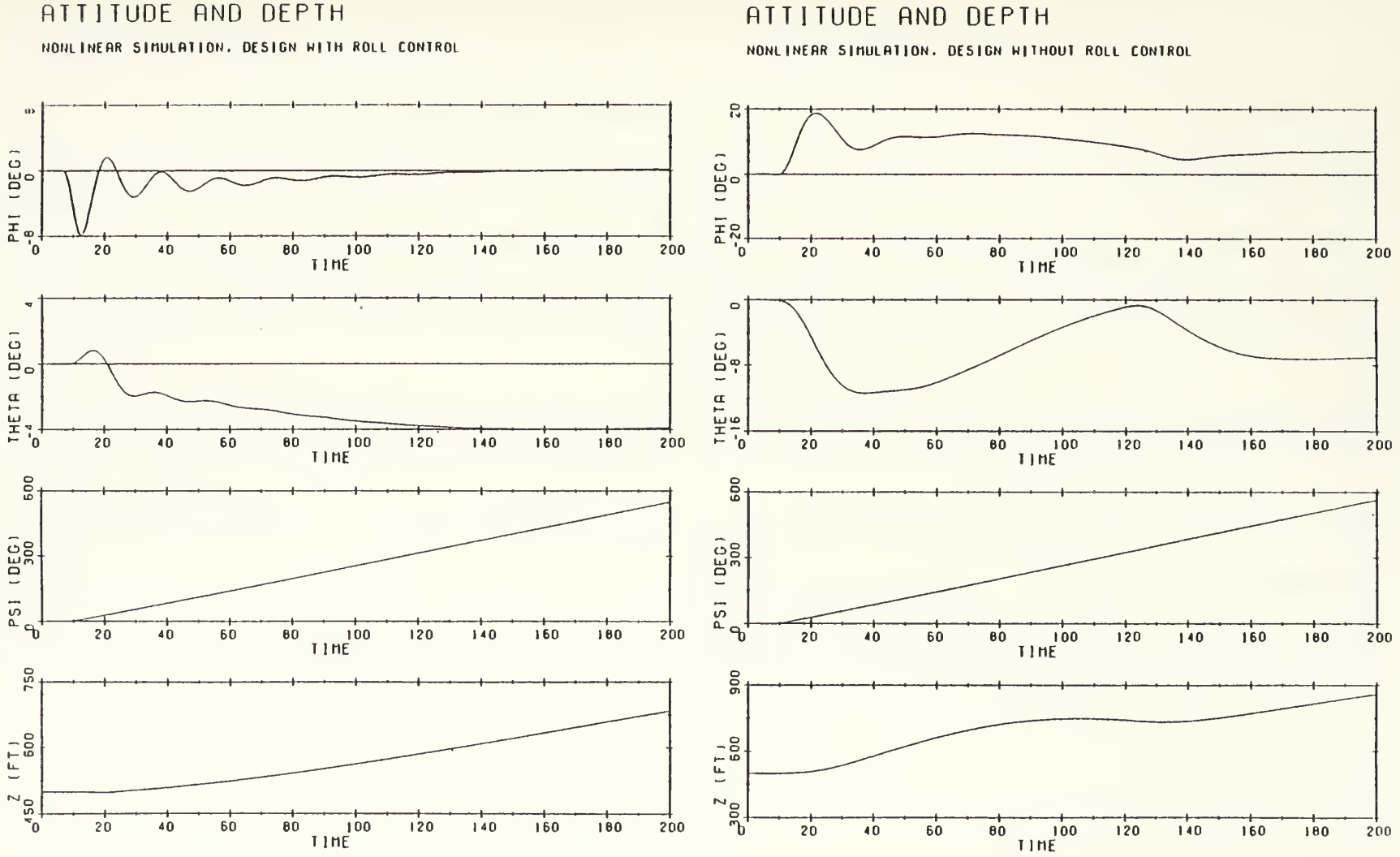


Figure 5.6(b) Comparison of the Non-linear Response of Models with and without Roll Control for a Hard Turn

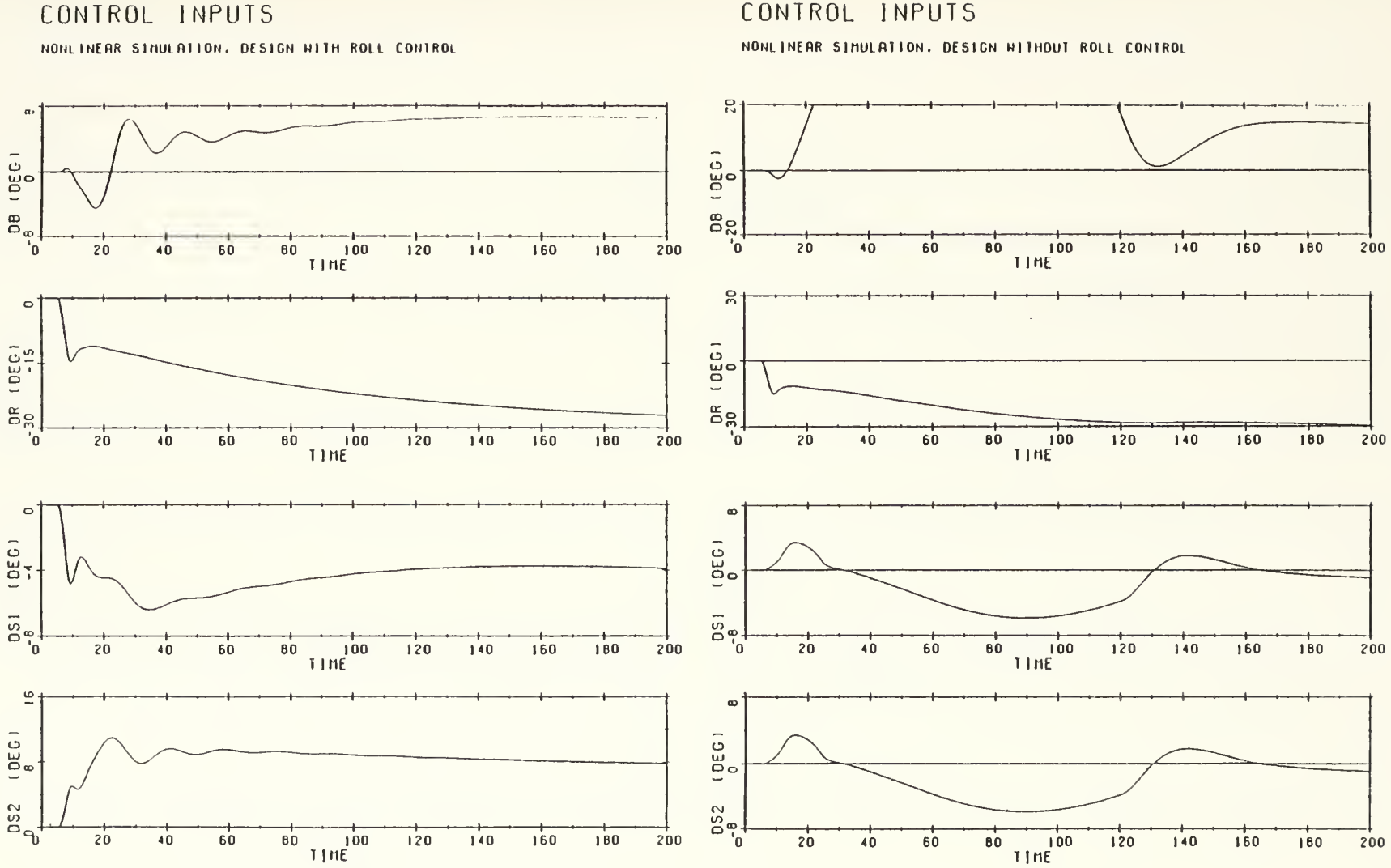


Figure 5.6(c) Comparison of the Non-linear Response of Models with and without Roll Control for a Hard Turn

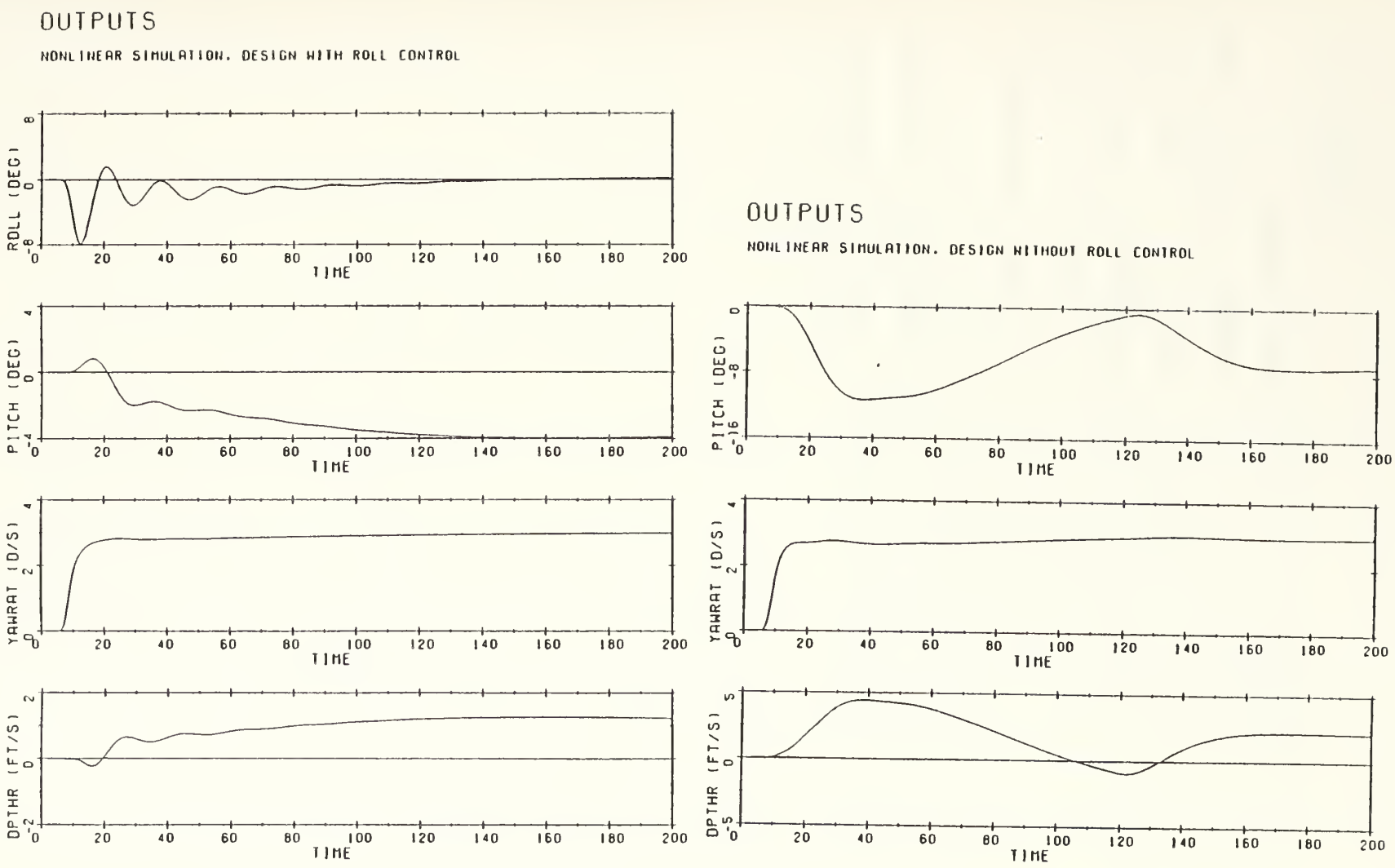


Figure 5.6(d) Comparison of the Non-linear Response of Models with and without Roll Control for a Hard Turn

5.6 Summary

This chapter has presented the implementation of the MBC designed in Chapter Four, and evaluation of the closed loop model. The linear and non-linear simulations were performed to demonstrate how the predictions for the Kalman filter loop of the linear can be used to validate the compensator's use on the non-linear model.

A second compensator, designed without roll control capability was presented, and then used to display the advantages of employing differential stern planes control on full scale submarines.

CHAPTER SIX

SUMMARY, CONCLUSIONS, AND DIRECTIONS FOR FUTURE RESEARCH

6.1 Summary

This thesis has presented a multivariable control design example for a submarine using active roll control capability.

The vehicle model was based on the NSRDC 2510 equations including vortex shedding and crossflow drag terms. These equations were linearized to generate linear models of the submarine which were then analyzed and verified.

The resulting models were reduced to eight order systems, scaled, and then subjected to modal analysis, which allowed the formulation of the prerequisites necessary to pursue the LQG/LTR design methodology.

Model Based Compensators with and without roll control capability were designed for the time and frequency domains. Specifications for the controller designs were presented, then, the methodology was applied to the design of submarine control systems. Compensators were designed and studied for various crossover frequencies, and a compensator was selected which provided desirable closed loop system response characteristics.

The selected compensator was evaluated by comparing the linear and non-linear dynamic simulations and determining how closely the performance specifications were met, and also, whether instabilities existed in the design. The MBC

was then compared with an equivalent compensator which did not have roll control capability.

6.2 Conclusions

Multivariable control system design using the LQG/LTR methodology has been successfully utilized to design a submarine control system with roll control capability.

It has been demonstrated that modal analysis and decomposition of the singular values of the plant can be used effectively in control system design. Modal analysis allows us to investigate the structure of the linear model and consider the ability to control and observe selected state variables. Singular value decomposition, once understood, can be used in a similar manner as Bode plots, and provides a convenient way to describe and ensure the performance requirements for the design.

The purpose of, and techniques used to scale the open loop plant were discussed in rigorous detail because the scaling strongly affects the singular value decomposition of the open loop plant, and the resulting compensator design.

The purpose of this thesis was to demonstrate the advantages of roll control on a full scale submarine. A limited number of simulations were performed, and the performance of the submarine with roll control is much improved over the design without roll control. The control system was designed for a submarine at 30 knots, and we observed the control system did fairly well, even for a

45% decrease in forward velocity of the ship. Additionally, the control system was designed using the inertial reference frame rather than the body reference frame of the ship. Use of the fixed inertial coordinate system provided better control of the submarine in maneuvering situations than for previous designs which used the body reference frame.

At this point it is important to stress the following observations:

- The performance characteristics of the submarine with active roll control are enhanced considerably over the design without roll control. The simulations demonstrated considerable depth improvement, and less control surface deflections and saturation in severe maneuvers, as demonstrated in Figure 5.6.
- This thesis demonstrates a technique to simulate performance characteristics of "paper" control systems for trade-off studies for specified performance criteria.
- One model cannot be used to globally control a submarine. Although the compensator performed well with large variations from the nominal operating point, reduced effectiveness of the control surfaces was observed.
- The fact that only small perturbations can be applied in validation of the design is not a limitation of the control design methodology. It is, however, a limitation of the linear model.
- Results of this thesis could be improved upon by including actuator dynamics, then selecting the compensator bandwidth and control gains to provide the best desirable ship response characteristics.
- To demonstrate the flexibility a controls engineer has when using multivariable control, the bow/fairwater planes were included in this thesis. Use of the bow/fairwater planes at 30 knots may not be considered practical due to flow noise and disturbances, and structural limitations.

6.3 Directions for Future Research

This thesis provides many of the building blocks necessary to refine the use of differential stern planes. Including actuator dynamics is an extension that needs to be completed. Additionally, limited designs were conducted which investigated the effects of compensator bandwidth and control gains. Much more work needs to be performed in this area.

Another area which needs additional research is in the use of propulsion as a dynamic control variable. If propeller rpm is allowed to vary, the control system design could effect maneuvers while minimizing speed loss in a turn (within propulsion constraints).

Finally, an area which is rather significant, and in which serious efforts have to be directed is in the area of casualty situations. This thesis has only looked at controlled maneuvers, in which the control system performs it's function completely. Failures of the control system during submerged operations must be fully investigated, understood, and designed into the compensator.

REFERENCES

1. Athans, M. "The Role and Use of the Stoichastic Linear-Quadratic-Gaussian Problem in Control System Design", IEEE Transactions on Automatic Control, Vol. AC-16, No. 6 (December, 1971): pp 529-552.

2. Athans, M. Multivariable Control Systems, Course Lecture Notes, MIT, Spring 1984.

3. Brogan, W. L. Modern Control Theory, New York, Quantum Publishers, Inc., 1974.

4. Doyle, J. C. and Stein, G. "Multivariable Feedback Design: Concepts for a Classical/Modern Synthesis", IEEE Transactions on Automatic Control, Vol. AC-26, No. 1 (February, 1981): pp 4-16.

5. Gertler, M. and Hagan, G. R. "Standard Equations of Motion for Submarine Simulation", Naval Ship Research and Development Report 2510, June 1967.

6. Kuo, B.C. Automatic Control Systems, Englewood Cliffs, N.J., Prentice Hall, Inc., 1982.

7. Kwakernaack, H. and Sivan, R. Linear Optimal Control Systems, New York, Wiley, 1972.

8. Ogata, K. Modern Control Engineering, Englewood Cliffs, N.J., Prentice Hall, Inc., 1972.

9. Triantafyllou, M. S., Bodson, M. and Athans, M. "Real Time Estimation of Ships Motion Using Kalman Filtering Techniques", IEEE Journal of Ocean Engineering, Vol. OE-8, No. 1 (January, 1983), pp 9-20.

10. Lively, K. A. "Multivariable Control System Design for a Submarine", Engineers Thesis, MIT, 1984.

11. Dreher, L. J. "Robust Rate Control System Designs for a Submersible", Engineers Thesis, MIT, 1984.

12. Milliken, L. G. "Multivariable Control of an Underwater Vehicle", Engineers Thesis, MIT, 1984.

13. Harris, K. A. "Automatic Control of a Submersible", Masters Thesis, MIT, 1984.

14. Bonnice, B. and Valavani, L. "Submarine Configuration and Control", CSDL Memo SUB 1-1083, 1983.

15. Bonnice, B. CONSTRPS Fortran and Executive Command Computer Programs, CSDL, May, 1984.

16. Abkowitz, M. Stability and Motion Control of Ocean Vehicles, MIT Press, Cambridge, MA., 1969.

17. Takahashi, Robins, and Auslander Control, Addison-Wesley, 1970, pp 65-86.

18. Athans, M. Multivariable Control System Design using the LQG/LTR Methodology, 6.232 Lecture Notes, MIT, Spring 1984.

19. Stein, G. "LQG-Based Multivariable Design: Frequency Domain Interpretation", AGARD, NATO, 1981.

20. Kappos, E. "Robust Multivarable Control for the F-100 Engine", Engineer's Thesis, MIT, 1983.

21. Boettcher, K. "Analysis of Multivarable Control Systems with Structural Uncertainty", Internal Report, MIT, 1983.

APPENDIX A

Detailed Definition of the Submarine Problem

Any submarine must meet certain minimum standards of controllability. Its course keeping and depth keeping stability must be adequate for transportation at the maximum speed and at a low but useful speed. While many surface ships and many submarines are directionally unstable to a small degree, requiring constant attention to steer an acceptable straight course, the consequences of a mistake or a temporary interruption of rudder or diving plane activity in a high speed submarine make it imprudent to accept even slight instability. For this reason, definite control-fixed stability is required.

Slow speed operation of a combatant submarine is often required. Because of the pendulum-like hydrostatic stability of the submarine, as the submarine moves very slowly through the water, the hydrodynamic effects of stern plane deflection are too small to change the submarine hull angle-of-attack by an amount large enough to develop rise or dive forces on the hull. The net vertical force on the submarine that results is due mostly to the force of the stern plane itself, which is always in the direction opposite to the conventional rise or dive command. This phenomenon is often referred to as "stern plane reversal". This particular effect can be controlled by proper design and building of the ship such that the vertical distance between the location of the center of buoyancy and the center of gravity of the ship are within prescribed max/min limits.

At or near zero ship speed, control of the ship's attitude and depth using forces generated by flow over the hull and control surfaces is not possible. Control of depth can be obtained by changing the weight of the submarine using the trim system.

In the absence of external force disturbances, such as are encountered near the surface under a seaway, hovering by application of small weight and/or buoyancy changes has become a common experience for submariners. Quiet seas, skill, experience, and an opportunity to improve the trim while slowing to hovering speeds are all necessary. Lacking any of these factors, and given a need to hover, one immediately recognizes a need for some form of properly engineered hovering system.

Each submarine must operate a portion of its service life on the surface, which generates a different set of steering parameters and requirements. Adequate surfaced steering with slight directional unstability is feasible, so that specific values of directional stability on the surface are not necessary or even useful. Some degree of steering

control while backing is also necessary when docking or for in-port maneuvering.

The attributes of combatant service that affect controllability and performance requirements range from those associated with stealth to those associated with maximum speed violent maneuvers. Violent maneuvers, involving full acceleration, possible course reversals, and severe depth changes could be necessary. The prescribed Submerged Operating Envelope (SOE) should be the same for peacetime and wartime operations. The maximum exploitation of speed, depth, and maneuvering capabilities will be a necessity to prepare for potential engagements or casualty environments that may be experienced over the lifetime of the submarine.

Underlying all combatant submarine attributes, and in many cases, dominating them, are the requirements to operate quietly. Mandatory noise requirements and even more stringent desirable goals are generally imposed on all systems; one of the most significant contributors to the overall noise characteristics are operations of the control surfaces, thus, the ship control system must now be optimized to minimize this noise source.

The fact that the submarine is a "dirigible" in space, within the bounds of the surface, the bottom, and collapse depth, mandates that its handling properties be described as a set of horizontal and vertical plane properties. The consequences of error in the vertical plane that can be imagined are dramatically different from those in the horizontal plane. Groundings and collisions due to horizontal plane error, no matter how distressing to the ship(s) involved, do not have the sense of finality that sinkings have. For this reason, the highest priority attention is given to vertical plane maneuvering properties and vertical plane consequences of horizontal plane maneuvers. The remaining mobility characteristics, course and speed, are ranked in priority in that order.

With depth factors as the first priority, the criteria for judging the quality of vertical plane maneuvers will be based upon reliability and precision of control at constant ordered depth, and upon the ease of making ordered depth changes.

In the horizontal plane, it is rare that a specific minimum value of turning diameter would be critical for a submarine. A much more useful turning quality to impose is the time to change heading by a given amount (for example 30°, 180°, etc.), with minimum depth keeping disruption and maximum speed remaining when the turn is completed. This is a property which can be perceived by the operators. Evasive maneuvers are very likely to involve large changes in

speed, course, and depth. The performance of the submarine during large changes should provide the most freedom to the operator. It must be possible, with confidence in the safety of the maneuver, to order simultaneous speed, course, and depth changes in any combination. This requirement leads to the addition of a parameter describing the required control authority in the vertical plane to the time to reach the heading change requirement within a specified time period. The depth change limitation associated with turns must be met using only a portion of the available depth control authority. The remaining depth control authority that is not used in a flat turn could be used to enforce a simultaneous depth change.

APPENDIX B

Summary of the SUBMODEL Program

The SUBMODEL program was written to perform any of the following tasks:

1) Integrate the nonlinear equations of motion of a submarine.

2) Search for a local equilibrium point in the nonlinear equations of motion. (A local equilibrium point is the point where the derivatives of the state variables chosen are zero.)

3) Calculate the linearized dynamics about a particular nominal point.

4) Integrate the linearized equations of motion.

This description of the SUBMODEL program consists of three sections. Section 2 describes briefly the equations of motion that are implemented in the program. Section 3 describes the program.

Section Two: Nonlinear and Linear Equations of Motion

This section describes the equations of motion which have been implemented in the SUBMODEL program.

The nonlinear equations are in the form

$$\underline{E}\dot{\underline{x}} = \underline{f}(\underline{x},\underline{u})$$

where

$\underline{x}$ = 10 x 1 state vector
$\underline{u}$ = n x 1 control vector (n=user specified)
$\underline{f}$ = 10 x 1 vector that is a nonlinear function of the states and the controls
$\underline{E}$ = 10 x 10 matrix

The first nine differential equations are the same as the 688 nonlinear equations documented in CSDL Memo SUB 2-1083 except for three propulsion and drag terms. These changes are documented in the memo on propulsion and drag models. The nine states are ordered as stated in the main body of this thesis (Chapter Two). The tenth differential equation and state is used to describe the propulsion dynamics.

There are two propulsion models - an rps propulsion model and an eta propulsion model. The rps propulsion model contains a first order differential equation in terms of rps

(revolutions per second) and is the more accurate model of the two models. The eta propulsion model contains a first order differential equation in terms of eta (η is defined to be u/U, where U is the actual speed of the submarine and u is the commanded forward velocity) and is a slightly simplified version of the rps model. The importance of the eta model lies in the fact that it was the propulsion model that was linearized and included in the linear equations of motion. These propulsion models are documented in another Draper memo.

The controls that may be specified are bow/fairwater planes, rudder, stern planes (which may be segmented), and WSTEAM (steam flow).

Section Three: Program Description

This section describes how the four main tasks listed in the introduction are accomplished.

Before linearized dynamics can be calculated, equations of motion integrated, and/or local equilibrium points searched for, the program must be read in and can print out upon request the mass properties, the hydrodynamic coefficients, and the propulsion and drag constants. These constants and coefficients describe the dynamics of a specified submarine, and with two exceptions, are assumed to be valid for any dynamic condition. The exceptions are the propulsion variables "thrded" and "wake". The rps propulsion model calculates these variables and, therefore, values that are read in are ignored. However, in reformulating the rps propulsion model into the eta propulsion model, these two propulsion variables were assumed to be constant. A method of determining appropriate values of these constants is to integrate the nonlinear equations with the rps propulsion model using the same initial conditions that will be used to integrate the equations with the eta model. Then, use the values of "thrded" and "wake" after the initial transients of the states have "died out". The program prints out the final values of "thrded" and "wake" at the end of integrating the nonlinear equations with the rps model.

The program then proceeds to calculate the $\underline{\underline{E}}$ and $\underline{\underline{E}}^{-1}$ matrices as the $\underline{\underline{E}}^{-1}$ matrix is needed for any of the four main tasks. An indication of the accuracy of the $\underline{\underline{E}}^{-1}$ matrix is obtained by multiplying the $\underline{\underline{E}}$ and $\underline{\underline{E}}^{-1}$ matrices. The program prints each one of these matrices (i.e., $\underline{\underline{E}}$, $\underline{\underline{E}}^{-1}$, and $\underline{\underline{E}}\underline{\underline{E}}^{-1}$).

If the option to integrate the nonlinear equations of motion was selected, the initial conditions necessary to integrate the equations are read in. There is an option that can be set in the input data file containing the

initial conditions on p, q, and r from initial conditions on psidot, phidot, and thetadot. Also, the input data file contains initial conditions for both the variables rps and eta. As mentioned in section 2, there are both an rps and an eta propulsion model. If the rps model was chosen, the initial condition on rps is used and eta is calculated. If the eta model was chosen, the initial condition on eta is used and the rps initial condition is ignored.

The program proceeds to integrate the nonlinear equations of motion using a fourth order Runge Kutta routine. The values of the controls can be set in two ways. They can be either initialized and kept constant at that value throughout the run or be read from a data file. Another possibility, if the rps model is being used, is to calculate the controls using full state feedback. For this condition, the gain matrix is read by the program. Therefore, it is necessary for the program to read in the nominal point which corresponds to the linearized model used to design the gain matrix. For the purposes of calculating the controls using full state feedback only, eta is calculated from rps and u. It is subsequently used as the tenth state.

When integrating the nonlinear equations of motion, the initial time, the final time, and the integration time step must be chosen. In addition, there are options to print the states and to store the values of the states and the controls for plotting. The program writes the plotting data using an unformatted write. A plotting program, such as XPLOT4B, must be run to actually plot the data. The frequency of printing and storing data for plotting can be individually specified in terms of time steps.

Also, the program has the option to search for a local equilibrium point. If this option is selected, the program needs an initial guess of the local equilibrium point to begin the search. This initial guess can be provided in either of two ways. One way is to integrate the nonlinear equations of motion using the eta propulsion model. The program will use the final condition from integrating the nonlinear equations as the guess for the search routines. The other way is to read in an initial guess in the same manner as reading in the initial conditions to integrate the nonlinear equations of motion.

When searching for a local equilibrium point, the program uses the set of nonlinear equations with the eta propulsion model. The reason for using the eta propulsion model is that the linearized propulsion model was derived from it. Presumably, the reason for searching for a local equilibrium point is to use that point as a point about which to linearize the nonlinear equations of motion. If the vehicle is in a turn, psidot will be nonzero and

therefore the search routines will be unable to find a local equilibrium point for this case. As psi has no effect on the other differential equations, deleting the differential equation in psi allows a local equilibrium point (except in psi) to be found when the vehicle is in a turn.

To search for a local equilibrium point, the program uses two IMSL search routines - ZSPOW and ZSCNT. These routines take a supplied initial guess of the point and iterate for a specified number of times before returning a point. The number of iterations per call to a routine must be specified by the user. The program iterates by perturbing the number of variables specified by the user (maximum of eight are allowed). The point returned may or may not be closer to a local equilibrium point than the initial guess. The closeness of a point to being a local equilibrium point is determined by the sum of the squares of the derivatives.

Finally, when searching for a local equilibrium point, there is one additional option that must be specified - the number of times to call each one of the search routines. The program calls the routines in the following manner. Using the initial guess supplied by either input data or by integrating the nonlinear equations with the eta propulsion model, the program calls the ZSPOW routine. After ZSPOW returns a point, the program will cause the ZSPOW routine again using the point returned as the initial guess. The program repeatedly calls the ZSPOW routine unless: (1) the point returned is not closer than the initial guess, or (2) the specified number of times to call the search routine is exceeded. Then the program follows the same procedure with the ZSCNT routine with the first guess being the closest to a local equilibrium point available.

If the option to calculate the linearized dynamics was selected, the program would read in the nominal point about which the nonlinear equations are linearized.

If the option to integrate the linearized dynamics was chosen, the program will read in the nominal point and calculate the linearized dynamics if the option to calculate the linearized dynamics was not already chosen before. The program will then read in the initial conditions on the states and on the controls, calculate the perturbatiosn from the nominal point, and integrate the linearized equations. As with integrating the nonlinear equations of motion, the user must specify the initial time, final time, and integration time step. Also, the options to store data for plotting, to print, as well as the frequency of carrying out each step are the same as in integrating the nonlinear case.

APPENDIX C

STATE SPACE MATRICES FOR THE LINEARIZED MODELS

The elements of the $\underline{A}$, $\underline{B}$, and $\underline{C}$ matrices are presented in the standard row and column format.

APPENDIX C1

ORIGINAL MATRICES PRIOR TO SCALING

$$\underline{x}^T = [\, u \;\; v \;\; w \;\; p \;\; q \;\; r \;\; \phi \;\; \theta \;\; \psi \;\; z \,]$$

A MATRIX

-3.8245E-02	-2.1911E-02	-2.7720E-03	-1.8964E-02	-2.9363E-01	3.1674E+00	0.0000E+00	2.9326E-04	0.0000E+00	0.0000E+00
1.1461E-03	-1.5919E-01	-1.9338E-03	-1.1464E+00	1.1276E-01	-1.5397E+01	1.3004E-01	-1.7564E-03	0.0000E+00	0.0000E+00
2.4225E-05	4.6499E-04	-1.0631E-01	-1.5984E+00	1.2070E+01	8.0194E-02	0.0000E+00	7.5597E-03	0.0000E+00	0.0000E+00
2.4614E-04	-1.1680E-02	-1.3226E-03	-4.3445E-01	-2.3879E-01	-7.1773E-03	-1.5995E-01	2.1603E-03	0.0000E+00	0.0000E+00
-5.3732E-06	-1.8585E-05	1.3207E-03	-1.1380E-02	-4.0755E-01	1.0074E-04	0.0000E+00	-2.4934E-03	0.0000E+00	0.0000E+00
-2.7564E-05	-2.0277E-03	2.4063E-05	-8.1034E-03	3.6042E-03	-3.8180E-01	2.5836E-04	-3.4895E-06	0.0000E+00	0.0000E+00
0.0000E+00	0.0000E+00	0.0000E+00	1.0000E+00	1.3427E-02	-1.2348E-01	-2.0244E-10	-1.2660E-02	0.0000E+00	0.0000E+00
0.0000E+00	0.0000E+00	0.0000E+00	0.0000E+00	9.9414E-01	1.0810E-01	1.2467E-02	0.0000E+00	0.0000E+00	0.0000E+00
0.0000E+00	0.0000E+00	0.0000E+00	0.0000E+00	-1.0893E-01	1.0018E+00	1.6423E-09	1.5605E-03	0.0000E+00	0.0000E+00
1.2326E-01	-1.0728E-01	9.8656E-01	0.0000E+00	0.0000E+00	0.0000E+00	1.5702E+00	-4.8493E+01	0.0000E+00	0.0000E+00

$$\underline{u}^T = [\, \delta b \;\; \delta r \;\; \delta s_1 \;\; \delta s_2 \,]$$

B MATRIX

-1.6315E-03	-5.8396E-02	2.8022E-03	2.8022E-03
0.0000E+00	2.3119E+00	-1.6950E-01	1.6950E-01
-1.4442E+00	-1.4815E-06	-9.8476E-01	-9.8476E-01
0.0000E+00	4.2586E-02	2.0848E-01	-2.0848E-01
1.3872E-02	4.8862E-07	-2.3825E-02	-2.3825E-02
0.0000E+00	-5.8593E-02	-3.3676E-04	3.3676E-04
0.0000E+00	0.0000E+00	0.0000E+00	0.0000E+00
0.0000E+00	0.0000E+00	0.0000E+00	0.0000E+00
0.0000E+00	0.0000E+00	0.0000E+00	0.0000E+00
0.0000E+00	0.0000E+00	0.0000E+00	0.0000E+00

APPENDIX C2

MATRICES TO PERFORM UNIT TRANSFORMATIONS

Matrix used to premultiply the A and B matrices:

1.0000E+00	0.0000E+00	0.0000E+00	0.0000E+00	0.0000E+00	0.0000E+00	0.0000E+00	0.0000E+00	0.0000E+00	0.0000E+00
0.0000E+00	1.0000E+00	0.0000E+00	0.0000E+00	0.0000E+00	0.0000E+00	0.0000E+00	0.0000E+00	0.0000E+00	0.0000E+00
0.0000E+00	0.0000E+00	1.0000E+00	0.0000E+00	0.0000E+00	0.0000E+00	0.0000E+00	0.0000E+00	0.0000E+00	0.0000E+00
0.0000E+00	0.0000E+00	0.0000E+00	5.7300E+01	0.0000E+00	0.0000E+00	0.0000E+00	0.0000E+00	0.0000E+00	0.0000E+00
0.0000E+00	0.0000E+00	0.0000E+00	0.0000E+00	5.7300E+01	0.0000E+00	0.0000E+00	0.0000E+00	0.0000E+00	0.0000E+00
0.0000E+00	0.0000E+00	0.0000E+00	0.0000E+00	0.0000E+00	5.7300E+01	0.0000E+00	0.0000E+00	0.0000E+00	0.0000E+00
0.0000E+00	0.0000E+00	0.0000E+00	0.0000E+00	0.0000E+00	0.0000E+00	5.7300E+01	0.0000E+00	0.0000E+00	0.0000E+00
0.0000E+00	0.0000E+00	0.0000E+00	0.0000E+00	0.0000E+00	0.0000E+00	0.0000E+00	5.7300E+01	0.0000E+00	0.0000E+00
0.0000E+00	0.0000E+00	0.0000E+00	0.0000E+00	0.0000E+00	0.0000E+00	0.0000E+00	0.0000E+00	5.7300E+01	0.0000E+00
0.0000E+00	0.0000E+00	0.0000E+00	0.0000E+00	0.0000E+00	0.0000E+00	0.0000E+00	0.0000E+00	0.0000E+00	1.0000E+00

Matrix used to postmultiply the A matrix:

1.0000E+00	0.0000E+00	0.0000E+00	0.0000E+00	0.0000E+00	0.0000E+00	0.0000E+00	0.0000E+00	0.0000E+00	0.0000E+00
0.0000E+00	1.0000E+00	0.0000E+00	0.0000E+00	0.0000E+00	0.0000E+00	0.0000E+00	0.0000E+00	0.0000E+00	0.0000E+00
0.0000E+00	0.0000E+00	1.0000E+00	0.0000E+00	0.0000E+00	0.0000E+00	0.0000E+00	0.0000E+00	0.0000E+00	0.0000E+00
0.0000E+00	0.0000E+00	0.0000E+00	1.7452E-02	0.0000E+00	0.0000E+00	0.0000E+00	0.0000E+00	0.0000E+00	0.0000E+00
0.0000E+00	0.0000E+00	0.0000E+00	0.0000E+00	1.7452E-02	0.0000E+00	0.0000E+00	0.0000E+00	0.0000E+00	0.0000E+00
0.0000E+00	0.0000E+00	0.0000E+00	0.0000E+00	0.0000E+00	1.7452E-02	0.0000E+00	0.0000E+00	0.0000E+00	0.0000E+00
0.0000E+00	0.0000E+00	0.0000E+00	0.0000E+00	0.0000E+00	0.0000E+00	1.7452E-02	0.0000E+00	0.0000E+00	0.0000E+00
0.0000E+00	0.0000E+00	0.0000E+00	0.0000E+00	0.0000E+00	0.0000E+00	0.0000E+00	1.7452E-02	0.0000E+00	0.0000E+00
0.0000E+00	0.0000E+00	0.0000E+00	0.0000E+00	0.0000E+00	0.0000E+00	0.0000E+00	0.0000E+00	1.7452E-02	0.0000E+00
0.0000E+00	0.0000E+00	0.0000E+00	0.0000E+00	0.0000E+00	0.0000E+00	0.0000E+00	0.0000E+00	0.0000E+00	1.0000E+00

APPENDIX C2

Matrix used to postmultiply the B matrix:

1.7452E-02	0.0000E+00	0.0000E+00	0.0000E+00
0.0000E+00	1.7452E-02	0.0000E+00	0.0000E+00
0.0000E+00	0.0000E+00	1.7452E-02	0.0000E+00
0.0000E+00	0.0000E+00	0.0000E+00	1.7452E-02

Matrix used to premultiply the C matrix:

5.7300E+01	0.0000E+00	0.0000E+00	0.0000E+00
0.0000E+00	5.7300E+01	0.0000E+00	0.0000E+00
0.0000E+00	0.0000E+00	5.7300E+01	0.0000E+00
0.0000E+00	0.0000E+00	0.0000E+00	1.0000E+00

Matrix used to postmultiply the C matrix:

1.0000E+00	0.0000E+00	0.0000E+00	0.0000E+00	0.0000E+00	0.0000E+00	0.0000E+00	0.0000E+00	0.0000E+00	0.0000E+00
0.0000E+00	1.0000E+00	0.0000E+00	0.0000E+00	0.0000E+00	0.0000E+00	0.0000E+00	0.0000E+00	0.0000E+00	0.0000E+00
0.0000E+00	0.0000E+00	1.0000E+00	0.0000E+00	0.0000E+00	0.0000E+00	0.0000E+00	0.0000E+00	0.0000E+00	0.0000E+00
0.0000E+00	0.0000E+00	0.0000E+00	1.7452E-02	0.0000E+00	0.0000E+00	0.0000E+00	0.0000E+00	0.0000E+00	0.0000E+00
0.0000E+00	0.0000E+00	0.0000E+00	0.0000E+00	1.7452E-02	0.0000E+00	0.0000E+00	0.0000E+00	0.0000E+00	0.0000E+00
0.0000E+00	0.0000E+00	0.0000E+00	0.0000E+00	0.0000E+00	1.7452E-02	0.0000E+00	0.0000E+00	0.0000E+00	0.0000E+00
0.0000E+00	0.0000E+00	0.0000E+00	0.0000E+00	0.0000E+00	0.0000E+00	1.7452E-02	0.0000E+00	0.0000E+00	0.0000E+00
0.0000E+00	0.0000E+00	0.0000E+00	0.0000E+00	0.0000E+00	0.0000E+00	0.0000E+00	1.7452E-02	0.0000E+00	0.0000E+00
0.0000E+00	0.0000E+00	0.0000E+00	0.0000E+00	0.0000E+00	0.0000E+00	0.0000E+00	0.0000E+00	1.7452E-02	0.0000E+00
0.0000E+00	0.0000E+00	0.0000E+00	0.0000E+00	0.0000E+00	0.0000E+00	0.0000E+00	0.0000E+00	0.0000E+00	1.0000E+00

APPENDIX C3

MATRICES USED TO PERFORM TRANSFORMATIONS FOR CONTROL SURFACE DEFLECTION AND RELATIVE WEIGHTING OF THE OUTPUTS

$\tilde{S}_u$

1.0000E+00	0.0000E+00	0.0000E+00	0.0000E+00
0.0000E+00	6.6700E-01	0.0000E+00	0.0000E+00
0.0000E+00	0.0000E+00	8.0000E-01	0.0000E+00
0.0000E+00	0.0000E+00	0.0000E+00	8.0000E-01

$\tilde{S}_u^{-1}$

1.0000E+00	0.0000E+00	0.0000E+00	0.0000E+00
0.0000E+00	1.4993E+00	0.0000E+00	0.0000E+00
0.0000E+00	0.0000E+00	1.2500E+00	0.0000E+00
0.0000E+00	0.0000E+00	0.0000E+00	1.2500E+00

$\tilde{S}_y$

1.0000E-01	0.0000E+00	0.0000E+00	0.0000E+00
0.0000E+00	1.0000E-01	0.0000E+00	0.0000E+00
0.0000E+00	0.0000E+00	1.0000E+00	0.0000E+00
0.0000E+00	0.0000E+00	0.0000E+00	1.0000E+00

APPENDIX C4

REDUCED AND SCALED PLANT MATRICES WITH APPROPRIATE C MATRIX
MODEL WITH ROLL CONTROL

$$\underline{x}^T = [\, u \;\; v \;\; w \;\; p \;\; q \;\; r \;\; \Phi \;\; \Theta \,]$$

A MATRIX

-3.8269E-02	-2.1964E-02	-2.7533E-03	-3.3173E-04	2.0734E-03	5.5394E-02	0.0000E+00	5.1285E-06
1.1417E-03	-1.5939E-01	-3.3786E-05	-2.3578E-02	2.8353E-03	-2.6860E-01	2.2745E-03	-2.5914E-05
-4.7476E-04	1.3910E-03	-9.6526E-02	-2.7949E-02	2.1163E-01	7.6140E-04	0.0000E+00	1.3221E-04
1.3945E-02	-6.6430E-01	-8.0931E-02	-4.3452E-01	-2.5262E-01	-2.1920E-02	-1.6030E-01	1.8264E-03
7.1418E-05	-2.5929E-04	7.8117E-02	-1.1406E-02	-4.0815E-01	-7.7327E-04	0.0000E+00	-2.4985E-03
-1.5782E-03	-1.1622E-01	3.4035E-04	-8.0011E-03	2.2809E-03	-3.8201E-01	2.5893E-04	-2.9501E-06
0.0000E+00	0.0000E+00	0.0000E+00	1.0000E+00	1.1328E-02	-1.0538E-01	-4.9352E-10	-1.2635E-02
0.0000E+00	0.0000E+00	0.0000E+00	0.0000E+00	9.9427E-01	1.0689E-01	1.2494E-02	0.0000E+00

$$\underline{u}^T = [\, \delta b \;\; \delta r \;\; \delta s_1 \;\; \delta s_2 \,]$$

B MATRIX

-1.2666E-03	-1.5279E-03	9.8625E-05	9.8625E-05
0.0000E+00	6.0491E-02	-3.6976E-03	3.6976E-03
-2.5204E-02	-3.8763E-08	-2.1483E-02	-2.1483E-02
0.0000E+00	6.3847E-02	2.6060E-01	-2.6060E-01
1.3873E-02	7.3256E-07	-2.9781E-02	-2.9781E-02
0.0000E+00	-8.7846E-02	-4.2094E-04	4.2094E-04
0.0000E+00	0.0000E+00	0.0000E+00	0.0000E+00
0.0000E+00	0.0000E+00	0.0000E+00	0.0000E+00

APPENDIX C4

$$\underline{y}^T = [\ \phi\ \theta\ \dot{\psi}\ \dot{z}\ ]$$

C MATRIX

0.0000E+00	0.0000E+00	0.0000E+00	0.0000E+00	0.0000E+00	0.0000E+00	1.0000E-01	0.0000E+00
0.0000E+00	0.0000E+00	0.0000E+00	0.0000E+00	0.0000E+00	0.0000E+00	0.0000E+00	1.0000E-01
0.0000E+00	0.0000E+00	0.0000E+00	0.0000E+00	-1.0749E-01	9.9984E-01	4.6827E-09	1.3316E-03
1.0539E-01	-1.0629E-01	9.8873E-01	0.0000E+00	0.0000E+00	0.0000E+00	2.7119E-02	-8.4843E-01

APPENDIX C4

REDUCED AND SCALED PLANT MATRICES WITH APPROPRIATE C MATRIX
MODEL WITHOUT ROLL CONTROL

$$\underline{x}^T = [\ u\ v\ w\ p\ q\ r\ \phi\ \theta\ ]$$

A MATRIX

-3.8269E-02	-2.1964E-02	-2.7533E-03	-3.3173E-04	2.0734E-03	5.5394E-02	0.0000E+00	5.1285E-06
1.1417E-03	-1.5939E-01	-3.3786E-05	-2.3578E-02	2.8353E-03	-2.6860E-01	2.2745E-03	-2.5914E-05
-4.7476E-04	1.3910E-03	-9.6526E-02	-2.7949E-02	2.1163E-01	7.6140E-04	0.0000E+00	1.3221E-04
1.3945E-02	-6.6430E-01	-8.0931E-02	-4.3452E-01	-2.5262E-01	-2.1920E-02	-1.6030E-01	1.8264E-03
7.1418E-05	-2.5929E-04	7.8117E-02	-1.1406E-02	-4.0815E-01	-7.7327E-04	0.0000E+00	-2.4985E-03
-1.5782E-03	-1.1622E-01	3.4035E-04	-8.0011E-03	2.2809E-03	-3.8201E-01	2.5893E-04	-2.9501E-06
0.0000E+00	0.0000E+00	0.0000E+00	1.0000E+00	1.1328E-02	-1.0538E-01	-4.9352E-10	-1.2635E-02
0.0000E+00	0.0000E+00	0.0000E+00	0.0000E+00	9.9427E-01	1.0689E-01	1.2494E-02	0.0000E+00

$$\underline{u}^T = [\ \delta b\ \delta r\ \delta s\ ]$$

B MATRIX

-1.2666E-03	-1.5279E-03	1.9725E-04
0.0000E+00	6.0491E-02	0.0000E+00
-2.5204E-02	-3.8763E-08	-4.2965E-02
0.0000E+00	6.3847E-02	0.0000E+00
1.3873E-02	7.3256E-07	-5.9562E-02
0.0000E+00	-8.7846E-02	0.0000E+00
0.0000E+00	0.0000E+00	0.0000E+00
0.0000E+00	0.0000E+00	0.0000E+00

APPENDIX C4

$$\underline{y}^T = [\ \theta\ \dot{\psi}\ \dot{z}\ ]$$

C MATRIX

0.0000E+00	0.0000E+00	0.0000E+00	0.0000E+00	0.0000E+00	0.0000E+00	0.0000E+00	1.0000E-01
0.0000E+00	0.0000E+00	0.0000E+00	0.0000E+00	-1.0749E-01	9.9984E-01	4.6827E-09	1.3316E-03
1.0539E-01	-1.0629E-01	9.8873E-01	0.0000E+00	0.0000E+00	0.0000E+00	2.7119E-02	-8.4843E-01

APPENDIX D

MODAL ANALYSIS RESULTS

The matrices are presented in the standard row and column format. Additionally, the data presented consists of complex numbers. As such, the numbers are always displayed with the inaginary part directly below the real part. The eigenvectors (modal matrices) are presented as complex column vectors.

APPENDIX D1

MODAL ANALYSIS FOR DESIGN WITH ROLL CONTROL

PLANT EIGENVALUES

-1.4176E-02 -4.0661E-02 -4.2886E-02 -7.1364E-02 -1.9689E-01 -1.9689E-01 -4.5114E-01 -5.0486E-01
 0.0000E+00 0.0000E+00 0.0000E+00 0.0000E+00 3.1300E-01 -3.1300E-01 0.0000E+00 0.0000E+00

TRANSMISSION ZEROS

 5.8302E+07 1.2014E+07 7.8269E+06 -3.8414E-02 -2.5097E-01 -1.3680E+01 -1.3579E+01 -2.6894E+08
 0.0000E+00 0.0000E+00 0.0000E+00 0.0000E+00 0.0000E+00 1.1609E+04 -1.1609E+04 0.0000E+00

EIGENVECTORS (MODAL MATRIX)

-6.8361E-03 -2.5658E-01 1.0505E-01 2.5104E-01 -1.3119E-03 -1.3119E-03 -1.0292E-03 1.7639E-02
 0.0000E+00 0.0000E+00 0.0000E+00 0.0000E+00 -1.6355E-03 1.6355E-03 0.0000E+00 0.0000E+00

 2.6727E-03 -2.0890E-02 2.4216E-03 1.8514E-01 -1.3216E-02 -1.3216E-02 2.9403E-02 -2.1901E-01
 0.0000E+00 0.0000E+00 0.0000E+00 0.0000E+00 -1.8009E-02 1.8009E-02 0.0000E+00 0.0000E+00

 4.0471E-02 1.5080E-01 1.7237E-01 8.5127E-02 -2.9186E-02 -2.9186E-02 2.1418E-01 -4.1687E-03
 0.0000E+00 0.0000E+00 0.0000E+00 0.0000E+00 -6.5275E-03 6.5275E-03 0.0000E+00 0.0000E+00

-1.2341E-02 -8.9644E-03 -6.2565E-03 5.9660E-02 -2.3086E-01 -2.3086E-01 -1.4102E-01 -4.4041E-01
 0.0000E+00 0.0000E+00 0.0000E+00 0.0000E+00 2.5728E-01 -2.5728E-01 0.0000E+00 0.0000E+00

 1.4711E-02 3.8749E-02 4.3690E-02 1.7590E-02 -6.9174E-03 -6.9174E-03 -3.7838E-01 -4.7868E-02
 0.0000E+00 0.0000E+00 0.0000E+00 0.0000E+00 -5.9444E-03 5.9444E-03 0.0000E+00 0.0000E+00

-4.3411E-04 8.8786E-03 -8.1227E-04 -7.2642E-02 5.1850E-03 5.1850E-03 4.3218E-02 -2.3648E-01
 0.0000E+00 0.0000E+00 0.0000E+00 0.0000E+00 -8.4312E-03 8.4312E-03 0.0000E+00 0.0000E+00

-3.4241E-02 -6.2985E-02 -1.5239E-01 -9.4101E-01 9.2397E-01 9.2397E-01 3.5497E-01 8.2716E-01
 0.0000E+00 0.0000E+00 0.0000E+00 0.0000E+00 1.5763E-01 -1.5763E-01 0.0000E+00 0.0000E+00

-9.9838E-01 -9.5150E-01 -9.6648E-01 2.8480E-02 -1.8602E-02 -1.8602E-02 8.1384E-01 1.2387E-01
 0.0000E+00 0.0000E+00 0.0000E+00 0.0000E+00 -4.9793E-03 4.9793E-03 0.0000E+00 0.0000E+00

APPENDIX D1

CONTROLLABILITY MATRIX

5.6156E-01	1.7840E-01	4.1655E-01	4.8436E-01
-1.9911E-10	1.4232E-09	-3.7882E-10	4.7169E-10
-2.8596E-01	3.5042E-01	-1.2380E-01	-1.5388E-01
-6.2679E-10	2.7076E-09	7.3586E-10	-5.1437E-10
-6.4135E-01	-5.2348E-01	-2.5188E-01	-2.6555E-01
8.6262E-10	-4.1367E-09	-4.7910E-10	1.4451E-10
-5.1517E-02	5.7248E-01	1.6873E-04	-4.3806E-02
-1.0340E-09	4.5318E-09	7.6296E-10	-3.8432E-10
4.2000E-02	1.5533E-01	-1.1720E-01	1.3250E-02
1.1239E-01	-2.9618E-01	-5.9723E-01	5.7354E-01
4.2000E-02	1.5533E-01	-1.1720E-01	1.3250E-02
-1.1239E-01	2.9618E-01	5.9723E-01	-5.7354E-01
-3.9615E-01	-2.3595E-02	7.4600E-02	8.4577E-02
3.8132E-12	-1.3261E-10	-5.0678E-10	5.0520E-10
-5.6283E-02	1.3913E-01	-3.6203E-02	6.2273E-02
2.5680E-10	3.5415E-10	2.0900E-09	-2.1848E-09

OBSERVABILITY MATRIX

-3.4241E-03	-6.2985E-03	-1.5239E-02	-9.4101E-02	9.2397E-02	9.2397E-02	3.5497E-02	8.2716E-02
0.0000E+00	0.0000E+00	0.0000E+00	0.0000E+00	1.5763E-02	-1.5763E-02	0.0000E+00	0.0000E+00
-9.9838E-02	-9.5150E-02	-9.6648E-02	2.8480E-03	-1.8602E-03	-1.8602E-03	8.1384E-02	1.2387E-02
0.0000E+00	0.0000E+00	0.0000E+00	0.0000E+00	-4.9793E-04	4.9793E-04	0.0000E+00	0.0000E+00
-3.3447E-03	3.4451E-03	-6.7951E-03	-7.4483E-02	5.9029E-03	5.9029E-03	8.4965E-02	-2.3113E-01
0.0000E+00	0.0000E+00	0.0000E+00	0.0000E+00	-7.7975E-03	7.7975E-03	0.0000E+00	0.0000E+00
8.8514E-01	9.2986E-01	9.9710E-01	4.1263E-02	1.3249E-02	1.3249E-02	-4.7233E-01	-6.1643E-02
0.0000E+00	0.0000E+00	0.0000E+00	0.0000E+00	3.7872E-03	-3.7872E-03	0.0000E+00	0.0000E+00

APPENDIX D2

MODAL ANALYSIS FOR DESIGN WITHOUT ROLL CONTROL

PLANT EIGENVALUES

-1.4176E-02 -4.0661E-02 -4.2886E-02 -7.1364E-02 -1.9689E-01 -1.9689E-01 -4.5114E-01 -5.0486E-01
 0.0000E+00 0.0000E+00 0.0000E+00 0.0000E+00 3.1300E-01 -3.1300E-01 0.0000E+00 0.0000E+00

TRANSMISSION ZEROS

 3.0779E+07 5.5553E+03 -3.8432E-02 -1.8029E-01 -1.8029E-01 -3.1812E-01 -5.5561E+03 -1.5282E+08
 0.0000E+00 0.0000E+00 0.0000E+00 3.0164E-01 -3.0164E-01 0.0000E+00 0.0000E+00 0.0000E+00

EIGENVECTORS (MODAL MATRIX)

-6.8361E-03 -2.5658E-01 1.0505E-01 2.5104E-01 -1.3119E-03 -1.3119E-03 -1.0292E-03 1.7639E-02
 0.0000E+00 0.0000E+00 0.0000E+00 0.0000E+00 -1.6355E-03 1.6355E-03 0.0000E+00 0.0000E+00

 2.6727E-03 -2.0890E-02 2.4216E-03 1.8514E-01 -1.3216E-02 -1.3216E-02 2.9403E-02 -2.1901E-01
 0.0000E+00 0.0000E+00 0.0000E+00 0.0000E+00 -1.8009E-02 1.8009E-02 0.0000E+00 0.0000E+00

 4.0471E-02 1.5080E-01 1.7237E-01 8.5127E-02 -2.9186E-02 -2.9186E-02 2.1418E-01 -4.1687E-03
 0.0000E+00 0.0000E+00 0.0000E+00 0.0000E+00 -6.5275E-03 6.5275E-03 0.0000E+00 0.0000E+00

-1.2341E-02 -8.9644E-03 -6.2565E-03 5.9660E-02 -2.3086E-01 -2.3086E-01 -1.4102E-01 -4.4041E-01
 0.0000E+00 0.0000E+00 0.0000E+00 0.0000E+00 2.5728E-01 -2.5728E-01 0.0000E+00 0.0000E+00

 1.4711E-02 3.8749E-02 4.3690E-02 1.7590E-02 -6.9174E-03 -6.9174E-03 -3.7838E-01 -4.7868E-02
 0.0000E+00 0.0000E+00 0.0000E+00 0.0000E+00 -5.9444E-03 5.9444E-03 0.0000E+00 0.0000E+00

-4.3411E-04 8.8786E-03 -8.1227E-04 -7.2642E-02 5.1850E-03 5.1850E-03 4.3218E-02 -2.3648E-01
 0.0000E+00 0.0000E+00 0.0000E+00 0.0000E+00 -8.4312E-03 8.4312E-03 0.0000E+00 0.0000E+00

-3.4241E-02 -6.2985E-02 -1.5239E-01 -9.4101E-01 9.2397E-01 9.2397E-01 3.5497E-01 8.2716E-01
 0.0000E+00 0.0000E+00 0.0000E+00 0.0000E+00 1.5763E-01 -1.5763E-01 0.0000E+00 0.0000E+00

-9.9838E-01 -9.5150E-01 -9.6648E-01 2.8480E-02 -1.8602E-02 -1.8602E-02 8.1384E-01 1.2387E-01
 0.0000E+00 0.0000E+00 0.0000E+00 0.0000E+00 -4.9793E-03 4.9793E-03 0.0000E+00 0.0000E+00

APPENDIX D2

CONTROLLABILITY MATRIX

5.6156E-01	1.7840E-01	8.2094E-01
-1.9911E-10	1.4232E-09	1.0434E-10
-2.8596E-01	3.5042E-01	-2.5325E-01
-6.2679E-10	2.7076E-09	1.7222E-10
-6.4135E-01	-5.2348E-01	-4.7091E-01
8.6262E-10	-4.1367E-09	-2.8973E-10
-5.1517E-02	5.7248E-01	-4.0715E-02
-1.0340E-09	4.5318E-09	3.1755E-10
4.2000E-02	1.5533E-01	-9.1490E-02
1.1239E-01	-2.9618E-01	5.8204E-03
4.2000E-02	1.5533E-01	-9.1490E-02
-1.1239E-01	2.9618E-01	-5.8204E-03
-3.9615E-01	-2.3595E-02	1.4500E-01
3.8132E-12	-1.3261E-10	2.2219E-11
-5.6283E-02	1.3913E-01	2.6012E-02
2.5680E-10	3.5415E-10	-1.8620E-10

OBSERVABILITY MATRIX

-9.9838E-02	-9.5150E-02	-9.6648E-02	2.8480E-03	-1.8602E-03	-1.8602E-03	8.1384E-02	1.2387E-02
0.0000E+00	0.0000E+00	0.0000E+00	0.0000E+00	-4.9793E-04	4.9793E-04	0.0000E+00	0.0000E+00
-3.3447E-03	3.4451E-03	-6.7951E-03	-7.4483E-02	5.9029E-03	5.9029E-03	8.4965E-02	-2.3113E-01
0.0000E+00	0.0000E+00	0.0000E+00	0.0000E+00	-7.7975E-03	7.7975E-03	0.0000E+00	0.0000E+00
8.8514E-01	9.2986E-01	9.9710E-01	4.1263E-02	1.3249E-02	1.3249E-02	-4.7233E-01	-6.1643E-02
0.0000E+00	0.0000E+00	0.0000E+00	0.0000E+00	3.7872E-03	-3.7872E-03	0.0000E+00	0.0000E+00

APPENDIX E

GAIN MATRICES AND PROPERTIES OF THE CLOSED LOOP SYSTEM

For the 4-input, 4-output design the Kalman filter, control gain, and L matrices are real matrices displayed as 12x4, 4x12, and 12x4 matrices, respectively. In the case of the control gain matrices, the 12 elements of each row are displayed as two rows, containing the first six elements in one row and the last six elements in the next. The eigenvalues and transmission zeros of the open and closed loop plant are 1x24 complex matrices. The 24 elements in the row are displayed as four rows, with six elements in each row. The imaginary part of each element is directly below the real part. Similar notation is used for the 3-input, 3-output design.

APPENDIX E1

PROPERTIES OF THE ROLL CONTROL MODEL

FILTER GAIN MATRIX

-1.0282E+00	-1.8198E+01	-8.1019E-01	-2.1680E+00
1.1923E-01	7.9327E-02	-7.5141E-01	2.8994E-02
1.9031E+00	1.7664E+00	-8.6529E-01	1.5857E-01
-1.4904E+00	4.2619E-01	1.2014E+00	1.1415E-01
9.3005E-03	4.4870E-01	9.2495E-02	5.4981E-02
6.8777E-03	-3.4783E-01	-2.6354E-01	-3.8983E-02
2.4814E-02	4.1892E+00	2.1197E-01	4.9849E-01
1.8704E-01	2.4765E-01	-3.5220E-01	4.9200E-02
-3.0473E-02	-4.2343E-03	-3.1907E-02	3.5337E-04
-4.2073E-02	2.1331E-02	3.8510E-01	-4.2349E-03
5.3431E+00	2.1792E-01	-3.8501E-01	-1.5210E-01
2.1792E-01	4.9887E+00	2.8426E-01	-4.8414E-03

CONTROL GAIN MATRIX

1.3487E+00	1.4722E-03	-1.8437E-03	3.2330E-03	-2.8935E+00	2.1865E+00
-2.3081E+01	4.6679E-02	2.3366E+01	2.0238E+00	-2.3789E-01	2.5951E+01
1.4722E-03	2.0983E+00	-1.1733E-02	-4.2671E-02	-4.7100E-02	2.5212E+00
-7.6947E-01	1.9053E-01	1.7016E+00	-2.3196E+01	8.8982E-02	3.6430E-01
-1.8437E-03	-1.1733E-02	1.3132E+00	-3.5292E-01	-7.9515E-01	-1.3192E+00
-8.6155E+00	2.5982E+00	-1.9569E+00	1.4596E+00	1.4934E+00	4.8954E+00
3.2330E-03	-4.2671E-02	-3.5292E-01	1.2835E+00	-9.4105E-01	2.7612E+00
-8.7112E+00	-2.5781E+00	-5.8551E-01	6.8046E-01	-1.9771E+00	5.4309E+00

APPENDIX E1

L MATRIX

-6.0839E-01	-3.6479E+01	5.6633E-01	-4.3555E+00
1.5610E-02	8.7114E-02	-1.5284E+00	6.4870E-03
3.3627E+00	3.5527E+00	-2.4355E+00	4.4871E-01
-2.6540E+00	8.8502E-01	2.7545E+00	1.5325E-01
-2.8582E-02	8.9419E-01	8.1547E-14	1.0539E-01
2.8826E-02	-9.0182E-01	-8.2242E-14	-1.0629E-01
-2.6814E-01	8.3888E+00	7.6502E-13	9.8873E-01
0.0000E+00	0.0000E+00	0.0000E+00	0.0000E+00
4.9774E-09	1.4154E-03	-1.0629E-01	-4.4369E-13
-4.6300E-08	-1.3166E-02	9.8873E-01	4.1272E-12
1.0000E+01	-1.4691E-09	-3.8444E-17	1.2488E-11
-1.3286E-10	1.0000E+01	6.9211E-12	-5.5841E-09

OPEN LOOP EIGENVALUES

9.5843E-09	0.0000E+00	0.0000E+00	0.0000E+00	-1.4176E-02	-3.8412E-02
-4.4084E-01	-4.4084E-01	-4.5114E-01	-5.0486E-01	-5.8965E-01	-5.8965E-01
-4.0661E-02	-4.2886E-02	-7.1364E-02	-1.9689E-01	-1.9689E-01	-2.5114E-01
-9.5148E-01	-9.5148E-01	-1.0104E+00	-1.3887E+00	-1.3887E+00	-1.4462E+00
0.0000E+00	0.0000E+00	0.0000E+00	0.0000E+00	0.0000E+00	0.0000E+00
4.7901E-01	-4.7901E-01	0.0000E+00	0.0000E+00	1.1366E+00	-1.1366E+00
0.0000E+00	0.0000E+00	0.0000E+00	3.1300E-01	-3.1300E-01	0.0000E+00
1.0148E+00	-1.0148E+00	0.0000E+00	1.3186E+00	-1.3186E+00	0.0000E+00

APPENDIX E1

OPEN LOOP TRANSMISSION ZEROS

1.0000E+30	1.0000E+30	1.0000E+30	1.0000E+30	1.1625E+08	1.0192E+08
-3.9767E-02	-3.9767E-02	-1.9869E-01	-2.0469E-01	-2.0469E-01	-2.5097E-01
1.2816E+05	1.4260E+04	1.2133E+00	1.2202E+00	-1.4256E-02	-3.8414E-02
-2.8357E-01	-4.5944E-01	-1.4263E+04	-1.2816E+05	-8.6484E+07	-5.8038E+09
0.0000E+00	0.0000E+00	0.0000E+00	0.0000E+00	0.0000E+00	0.0000E+00
1.6540E-03	-1.6540E-03	0.0000E+00	2.8343E-01	-2.8343E-01	0.0000E+00
0.0000E+00	0.0000E+00	1.0851E+04	-1.0851E+04	0.0000E+00	0.0000E+00
0.0000E+00	0.0000E+00	0.0000E+00	0.0000E+00	0.0000E+00	0.0000E+00

CLOSED LOOP EIGENVALUES

-1.4220E-02	-3.8414E-02	-3.8479E-02	-4.1399E-02	-1.0317E-01	-1.0317E-01
-5.1064E-01	-5.1064E-01	-5.1516E-01	-5.2355E-01	-5.2355E-01	-7.1513E-01
-2.3970E-01	-2.3970E-01	-2.5106E-01	-2.7292E-01	-2.7292E-01	-4.1228E-01
-7.4533E-01	-7.5232E-01	-7.5232E-01	-1.0388E+00	-1.1957E+00	-1.1957E+00
0.0000E+00	0.0000E+00	0.0000E+00	0.0000E+00	1.0659E-01	-1.0659E-01
7.0401E-02	-7.0401E-02	0.0000E+00	9.2146E-01	-9.2146E-01	0.0000E+00
3.3649E-01	-3.3649E-01	0.0000E+00	2.7737E-01	-2.7737E-01	0.0000E+00
0.0000E+00	8.5953E-01	-8.5953E-01	0.0000E+00	1.1639E+00	-1.1639E+00

CLOSED LOOP TRANSMISSION ZEROS

7.5203E+10	1.1350E+04	8.6830E+03	6.7422E+03	2.5300E+02	2.5300E+02
-3.9768E-02	-3.9768E-02	-1.9869E-01	-2.0469E-01	-2.0469E-01	-2.5097E-01
1.5900E+00	1.4499E+00	2.5446E-01	7.5507E-01	-1.4253E-02	-3.8414E-02
-2.8357E-01	-4.5944E-01	-5.0698E+02	-6.7412E+03	-8.6823E+03	-1.1349E+04
0.0000E+00	0.0000E+00	0.0000E+00	0.0000E+00	4.3878E+02	-4.3878E+02
1.6527E-03	-1.6527E-03	0.0000E+00	2.8343E-01	-2.8343E-01	0.0000E+00
2.4470E+05	-2.4470E+05	1.5450E+04	-1.5450E+04	0.0000E+00	0.0000E+00
0.0000E+00	0.0000E+00	0.0000E+00	0.0000E+00	0.0000E+00	0.0000E+00

APPENDIX E2

PROPERTIES OF THE MODEL WITHOUT ROLL CONTROL

FILTER GAIN MATRIX

-1.8104E+01	-9.9739E-01	-1.9187E+00
8.3100E-02	-7.5396E-01	-2.4242E-03
1.0178E+00	2.9009E-01	1.2935E-01
4.4848E-01	9.4995E-02	4.6515E-02
-3.2777E-01	-2.9706E-01	-4.0709E-02
4.2139E+00	1.7960E-01	4.3854E-01
-8.2718E-02	1.1100E-01	-3.5626E-03
8.5074E-03	-5.1439E-02	6.8779E-05
2.0580E-02	3.8598E-01	5.4579E-03
-1.9794E-01	3.5426E-01	-5.2399E-03
5.0090E+00	2.6332E-01	-6.6166E-02

CONTROL GAIN MATRIX

1.3399E+00	2.4951E-03	-4.1531E-02	-2.8549E+00	2.1877E+00	-2.2711E+01
2.8530E-02	2.3251E+01	1.9938E+00	-2.3664E-01	2.5708E+01	
2.4951E-03	2.0950E+00	-4.4818E-02	-6.1695E-02	2.5273E+00	-9.1184E-01
8.4496E-02	1.7283E+00	-2.3191E+01	-5.5890E-02	4.6906E-01	
-4.1531E-02	-4.4818E-02	1.1898E+00	-1.3346E+00	1.2073E+00	-1.3296E+01
-7.3320E-02	-2.3292E+00	1.7524E+00	-4.3088E-01	8.1221E+00	

APPENDIX E2

L MATRIX

-3.6209E+01	4.1533E-02	-4.3257E+00
8.0193E-02	-1.5149E+00	5.7204E-03
2.0617E+00	4.6520E-01	2.8358E-01
8.9353E-01	-1.3558E-11	1.0532E-01
-9.0115E-01	1.3674E-11	-1.0621E-01
8.3826E+00	-1.2719E-10	9.8801E-01
0.0000E+00	0.0000E+00	0.0000E+00
1.4154E-03	-1.0629E-01	1.4658E-11
-1.3166E-02	9.8873E-01	-1.3635E-10
2.2992E-01	4.6272E-09	2.7099E-02
1.0000E+01	1.1950E-11	-3.4596E-10

OPEN LOOP EIGENVALUES

1.4791E-08	0.0000E+00	0.0000E+00	-1.4176E-02	-3.8430E-02	-4.0661E-02
0.0000E+00	0.0000E+00	0.0000E+00	0.0000E+00	0.0000E+00	0.0000E+00
-4.2886E-02	-7.1364E-02	-1.8012E-01	-1.8012E-01	-1.9689E-01	-1.9689E-01
0.0000E+00	0.0000E+00	3.0158E-01	-3.0158E-01	3.1300E-01	-3.1300E-01
-3.1857E-01	-4.5114E-01	-4.5954E-01	-4.5954E-01	-5.0486E-01	-1.0233E+00
0.0000E+00	0.0000E+00	4.9673E-01	-4.9673E-01	0.0000E+00	1.1072E+00
		-1.0233E+00	-1.0643E+00	-1.3940E+00	-1.3940E+00
		-1.1072E+00	0.0000E+00	1.3186E+00	-1.3186E+00

APPENDIX E2

OPEN LOOP TRANSMISSION ZEROS

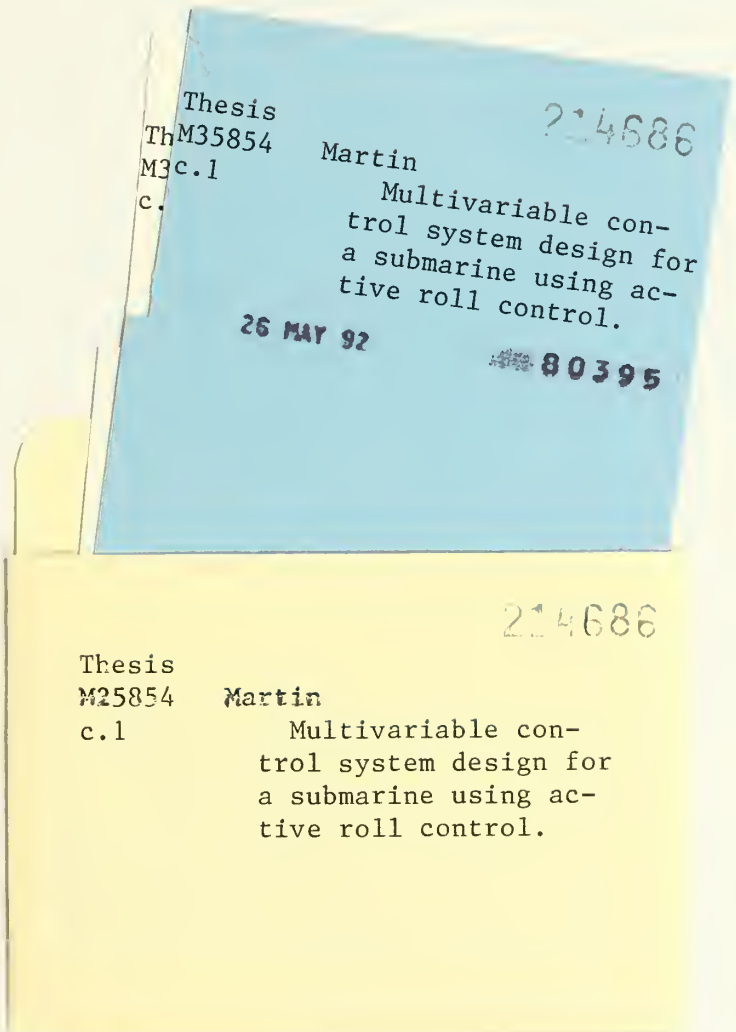
1.0000E+30	1.0000E+30	1.0000E+30	1.7438E+11	2.5380E+10	1.2540E+08
0.0000E+00	0.0000E+00	0.0000E+00	0.0000E+00	0.0000E+00	0.0000E+00
2.4318E+04	1.3204E+04	-1.4324E-02	-3.8432E-02	-3.9719E-02	-3.9719E-02
0.0000E+00	0.0000E+00	0.0000E+00	0.0000E+00	9.8294E-04	-9.8294E-04
-1.5509E-01	-1.8029E-01	-1.8029E-01	-1.9034E-01	-1.9034E-01	-3.1812E-01
0.0000E+00	3.0164E-01	-3.0164E-01	3.1017E-01	-3.1017E-01	0.0000E+00
	-3.5414E-01	-4.5896E-01	-1.3205E+04	-2.4309E+04	
	0.0000E+00	0.0000E+00	0.0000E+00	0.0000E+00	

CLOSED LOOP EIGENVALUES

-1.4259E-02	-3.8432E-02	-3.8768E-02	-4.0957E-02	-1.3245E-01	-1.3245E-01
0.0000E+00	0.0000E+00	0.0000E+00	0.0000E+00	1.0424E-01	-1.0424E-01
-1.7991E-01	-1.7991E-01	-1.9902E-01	-1.9902E-01	-2.8854E-01	-2.8854E-01
3.0178E-01	-3.0178E-01	3.0667E-01	-3.0667E-01	2.9348E-01	-2.9348E-01
-3.1880E-01	-4.5868E-01	-4.8610E-01	-5.2124E-01	-6.8742E-01	-7.5761E-01
0.0000E+00	0.0000E+00	0.0000E+00	0.0000E+00	0.0000E+00	0.0000E+00
	-8.4879E-01	-8.4879E-01	-1.1972E+00	-1.1972E+00	
	9.4987E-01	-9.4987E-01	1.1636E+00	-1.1636E+00	

CLOSED LOOP TRANSMISSION ZEROS

1.0000E+30	7.5842E+08	3.0352E+04	1.3159E+04	5.1442E+02	-1.4324E-02
0.0000E+00	0.0000E+00	0.0000E+00	0.0000E+00	0.0000E+00	0.0000E+00
-3.8432E-02	-3.9718E-02	-3.9718E-02	-1.5509E-01	-1.8029E-01	-1.8029E-01
0.0000E+00	9.8524E-04	-9.8524E-04	0.0000E+00	3.0164E-01	-3.0164E-01
-1.9034E-01	-1.9034E-01	-3.1812E-01	-3.5414E-01	-4.5896E-01	-2.5748E+02
3.1017E-01	-3.1017E-01	0.0000E+00	0.0000E+00	0.0000E+00	4.4566E+02
	-2.5748E+02	-1.3166E+04	-3.0347E+04	-8.0668E+09	
	-4.4566E+02	0.0000E+00	0.0000E+00	0.0000E+00	


Thesis
M35854
c.1
Th
M3
c.
214686
Martin
Multivariable control system design for a submarine using active roll control.
26 MAY 92
80395
214686
Thesis
M25854
c.1
Martin
Multivariable control system design for a submarine using active roll control.

Multivariable control system design for
3 2768 000 68165 4
DUDLEY KNOX LIBRARY